REACTION OF PEROXYNITRITE AND URIC ACID STUDIED BY ESR SPIN TRAPPING AND MASS SPECTROMETRY: FREE RADICAL FORMATION AND PRODUCT IDENTIFICATION

By

WITCHA IMARAM

A DISSERTATION PRESENTED TO THE GRADUATE SCHOOL
OF THE UNIVERSITY OF FLORIDA IN PARTIAL FULFILLMENT
OF THE REQUIREMENTS FOR THE DEGREE OF
DOCTOR OF PHILOSOPHY

UNIVERSITY OF FLORIDA

2008

To my parents, to my brother, and to my grandparents

ACKNOWLEDGMENTS

I particularly owe my deepest gratitude to my advisor Dr. Alexander Angerhofer for his encouragement, valuable guidance and support throughout this study. I would like to express my sincere gratitude to Dr. Richard J. Johnson for inspiring me to be involved in the exciting field of biochemistry, in uric acid study. I am pleased to thank Dr. George N. Henderson for making the MS work a reality, as well as his invaluable suggestions and discussion. I would like to thank my doctoral dissertation committee members (Dr. William R. Dolbier, Dr. Lisa McElwee-White, and Dr. Kirk S. Schanze) for their input and constructive comments. This study was supported by grants from Gatorade and the University of Florida through an opportunity grant from its Division of Sponsored Research, and by the University of Florida Chemistry Department. I am grateful for the graduate stipend and tuition sponsored by the Development and Promotion of Science and Technology Talent Project (DPST) scholarship from the Institute for the Promotion of Teaching Science and Technology, Thailand.

I would also like to take this opportunity to further express my appreciation to my uric acid project collaborators Dr. Christine Gersch, Dr. Sergiu P. Palii, and Dr. Kyung Mee Kim for their invaluable training and guidance. I am also thankful to Dr. Yuri Y. Sautin for his helpful suggestion. In addition to Dr. George N. Henderson and Dr. Kyung Mee Kim, I owe a debt of gratitude to my MS collaborators Dr. David H. Powell and Dr. Jodie V. Johnson of the Mass Spectrometry Services at the University of Florida Chemistry Department.

I am grateful to my colleagues and friends Dimitri Dascier, Fabrizio Guzzetta, Dooho Park Vijay B. Krishna, Jirapat Jangjamras**,** Yun Wang, Suwussa Bamrungsap, and Pattaraporn Vanachayangkul for their help, suggestion, and friendship.

I thank Dr. Ben Smith, Graduate Coordinator and chemistry departmental staff members Lori Clark, Beth Douglas, and Vivian Thompson for their help and advice. I gratefully acknowledge Rich Athey for his friendship and critical reading of this dissertation.

Finally, I would like to acknowledge my parents who have always supported, encouraged, and inspired me to complete my dream.

TABLE OF CONTENTS

page

LIST OF TABLES

LIST OF FIGURES

Abstract of Dissertation Presented to the Graduate School
of the University of Florida in Partial Fulfillment of the
Requirements for the Degree of Doctor of Philosophy

REACTION OF PEROXYNITRITE AND URIC ACID STUDIED BY ESR SPIN TRAPPING AND MASS SPECTROMETRY: FREE RADICAL FORMATION AND PRODUCT IDENTIFICATION

By

Witcha Imaram

December 2008

Chair: Name Alexander Angerhofer
Major: Chemistry

Uric acid is the most abundant antioxidant in plasma. However, under conditions of elevated uric acid levels and oxidative stress, it becomes a pro-oxidant and causes endothelial dysfunction. It is hypothesized that the generation of reactive intermediates such as free radicals from the reaction of peroxynitrite and other oxidants mediate the pathological pro-oxidant properties of uric acid. Peroxynitrite is a reactive oxidant produced *in vivo* in response to oxidative and other stress by the diffusion-limited reaction of nitric oxide and superoxide. Our research is focused on the identification of free radical metabolites of uric acid formed from its reaction with peroxynitrite. Our experimental approach included the electron spin resonance (ESR) spin trapping of the radical generated from the reaction between uric acid and peroxynitrite at pH 7.4. Using PBN (N-*tert*-butyl-alpha-phenylnitrone) as the spin trapping agent, a six-line ESR spectrum was obtained and its hyperfine coupling constants, a(N) = 15.6 G; and a(H) = 3.6 G, corresponded to two carbon-based radicals. Further structural identifications of the PBN-radical adducts were carried out using liquid chromatography-mass spectrometry (LC-MS). After comparison with the control reactions, we could identify two molecules, corresponding to the fragment ions of m/z 352 and 223, respectively. The PBN-triuretcarbonyl

radical adduct was characterized for m/z 352 and the latter was identified as a PBN-aminocarbonyl radical adduct.

The pH dependence study of the reaction between uric acid and peroxynitrite revealed the formation of hydrogen adduct at high pH and could be observed even without urate. Its formation was proposed to undergo the inverted spin trapping mechanism, in which the spin trap was initially oxidized rather than the antioxidant substrate, and followed by electron transfer.

We extended our studies to investigate the effect of methyl substitution at various nitrogen positions on product and radical formation. No ESR signal was observed when conducting the reactions with N-7 methylated uric acids in phosphate buffer pH 7.4. Moreover, the reactions were purposely conducted in methanol to trap the reaction intermediate. Various products have been identified by LC-MS, and those products indicated that a common intermediate in various urate oxidation conditions, dehydroisouric acid, was formed.

CHAPTER 1
INTRODUCTION

General Overview of Electron Spin Resonance Spin Trapping

Free radicals are any chemical species capable of independent existence possessing one or more unpaired electrons (*1*). Free radicals, and especially reactive oxygen species, play an important role in living systems and they are widely believed to contribute to the development of several age-related diseases and implicated in the pathology of a range of diseases including ischemic and post-ischemic reperfusion damage, inflammation processes, cancers, and neurodegenerative diseases (*1-5*). In these pathologies, oxidative damage initiated by free radicals, such as lipid peroxidation process (*6*), DNA damage (*7*), and proteins and enzyme inactivation, is occurring. Thus, the development of methods capable of detecting free radicals in biological systems is very important and has become an active field in free radical research.

Electron spin resonance (ESR), known by many synonyms such as, electron paramagnetic resonance (EPR), or electron magnetic resonance (EMR), has emerged as a powerful method for direct detection and characterization of free radicals (*2*). Because of its high selectivity to detect paramagnetic species such as free radicals, ESR is one of the most widely chosen methods for studying the free-radical mediated process in a complex biological system (*8*). However, ESR alone has some disadvantages, one of which is a short time-period for free radical detection (half life $t_{1/2}$ 10^{-9} to 10 s). In many occasions, some radical processes may not be ESR detectable under various physiological conditions because some free radicals are very short-lived. These short-lived free radical species may not have sufficient enough time to accumulate their concentration to reach a steady state level above the detection limit of ESR (~10^{-8} M) (*8*). Moreover, if free radicals have very short spin relaxation time, this will make their line width too broad to be

observed by ESR (*9*). To circumvent this drawback, the spin trapping technique was introduced in late 1960s (*10*).

Named by Janzen and Blackburn in 1969 (*11*), spin trapping is the chemical reaction (Equation 1-1) in which a reactive free radical ($R^{\bullet}$) adds to a diamagnetic compound and spin trapping agent (ST) to form a more stable radical, the spin adduct ($[ST\text{-}R]^{\bullet}$).

$$R^{\bullet} + ST \rightarrow [ST\text{-}R]^{\bullet} \qquad (1\text{-}1)$$

The spin adduct (usually a nitroxide) that is paramagnetic gives the ESR spectrum which contains useful information called hyperfine parameters. In general, one can characterize the original free radical, from which the spin adduct was derived, by analyzing the number of hyperfine parameters and the magnitude of the hyperfine coupling constants in the ESR spectrum (*8*). Practically, such a full characterization is rarely obtained; however, it is still possible to extract some information about the type of the radical (i.e., whether it is carbon-centered, oxygen-centered, or nitrogen-centered) (*9*).

Nitrone and nitroso compounds are the most popular spin trapping agents. Although the spin adducts of nitroso compounds are relatively less stable, more information in the hyperfine splitting parameters can be obtained from nitroso compounds, such as 2-methyl-2-nitrosopropane (MNP), than nitrone because the radical adds directly to the nitroso nitrogen (Equation 1-2),

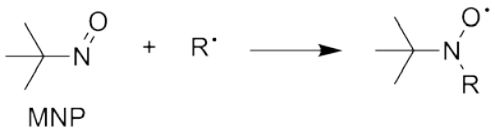

MNP (1-2)

The spin adducts from nitrones are quite stable, but some information is lost because the nitroxyl radical is far away from the original radical by one carbon atom. Nevertheless, useful information can still be obtained from a β-hydrogen that is present in many widely used nitrone spin traps: DMPO, PBN, and POBN (Figure 1-1).

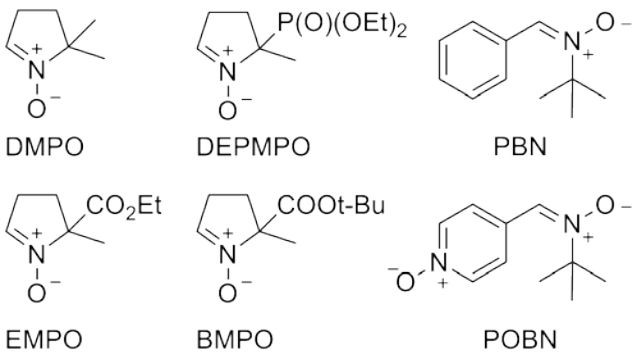

Figure 1-1. Examples of nitrone spin trapping agents.

The spin-trapping technique of short-lived free radicals, especially reactive oxygen species (ROS), coupled with ESR has become a valuable tool in the study of the fate of the radicals in the biological milieu. However, the use of the spin-trapping technique has been limited when applied to the biological system due to the short persistence of the spin adducts, in which the aminoxyls are reduced to ESR silent products by the biological antioxidants such as ascorbate anion and glutathione peroxidase (*12*). In an effort to develop more efficient spin traps, in the past decade, a number of different nitrone spin traps, such as DEPMPO (*13*), EMPO (*14*), and BMPO (*15*) (Figure 1-1) have been synthesized. The challenge of designing a new spin trap is not only getting more persistent spin adducts, but also improving the spectral resolution between the different spin adducts. Moreover, the development of spin traps that can accumulate in relevant sites and cell compartments is an important issue as well.

Uric Acid

Generation and Degradation

Uric acid is a purine degradation product from RNA, DNA and adenine nucleotides (*16*). Its immediate precursor, xanthine, is converted to uric acid via the enzymatic reaction with xanthine oxidase or xanthine dehydrogenase (Equation 1-3).

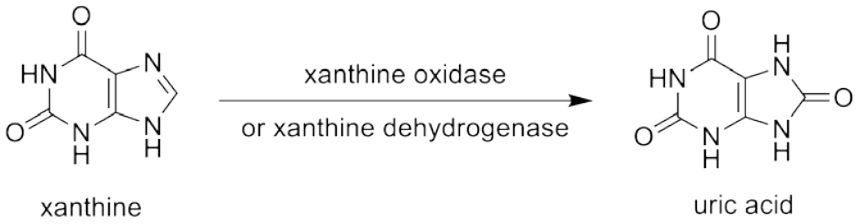

(1-3)

The former enzyme generates oxidants (O_2^- and H_2O_2) during this reaction. In most mammals, uric acid is degraded to allantoin by the enzyme urate oxidase (uricase) which is present in the liver. However, during primate evolution, 5 to 20 million years ago, two parallel but distinct mutations occurred in early humanoids that rendered the uricase gene nonfunctional (*17*). As a result, humans and the great apes have higher uric acid levels (range 3-14 mg/dL) compare with most mammals (1mg/dL) (*18*).

In plasma, uric acid is largely present as monoanion urate (pKa = 5.4) (*19*). Serum uric acid can be generated from endogenous and exogenous sources. Exogenous sources include foods rich in purines, such as fatty meats, beer, and organ meats. Interestingly, fructose can increase the level of uric acid in serum (*20*). Fructose is different from other sugars in that it is degraded by a specific enzyme pathway (fructokinase-aldolase B) that results in the rapid generation of uric acid. The mechanism is due to the unregulated rapid phosphorylation of fructose to fructose-1-phosphate, resulting in ATP depletion, phosphate depletion, AMP deaminase synthesis, and generation of urate (*21*). Because of the lack of uricase and the ability to regulate uric acid tightly, dietary intake of purines or fructose can lead to a rapid rise in serum uric acid. In addition to exogenous sources, uric acid can be generated under conditions of high cell turnover or in the setting of ischemia (*22*).

Being an antioxidant, uric acid can react with a variety of substances that can lead to its stepwise degradation. It can react with O_2^-, H_2O_2, and peroxynitrite ($OONO^-$) (*23,24*). These

reactions lead to the complete degradation of uric acid and result in the generation of a number of stable end products, including allantoin, alloxan, parabanic acid, and triuret (*25*,*26*).

Uric Acid: The Oxidant-Antioxidant Paradox

Because of the lack of uricase in humans after the primate evolution, uric acid has been theorized to replace vitamin C and become a major antioxidant in human (*23*). Urate has been proposed to inhibit the formation of nitrotyrosine resulted from peroxynitrite-mediated damage (*27*) by scavenging the radical intermediates, the decomposition products of peroxynitrite (*28*), which are responsible for nitration of tyrosine. Moreover, uric acid can chelate transition metal ions and scavenge many reactive oxygen and nitrogen species; for example, superoxide, the hydroxyl radical, singlet oxygen, and peroxynitrite (*19*,*29*).The antioxidant properties of uric acid have been thought to be initiated by the donation of an electron by uric acid to generate the urate radical (with a redox potential of 0.59V), followed by its nonreversible degradation to a variety of products (*25*,*26*). In this regard the urate reaction is distinct from ascorbate, for although ascorbate will also generate the ascorbyl radical, this latter reaction is reversible (*30*).

Despite the role of antioxidant in plasma, the growing evidence of uric acid being a true risk factor to develop obesity, hypertension, and cardiovascular disease, conditions associated with oxidative stress, has recently been reported (*18*,*31*). Uric acid can be a pro-oxidant by forming free radials in various reactions. Maples and Mason detected the urate radical in a flow-cell ESR experiment with both permanganate and the peroxidase/H_2O_2 system (*32*). The data suggested that the UA radical was a π-delocalized radical that resided on the 5-membered ring. Kahn et al. studied the oxidative reaction of urate (anion form of uric acid) by xanthine oxidase (XO) and found that hydroperoxide and dehydrourate were two distinct intermediates (Figure 1-2) (*33*,*34*). 5-hydroxyisourate was the primary product of the enzymatic oxidation and through

subsequent non-enzymatic ring opening leads to allantoin (*33*,*35*). This is an effective $2e^{-}/2H^{+}$ oxidation mechanism which can also be observed by electrochemical oxidation (*26*,*35*).

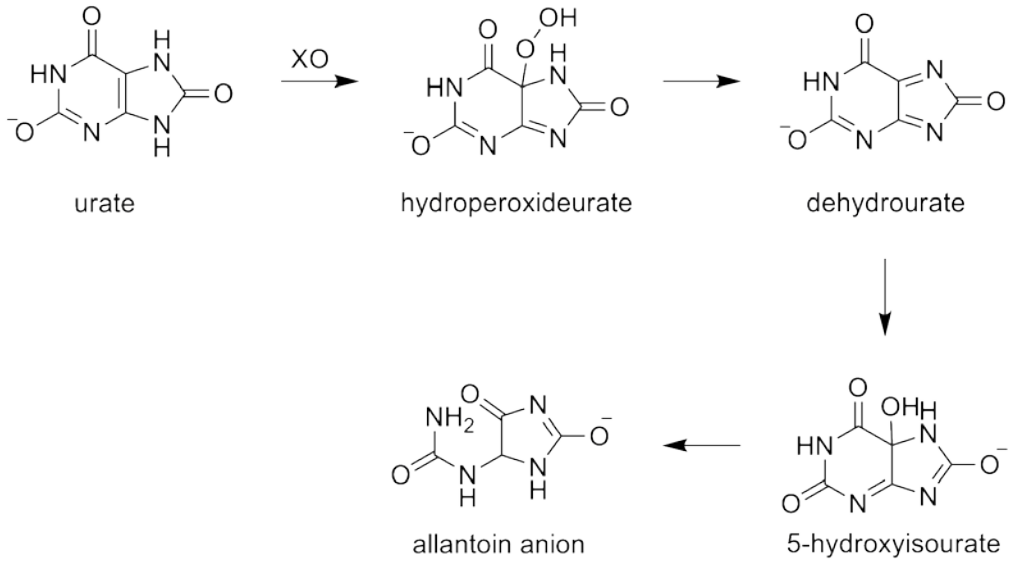

Figure 1-2. The oxidative reaction of urate by xanthine oxidase (XO).

Attacked by peroxynitrite, urate was decomposed to form urate-derived radicals, which are responsible for the amplification of lipid oxidation products found in liposomes and LDL when treated with peroxynitrite (*36*). The fact that urate can be oxidized via a radical mechanism is significant since this opens up the possibility for an explanation of the pro-oxidant effect of uric acid (*20*,*37-39*). If the oxidation of uric acid *in vivo* processes via radical mechanism, it is possible that radical chain reactions may be started and damage the cell (*16*).

Whether uric acid functions as an antioxidant or pro-oxidant remains ambiguous. Sautin et al. suspected that uric acid may have a protective effect only in the hydrophilic environment, like in plasma (*16*). On the other hand, the pro-oxidative effects of uric acid, which are usually associated with lipid, may take place only in the hydrophobic environment created by lipid within the cell (*16*). Thus, one may determine the true function of uric acid by analyzing the effect of uric acid in various circumstances.

Peroxynitrite

Peroxynitrite ($OONO^-$) or oxoperoxynitrate(1-) has been receiving great interest in several fields. Beside earth, peroxynitrite was observed by the Mars Viking biology experiments to be generated by photolysis on Mars (*40*). It can be formed by the fast reaction ($k = 5\text{-}19 \times 10^9\ M^{-1} \cdot s^{-1}$) between nitric oxide ($^{\bullet}NO$)and superoxide ($O_2^{\bullet-}$) (*41-43*) (Equation 1-4).

$$^{\bullet}NO + O_2^{\bullet-} \rightarrow ONOO^- \quad (1\text{-}4)$$

In *vivo*, this reaction frequently occurs in the vasculature due to the presence of superoxide generated by NADPH oxidase or by xanthine oxidase, and nitric oxide generated by endothelial nitric oxide synthase (eNOS) (*44*). The formation of peroxynitrite from relatively unreactive radicals, $^{\bullet}NO$ and $O_2^{\bullet-}$, is regulated by superoxide dismutase (SOD), an enzyme capable of lowering superoxide ($O_2^{\bullet-}$) (Figure 1-3).

From thermodynamic calculations, the oxidation potential of peroxynitrite was calculated. It indicated that peroxynitrite is a strong oxidant, with a one-electron reduction potential, E° ($OONO^-$, $2H^+$/ $NO_2^{\bullet}$, H_2O), around 1.6 V at pH 7, and that it is unstable with respect to disproportionation to nitrogen dioxide and the nitrosyldioxyl radical, $ONOO^{\bullet}$ (*45*).

Moreover, the product, nitrogen dioxide, is also a strong oxidant, with a one-electron reduction potential, E° ($NO_2^{\bullet}/NO_2^-$) = 1.04 V (*46*). Peroxynitrite is somewhat stable, though decomposes slowly to nitrite and dioxygen at and above pKa, and at high concentration (exceed 0.1 mM) (Equation 1-5) (*47*).

$$2ONOO^- \rightarrow O_2 + 2NO_2^- \quad (1\text{-}5)$$

Peroxynitrite anion can exist in two geometries, the *cis* and *trans* isomers (Figure 1-4). In solution, it is present in the *cis*-form (*48*), which is 3-4 kcal/mol more stable than the *trans*-form

(*49*). The energy barrier between the two conformers is approximately 24 kcal/mol for the anion, and 10 kcal/mol less for the protonated form (*49*).

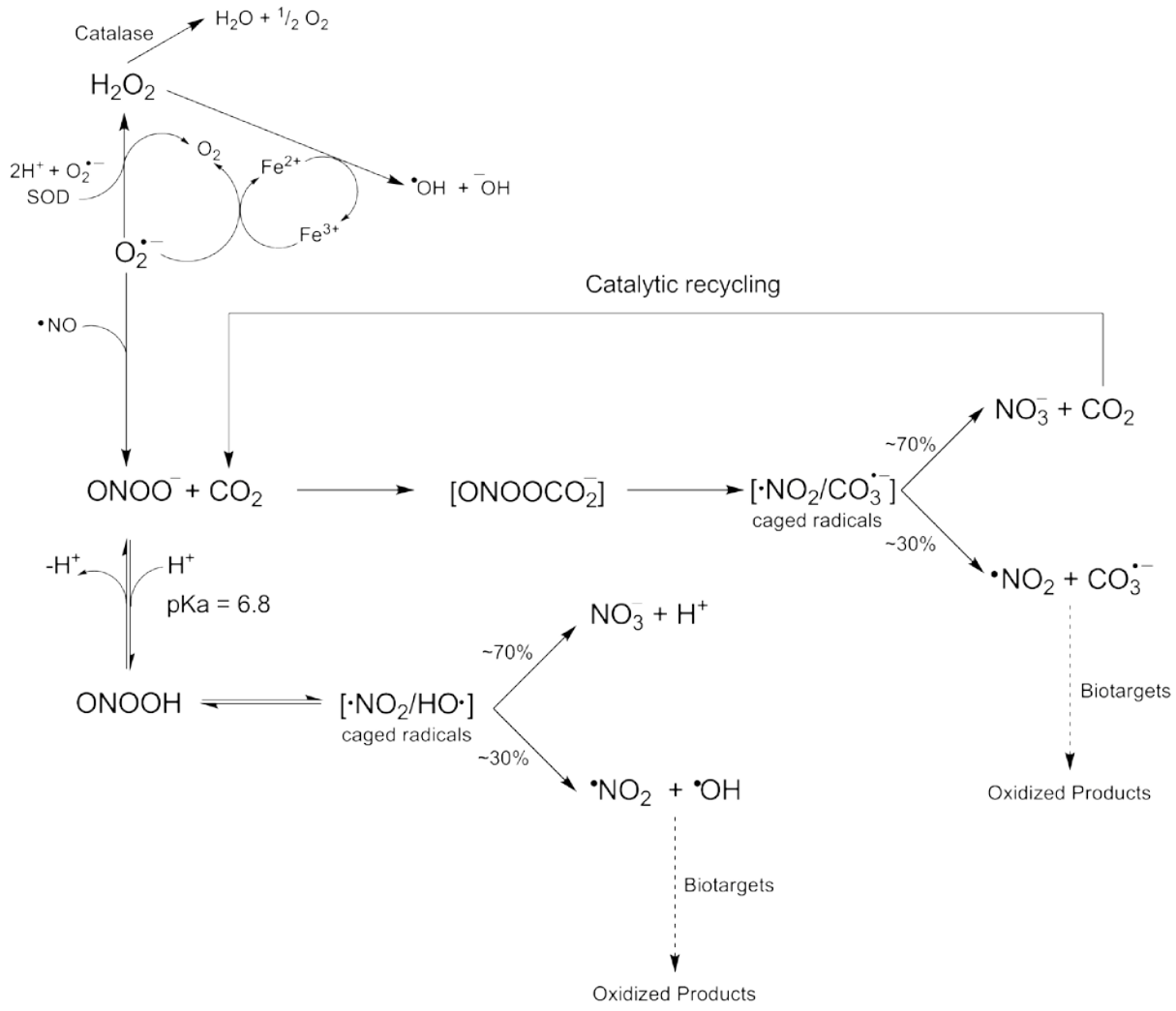

Figure 1-3. Scheme summarized the chemistry of peroxynitrite, including the postulated formation of peroxynitrite *in vivo*, the reaction between peroxynitrite and CO_2, the decomposition of peroxynitrous acid, and the reaction pathways leading to the oxidation products.

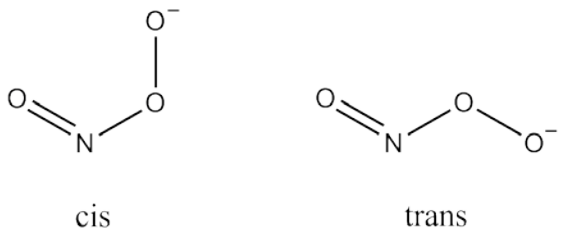

Figure 1-4. Geometrical isomers of peroxynitrite.

Known to react as a nucleophile, peroxynitrite anion ($OONO^-$) can undergo nucleophilic addition with CO_2 (*50*,*51*), aldehydes (*52*), and ketones (*53*), while peroxynitrous acid (ONOOH) mediates ebselen oxidaton (*52*,*54*).

Peroxynitrous acid (ONOOH), a conjugate acid of peroxynitrite, is a strong both one- and two-electron oxidizing agent (*55*), with a pKa of 6.5-7.5, depending on the ionic strength of the medium (*47*). Unlike peroxynitrite anion, peroxynitrous acid isomerizes to nitrate (70%) with a rate of 1.2 s^{-1} at 25 °C. In addition to isomerisation pathway, peroxynitrous acid has been proposed to undergo homolysis (30%) to form the hydroxyl radical and nitrogen dioxide (Equation 1-6) (*56*). However, Kissner et al. suggested that homolysis of the O-O bond in peroxynitrous acid is unlikely(*55*), and concluded that peroxynitrous acid is not the source of hydroxyl radicals (*46*).

$$ONOOH \rightarrow HO^{\bullet} + {}^{\bullet}NO_2 \qquad (1\text{-}6)$$

The actual nature of the decomposition of peroxynitrite is still debated. However, whether peroxynitrous acid undergoes homolysis is irrelevant in a biological system, where the carbon dioxide (CO_2) exists in a high concentration (approximately 1 mM). The reaction of peroxynitrite with CO_2 is one of the main pathways of peroxynitrite chemistry in physiology. The rate constant for reaction of CO_2 with $OONO^-$ is large (approximately 5.8×10^4 $M^{-1} \cdot s^{-1}$ depending on pH), and faster than the rate of direct reaction between peroxynitrite and biological target molecules such as ascorbate, glutathione, and urate (*57*). As a result, only a limited number of biomolecules can compete with CO_2 to scavenge peroxynitrite.

Nitrosoperoxycarbonate ($ONOOCO_2^-$) is the first intermediate formed by the reaction of $ONOO^-$ and CO_2 (Equation 1-7). This intermediate is very short-lived and decomposes to regenerate CO_2 and NO_3^- in ca. 70% yield (Equation 1-8), and produce the free radicals (in ca.

30% yield) $CO_3^{\bullet-}$ and $^{\bullet}NO_2$ (Equation 1-9) that are responsible for the oxidations and nitrations of many biological species (*58*).

$$ONOO^- + CO_2 \rightarrow ONOOCO_2^- \quad (1\text{-}7)$$
$$ONOOCO_2^- \rightarrow CO_2 + NO_3^- \quad (1\text{-}8)$$
$$ONOOCO_2^- \rightarrow CO_3^{\bullet-} + {}^{\bullet}NO_2 \quad (1\text{-}9)$$

The decomposition processes of nitrosoperoxycarbonate ($ONOOCO_2^-$) described above is postulated to undergo via a second intermediate, which is proposed to be the caged radicals (Figures 1-3). These caged radicals can break apart to give free radicals and react further with scavengers, or reform and give a new cage product (*57*).

Peroxynitrite vs. Uric Acid

It was proposed in 1990 that peroxynitrite exists *in vivo* (*59*). Under oxidative stress, peroxynitrite ($OONO^-$) can react with various biomolecules (*60*). It has been shown that peroxynitrite reacts with tyrosine residue to produce nitrotyrosine; this is major evidence for peroxynitrite-mediated cell damage (*61*). Furthermore, peroxynitrite can induce DNA base damage (*62*) and lipid peroxidation (*63*). The finding of the potential scavengers of peroxynitrite is important, and has become one of the most interesting topics in the field (*60*).

Among scavengers, uric acid is one of the most abundant in human. In many cases, its reaction with peroxynitrite has been reported to benefit the cells from peroxynitrite-mediated damage (*16*). In the mice model of experimental allergic encephalomyelitis (EAE), uric acid can block peroxynitrite activity by preventing the nitration of neuronal proteins (*64*). Interestingly, the protective properties of uric acid in EAE against peroxynitrite related chemical reaction is even more superior than ascorbic acid (*65*). Recently, uric acid was found to have a high potential to scavenge peroxynitrite (*24*). Peroxynitrite reacts with uric acid 16 times faster than with ascorbate, and 3 times quicker than with cysteine; however, to achieve the maximum

protection, ascorbate and cysteine must be present along with urate in scavenging of peroxynitrite (*24*).

As described in the previous topic, uric acid can become a pro-oxidant under a certain condition, by forming radicals after reacting with oxidants including peroxynitrite. Santos et al. observed a carbon-centered radical by ESR spin-trapping with the spin trap DMPO in reaction mixtures of uric acid and peroxynitrite (*36*). It was identified as the aminocarbonyl radical and its presence explained due to follow-up reactions between peroxynitrite and the primary reaction products such as alloxan and parabanic acid (*36*). The generation of the aminocarbonyl radical from urate was proposed to be responsible for amplified oxidation of LDL and liposomes.

Research Objectives

In recent years, Johnson et al. (*31,66-71*) demonstrated in a series of cell culture, animal, and human studies that uric acid may be a true risk factor for hypertension, kidney disease, and metabolic syndrome. A key issue is the upstream mechanism of how urate mediates these biological effects. It is thus important to know that when uric acid gives up an electron and proton as an anti-oxidant, it then becomes a urate radical (*32*) that can act as a pro-oxidant. A major question is whether the effects of uric acid to activate cells is due to the uric acid itself or to the urate radical, which is easily generated from uric acid in the presence of mild oxidative stress (*32,36*). This has led us to hypothesize that uric acid, particularly in the presence of oxidative stress, may convert to a urate radical or to an oxidative radical product of urate which could then activate cells contributing to the pathogenesis of hypertension, the metabolic syndrome, renal disease, and cardiovascular disease. Although the presence of the urate radical has been shown previously (*32,36*), as well as its ability to act as a pro-oxidant (*72-75*), to date there has been minimal study of the major urate radicals that are generated under physiological

conditions following reactions with oxidants, particularly as it relates to their structure, kinetics and possible mechanisms of generation.

Here we examined the reaction between urate and peroxynitrite using electron spin resonance (ESR) coupled with spin trapping as a primary tool to identify the radicals generated from this reaction. Moreover, the structure of the radical adduct was also characterized by LC-MS.

CHAPTER 2
RADICAL FORMATION FROM THE REACTION BETWEEN URIC ACID AND PEROXYNITRITE

Introduction

A comprehensive study of uric acid oxidation by peroxynitrite has been done by Santos et al (36). An apparent second order rate constant of this reaction has been determined ($k = 4.8 \times 102\ M^{-1} \cdot s^{-1}$), and oxygen consumption has been observed (36). The reaction was proposed to involve multiple interactions between uric acid and peroxynitrite, and generated various products including radicals. The radical formation has been claimed to be produced by the addition of peroxynitrite anion to the oxidation products that contain a carbonyl vicinal to aminocarbonyl group such as alloxan and parabanic acid. This assumption is unlikely because no radical was detected by ESR in incubations of peroxynitrite with those urate oxidation products in their study (36).

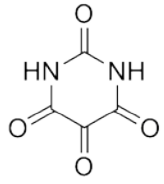

alloxan

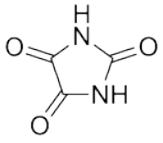

parabanic acid

Due to the complexity of the peroxynitrite-mediated oxidation of uric acid, its mechanism has not been well established. During our investigation to unfold the chemistry of uric acid when treated with peroxynitrite at pH 7.4, we discovered a novel urate-derived radical—triuretcarbonyl radical—which could be an intermediate for the production of the aminocarbonyl radical. The radicals were studied by electron spin resonance spectroscopy using spin trapping method, and PBN was used as a spin trapping agent. The structure of the PBN-radical adducts were characterized by liquid chromatography-mass spectrometry (LC-MS)

Materials and Methods

Chemicals. Uric acid was purchased from Sigma. Diethylenetriaminepentaacetic- acid (DTPA) was purchased from Fluka. N-tert-butyl-α-phenylnitrone (PBN) was obtained from Alexis Biochemicals. Peroxynitrite was synthesized following the method reported by Uppu and Pryor (*76*). The peroxynitrite concentration was measured spectrophotometrically at 302 nm (ε = 1670 M^{-1} cm^{-1}).

ESR Experiments. 100 mM stock solutions of uric acid (1) was prepared in 0.3 M potassium hydroxide. The reaction mixtures, typically conducted in 0.3-0.5 M potassium phosphate buffer at pH 7.4, contained the final concentration of 3 mM urate, 30 mM N-tert-butyl-α-phenylnitrone (PBN), 0.1 mM DTPA, and 9 mM peroxynitrite. Then, the reaction mixture was transferred into a quartz capillary of approximately 1×2 mm ID×OD for ESR measurement. After two minutes, the ESR spectrum was recorded at room temperature, using a commercial Bruker Elexsys E580 spectrometer, employing Bruker's high-Q cavity (ER 4123SHQE). Spectral parameters were typically: 100 kHz modulation frequency, 1 G or 0.1 G modulation amplitude, 20 mW microwave power, 9.87 GHz microwave frequency, 82 ms time constant, and 164 ms conversion time/point.

Sample Preparation for Liquid Chromatography-Mass Spectrometry. The reaction mixtures were prepared at room temperature in 0.3 M potassium phosphate buffer pH 7.4 and contained a final concentration of 10 mM uric acid, 30 mM PBN, 0.1 mM DTPA, and 30 mM peroxynitrite with the final volume of 10 mL. Then, the reaction mixtures were subsequently extracted by 2×20 ml of CH_2Cl_2, dried under nitrogen gas, and re-suspended in 1 mL CH_3CN.

Liquid Chromatography-Mass Spectrometry Analysis. The LC-MS analyses were carried out with an Agilent 1100 liquid chromatography system (Agilent Technologies, Palo

Alto, CA, USA) and an TSQ 7000 triple-quadruple mass spectrometer (ThermoFinnigan, San Jose, CA, USA) equipped with APCI interface operated in positive-ion mode detection. In a TSQ 7000 instrument, nitrogen was used as both the sheath and the auxiliary gases. The second quadrupole was used as a collision chamber, with argon as a collision gas, at a pressure in vicinity of 2.5×10^{-3} Torr. The operation of the LC-MS and data analyses was performed using the ThermoFinnigan Xcalibur 1.4 software.

Fullscan liquid chromatography-mass spectrometry. Liquid chromatography analyses were performed in a gradient elution mode using Phenomenex Luna 5µ C18(2) 100Å (150 mm × 4.6 mm) column (Phenomenex, Torrance, CA, USA) coupled with a Phenomenex Luna C18 (2), 5 µm particle size guard column. The mobile phase used included 5 mM ammonium acetate / 0.1 % acetic acid (A) and methanol (B) as a gradient. The mobile phase flow was 0.6 mL min-1, and the injection volume was 20 µL. The gradient began at 90% A. Composition was linearly ramped to 95% B over the next 10 min, remained constant for 3 min, then reversed to the original composition of 90% A over 1 min, after which it was kept constant for 1 min to re-equilibrate the column. The extracted reaction products, control samples and standard samples, were analyzed in the fullscan mode at a mass range of m/z 90-450.

Liquid chromatography-mass spectrometry tandem mass spectrometry analysis. LC analysis was performed as outlined above. The MS/MS analysis performed for M+1 ion 223 and 352 in the positive mode at a collision energy of 20V, with a mass scan range of m/z 40-230 for M+1 ion 223, and a mass scan range of m/z 45-360 for the latter.

Results

Electron Spin Resonance Spin Trapping. To probe the generation of the PBN-radical adducts at pH 7.4, the reaction between urate with peroxynitrite was monitored by ESR using spin trapping method. The reaction between urate and peroxynitrite resulted in a six-line ESR

spectrum (Figure 2-1A). The trapped radical adducts displayed the average hyperfine coupling constants a(N) = 15.6 G, and a(H) = 3.6 G. No trapped radicals were observed when the reactions were conducted without urate or peroxynitrite. PBN alone, or mixed with urate or peroxynitrite, did not yield any ESR signal (Figure 2-1C).

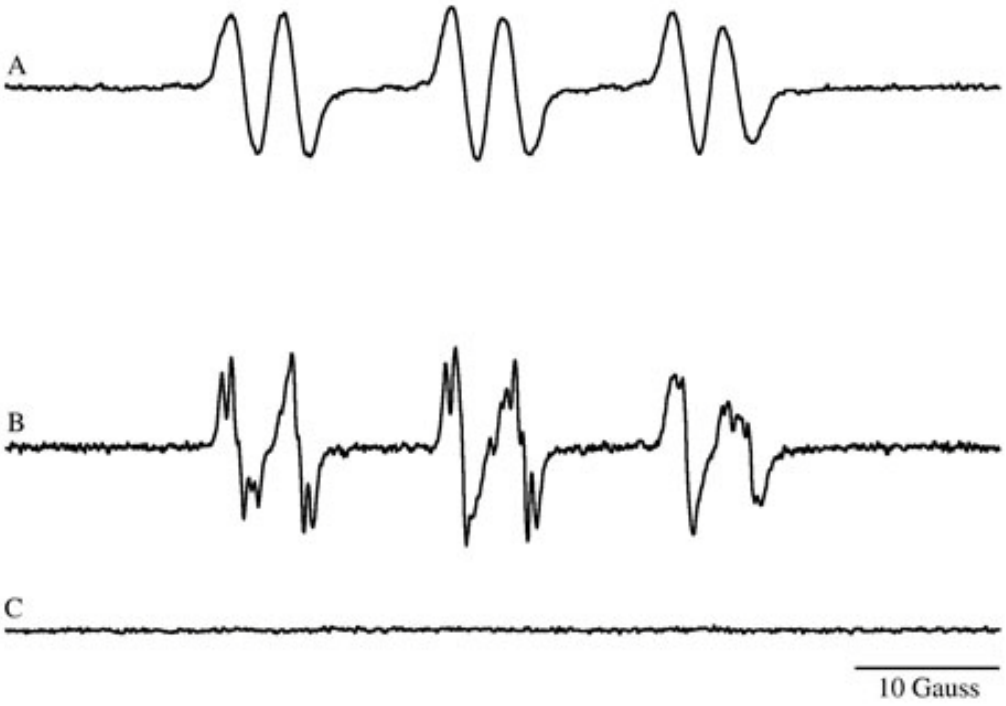

Figure 2-1. ESR spectra of PBN radical adducts obtained from the incubation of 3 mM urate, 30 mM N-tert-butyl-α-phenylnitrone (PBN), 0.1 mM DTPA, and 9 mM peroxynitrite in phosphate buffer pH 7.4. At room temperature, the ESR spectrum was recorded at 2 minutes after adding peroxynitrite. (A) The ESR spectrum of the PBN-radical adducts using spectral parameters at 100 kHz modulation frequency, 1 G modulation amplitude, 20 mW microwave power, 9.87 GHz microwave frequency, 82 ms time constant, and 164 ms conversion time/point. (B) The high resolution ESR spectrum of the PBN-radical adducts using spectral parameters at 100 kHz modulation frequency, 0.1 G modulation amplitude, 20 mW microwave power, 9.87 GHz microwave frequency, 82 ms time constant, and 164 ms conversion time/point. (C) The control reaction conducted in the same condition as described in (A) but without urate.

Furthermore, the ESR intensities increased when the urate concentration was increased (Figure 2-2). These experiments confirmed that the observed radicals were derived from urate, not artifacts. Moreover, when the experiment was performed at higher resolution (lower modulation amplitude), we found that PBN could trap at least two different carbon-based radicals (Figure 2-1B). The radical formation increased with the concentration of peroxynitrite, but yielded maximum at a four-fold molar excess of peroxynitrite over urate (Figure 2-3).

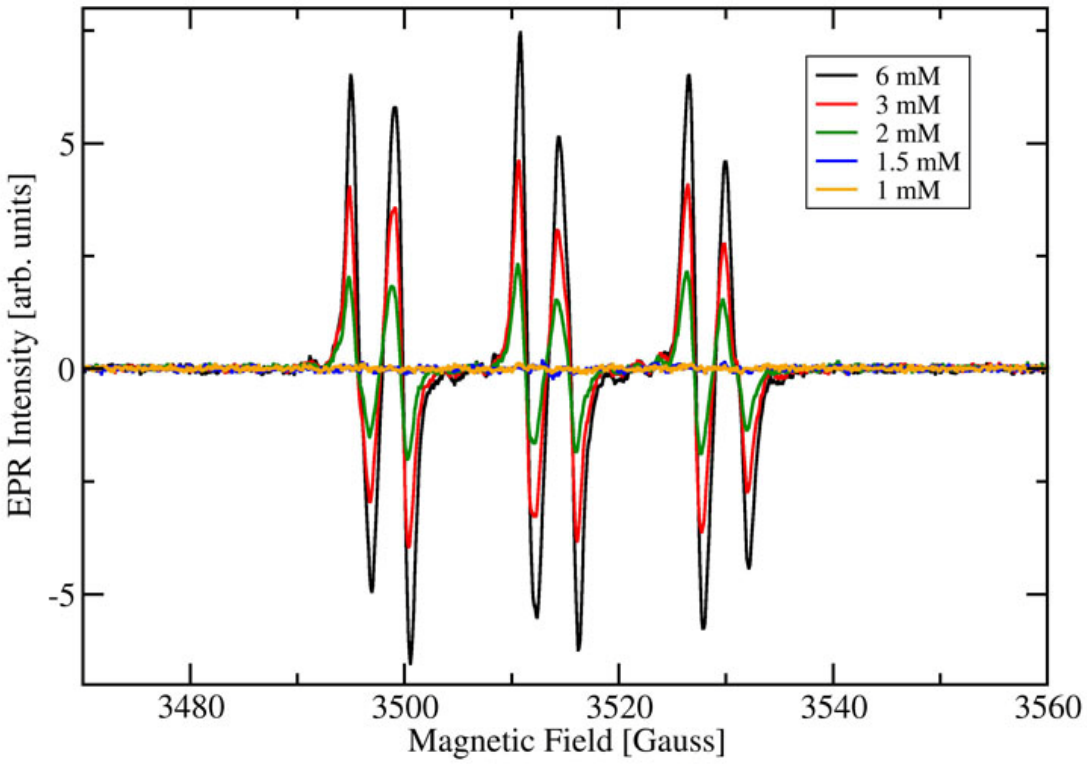

Figure 2-2. Effect of urate concentration on the production yield of the PBN-radical adduct derived from urate obtained from the oxidation of urate by peroxynitrite. The ESR spectra were recorded after 2 min of incubation of various urate concentraions, 19 mM N-tert-butyl-α-phenylnitrone (PBN), 0.1 mM DTPA, and 23 mM peroxynitrite in 0.3 M phosphate buffer pH 7.4. The instrumental parameters were 100 kHz modulation frequency, 0.5 G modulation amplitude, 20 mW microwave power, 9.87 GHz microwave frequency, 82 ms time constant, and 164 ms conversion time/point.

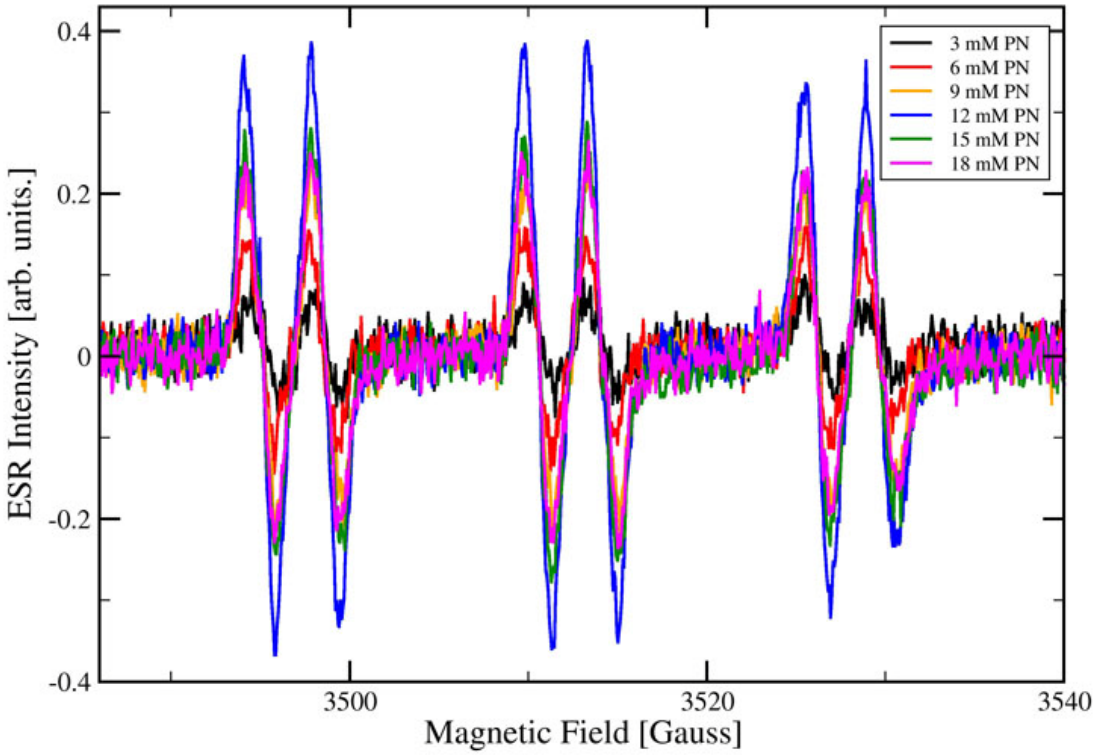

Figure 2-3. Effect of peroxynitrite concentration on the production yield of the PBN-radical adduct derived from urate obtained from the oxidation of urate by peroxynitrite. The ESR spectra were recorded after 2 min of incubation of 3 mM urate, 30 mM N-tert-butyl-α-phenylnitrone (PBN), 0.1 mM DTPA, and various concentrations of peroxynitrite in 0.5 M phosphate buffer pH 7.4. The instrumental parameters were 100 kHz modulation frequency, 1 G modulation amplitude, 20 mW microwave power, 9.87 GHz microwave frequency, 20 ms time constant, and 82 ms conversion time/point.

Depending on pH, both uric acid and peroxynitrite can exist in either neutral or anion form. Therefore, the radical formation should be affected by pH as well. Indeed, the pH profiles show that the urate-peroxynitrite reaction yielded more trapped radicals when pH increased (Figure 2-4). This indicates that the radicals may not be produced by the direct reaction between peroxynitrous acid or its decomposition products with uric acid. The simulated ESR titration curve obtained a better fitting when the initial pHs of the buffers were used. Although the final pHs of the solutions were preferred, we have not been able to find proper parameters to fit the

data obtained from the shifted pHs. Nevertheless, both pH profiles exhibited the same results; the yield of radical adducts increased with pH. The obtained pH sigmoidal curve shows an inflection point of 8.1, which is near the pKa of peroxynitrous acid determined previously by Kissner et al. (*47*).

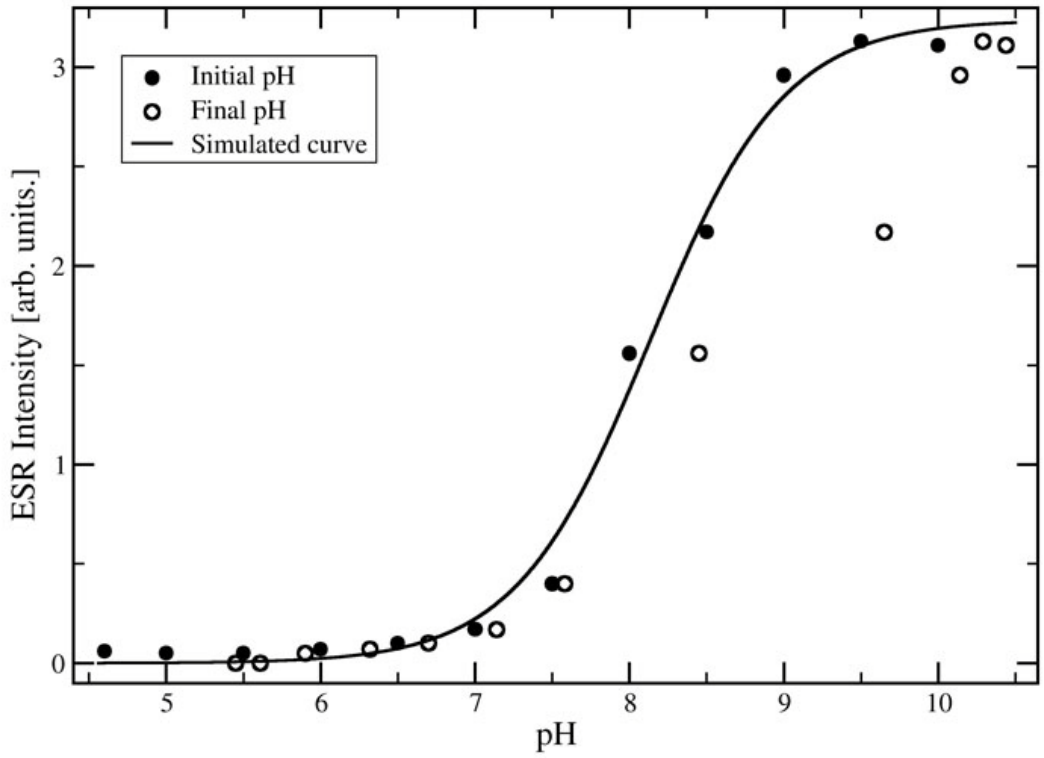

Figure 2-4. Effect of pH on the production yield of the PBN-radical adduct derived from urate obtained from the oxidation of urate by peroxynitrite. The ESR spectra were recorded after 2 min of incubation of 3 mM urate, 30 mM N-tert-butyl-α-phenylnitrone (PBN), 0.1 mM DTPA, and 9 mM peroxynitrite in 0.5 M phosphate buffer at various pHs. The instrumental parameters were 100 kHz modulation frequency, 1 G modulation amplitude, 20 mW microwave power, 9.87 GHz microwave frequency, 20 ms time constant, and 82 ms conversion time/point. The measured ESR intensities corresponded to the first PBN-radical adduct peak to peak heigthts.

In addition to the effect of pH, we have investigated the effect of CO_2 on the production of radical adducts. The administration of CO_2 decreased the observed ESR signals (Figure 2-5). Interestingly, a four-fold excess of bicarbonate over peroxynitrite was required to completely prevent the formation of the radical adducts. This is probably because the reactions were not

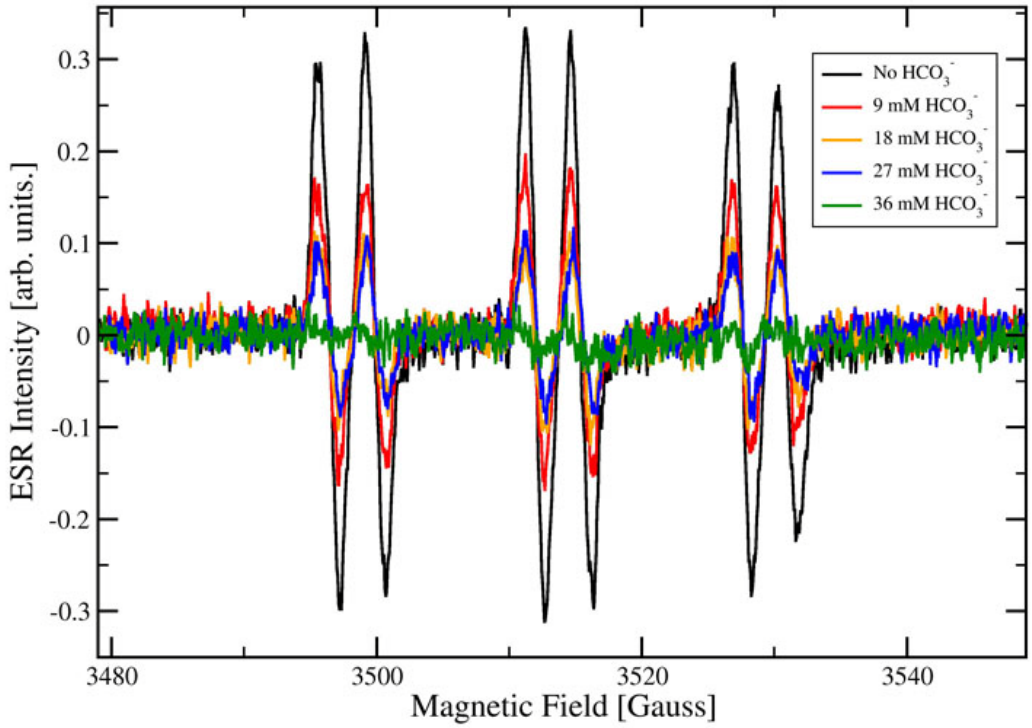

Figure 2-5. Effect of CO_2 on the production yield of the PBN-radical adduct derived from urate obtained from the oxidation of urate by peroxynitrite. The ESR spectra were recorded after 2 min of incubation of 3 mM urate, 30 mM N-tert-butyl-α-phenylnitrone (PBN), 0.1 mM DTPA, and 9 mM peroxynitrite in 0.5 M phosphate buffer at pH 7.4 in the present of various concentrations of bicarbonate (HCO_3^-). The instrumental parameters were 100 kHz modulation frequency, 1 G modulation amplitude, 20 mW microwave power, 9.87 GHz microwave frequency, 82 ms time constant, and 164 ms conversion time/point.

conducted in the gas-tight system. Therefore, some carbon dioxide gas could escape the reaction mixtures. As a result, the excess amount of bicarbonate is required in order to completely quench peroxynitrite.

Product Identification of the Radical Adducts by Liquid Chromatography-Mass Spectrometry Analysis. From the reaction between urate and peroxynitrite in phosphate buffer pH 7.4, the extracted radical adducts were separated and characterized by liquid chromatography coupled with mass spectrometry (LC-MS). After comparison with the control reaction (Figure 2-6B)—the reaction without urate—the fullscan LC-MS showed two products, at the retention time

of 10:56 minutes corresponding to the quasi ions at m/z 223; and at 13:13 minutes corresponding to the quasi ion at m/z 352 (Figure 2-6A). As displayed in Figure 2-6A and 2-6B, the large area of the LC traces at the retention time stating from 11.12 minutes to 15.00 minutes belonged to the mass derived from PBN (M+1 = 178), and the small peak at 9 minutes was consistent with benzaldehyde oxime (M+1 = 122), which is the decomposition product of PBN.

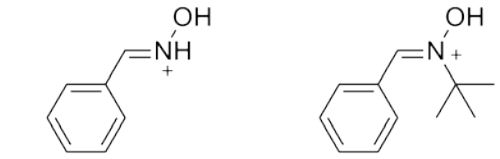

benzaldehyde oxime
$[M+1]^+ = 122$

PBN
$[M+1]^+ = 178$

In addition to the fullscan, the ions at m/z 223 and 352 were selected and analyzed by tandem mass spectrometry (MS/MS). At m/z 223, the following ions were identified: m/z (% intensity): 223 (4%; M+1), 167 (30), 149 (29), 134 (12), 132 (5), 122 (24) and 104 (100%), see Figure 2-7, and the fragment of m/z 352 exhibited the following ions m/z (% intensity): 352 (2%; M+1), 335 (13%), 296(33), 279(25), 263 (100), 246 (83), 218 (7), 193(12), 177(24), 175 (22), 167 (9), 147(24), 122(8), 118 (6), 104 (9); and 61 (1), see Figure 2-8.

Discussion

Spin trapping allows the trapping of short lived radicals with a more stable radical adduct, thereby allowing analysis. It is the method of choice to study short-lived radical intermediates (*77*). The identification of the radical adducts and their proposed formation mechanism from the peroxynitrite-urate reaction will be discussed.

The first spin-trapping studies on urate-derived radicals were reported by Santos et al. on the peroxynitrite-urate system (*36*). A carbon-centered radical was trapped with the spin trap

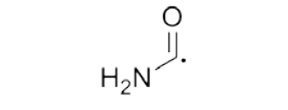

DMPO (Figure 1-1) and analyzed by CW-ESR. It was tentatively identified as an aminocarbonyl radical.

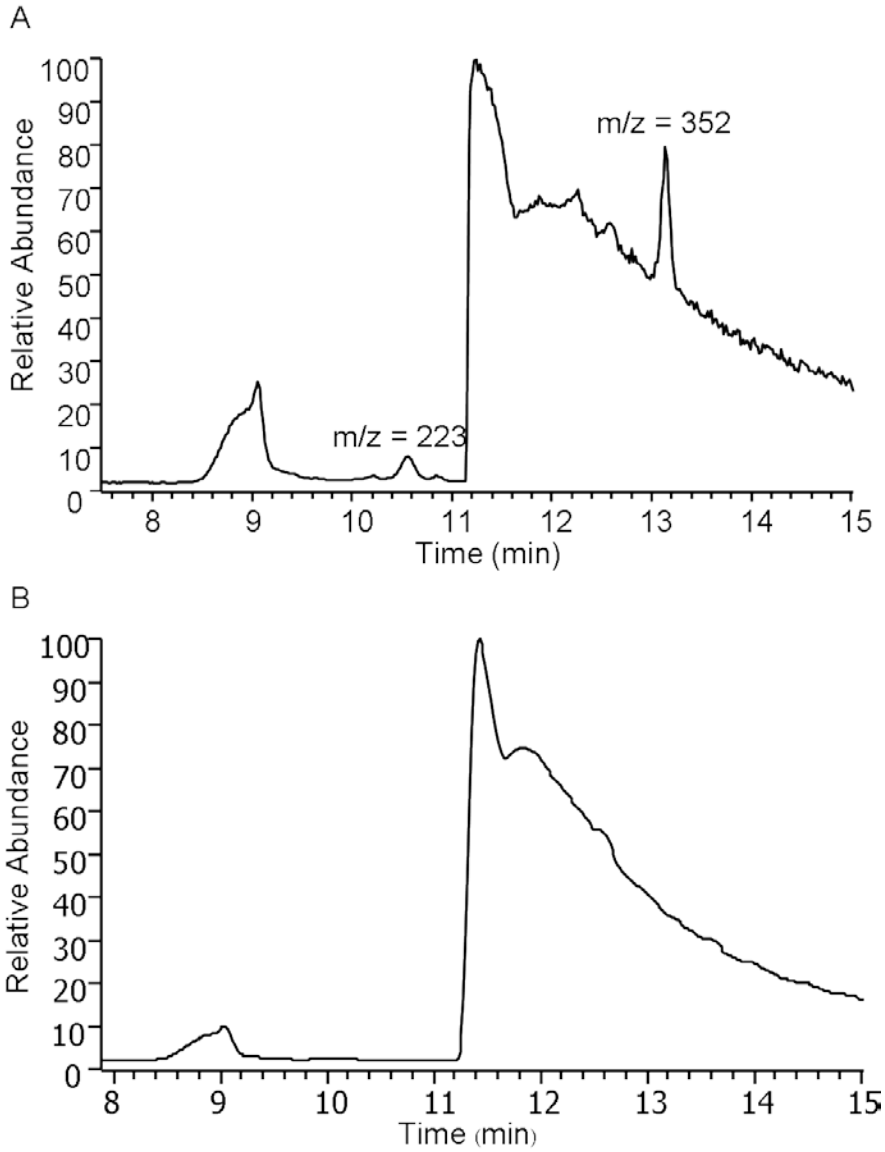

Figure 2-6. LC-MS study of the reaction between urate and peroxynitrite in phosphate buffer pH 7.4. Before submitting to LC, the reaction products were extracted by methylene chloride (CH_2Cl_2), dry under nitrogen gas, and resuspended in acetronitrile. (**A**) LC chromatogram of 10 mM urate treated with 30 mM peroxynitrite in the presence of 30 mM PBN and 0.1 mM DTPA. (**B**) LC chromatogram of the control reaction, which every reagent contained the same concentration as described in a) but without urate.

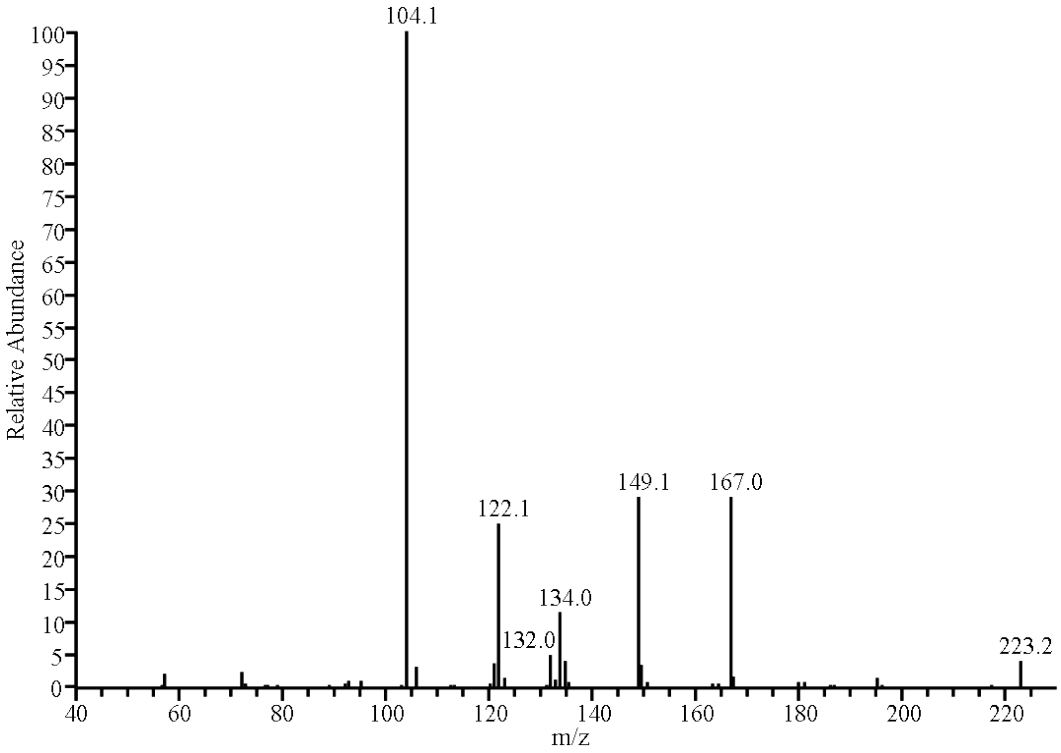

Figure 2-7. MS/MS spectrum of the PBN-aminocarbonyl radical adduct.

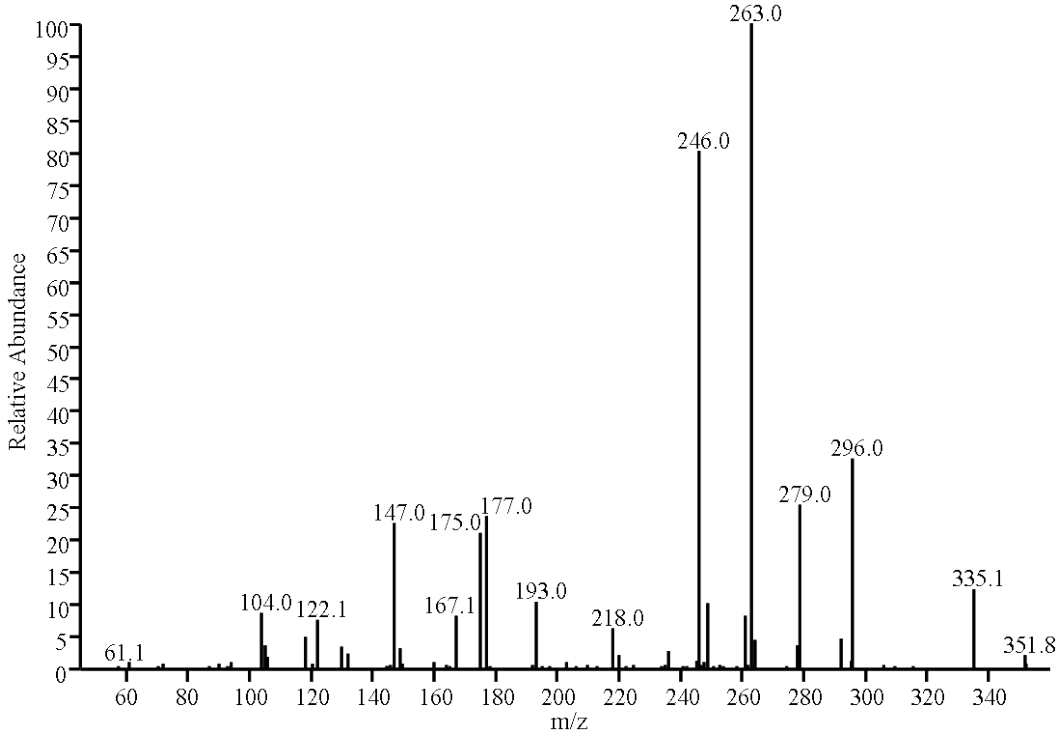

Figure 2-8. MS/MS spectrum of the PBN-triuretcarbonyl radical adduct.

Unlike reported by Santos et al (i.e., only spin trapping agent DMPO gave stable radical adducts) (*36*), our experiment showed that PBN could trap at least two radicals. After a comparison with data reported in a review by Buettner (*9*), the PBN adducts were found to belong to carbon-centered radicals. The information from ESR spectra only gave a rough estimation of the type of trapped radicals. Thus, the LC-MS analysis was performed to acquire more structural information of the radical adducts. The fullscan LC-MS study showed two distinctive products with m/z 223 (M+1) and 352 (M+1), which were absent in the control reaction (Figure 2-6).

The analysis of the LC-MS/MS spectra (Figure 2-7 and 2-8) revealed that both ions showed the same initial fragment loss of a neutral compound with a molecular weight (MW) of 56, corresponding to the loss of 2-methylpropene ($[M+H-C_4H_8]^+$). This fragment loss could be originated from the cleavage of tert-butyl group from the PBN moiety. Moreover, the fragmentation pattern of both parent ions contained the same fragment daughter ion at m/z 122. This ion was identified as benzaldehyde oxime (Figure 2-9 and 2-10), which was converted from PBN as well. These results indicated that both parent ions were derived from PBN. Furthermore, the loss of formamide (MW 45), in both 223 and 352 ions, and isocyanic acid (HNCO, MW 43), in the case of 352 ion, indicated that at least one amide group was present in both compounds. This hypothesis is further supported by the loss of ammonia (MW 17) in both 223 and 352 ions, which reflects that the parent compounds have a functional group that contained a primary amine such as amide. Based on the observations described above, the MS/MS fragmentation analysis confirmed that the structure of the product corresponding to m/z 223 was consistent with the hydroxylamine form of the PBN-aminocarbonyl radical adduct **2** (Figure 2-11), and the structure corresponding to m/z 352 was proposed to be the hydroxylamine form of the PBN-

triuretcarbonyl radical adduct **3** (Figure 2-11). The existence of triuret moiety in compound **3** is confirmed by the fragment ions at m/z 147, 104, and 61(Figure 2-10), which is a signature fragmentation pattern of triuret (M+1 = 147) (*25*).

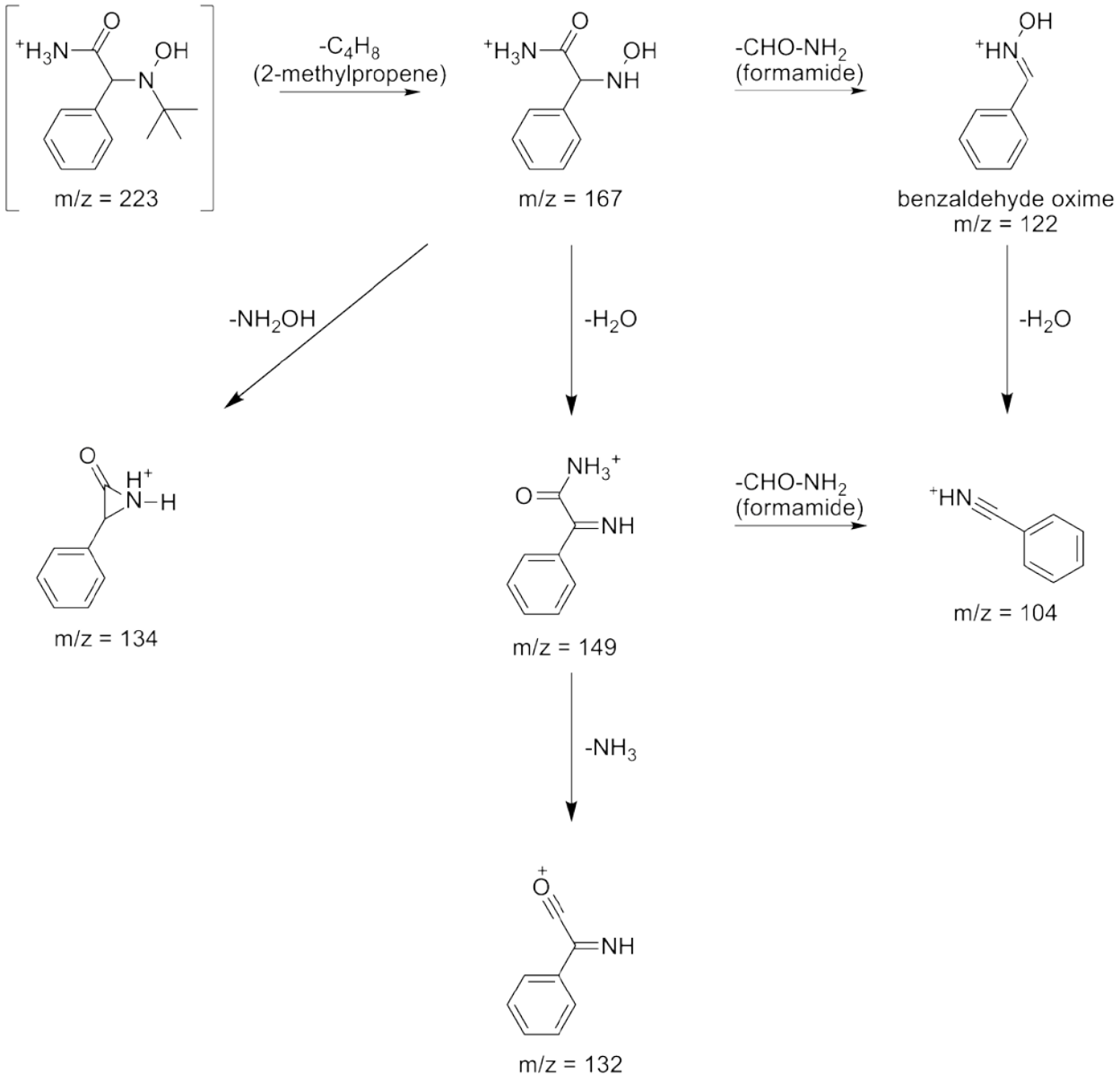

Figure 2-9. Fragmentation pattern of the hydroxylamine form of PBN-aminocarbonyl radical adduct.

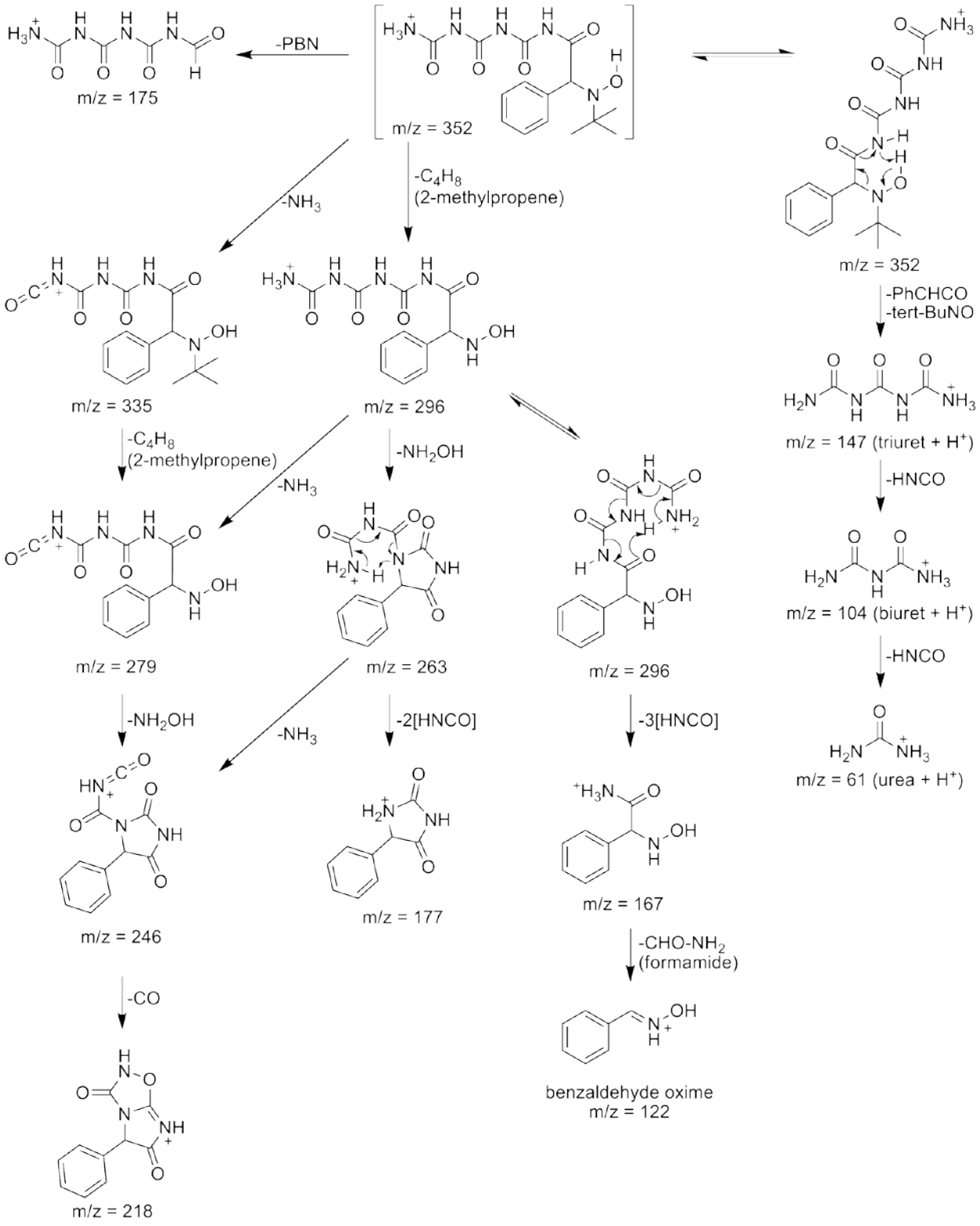

Figure 2-10. Fragmentation pattern of the hydroxylamine form of PBN-triuretcarbonyl radical adduct.

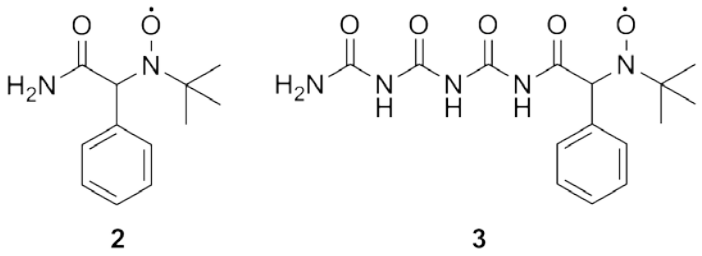

Figure 2-11. The structures of PBN-radical adducts of aminocarbonyl radical **2**, and triuretcarbonyl radical **3**.

Although the aminocarbonyl radical has been previously characterized, little is known about its formational mechanism. Many possible pathways have been proposed for the generation of aminocarbonyl radical. Santos et al. suggested that the aminocarbonyl radical was produced from one of the products of a urate-peroxynitrite reaction, such as alloxan, parabanic acid, or allantoin (*36*). Robinson et al. later suggested that triuret, a novel product from peroxynitrite-induced oxidation of urate, could be accounted for the detection of aminocarbonyl radical (*25*). These hypotheses, however, is unlikely because we have tested the reaction of these products with peroxynitrite under the same condition as the oxidation of urate, and we did not observe any radical adduct formation. Our observation indicated that aminocarbonyl radical was not derived from these known urate-derived products.

In our study, the trapping of radical adduct **3** led us to postulate that triuretcarbonyl radical **12** can be an intermediate for the production of aminocarbonyl radical **13**, and their formations are proposed as depicted in (Figure 2-12). At pH 7.4, peroxynitrite, which its pKa is about 6.8, can exist as a mixture of peroxynitrite anion, peroxynitrous acid, or its decomposition products (*25*,*46*). We propose that urate is oxidized via one electron transfer by peroxynitrous acid, forming urate radical **4** (Equation 2-1 to 2-2). Because we did not observe the PBN-OH radical adduct, so the electron is likely transferred to oxygen of the hydroxyl moiety of peroxynitrous acid, forming a hydroxide ($^{-}$OH) and a nitrogen dioxide radical ($NO_2^{\bullet}$) (Equation 2-2).

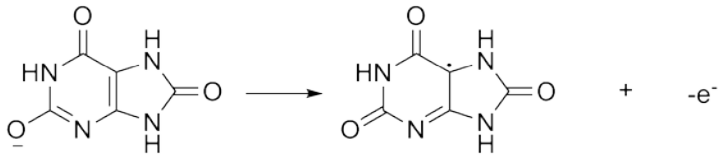

(2-1)

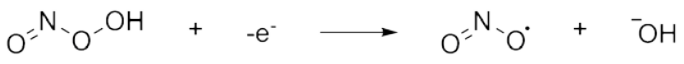

(2-2)

Then diimine **5**, an oxidative intermediate of uric acid described in many urate oxidation studies (*26*,*36*), can be produced by one electron and one proton transfer from urate radical **4** to peroxynitrous acid. This second electron oxidation can be initiated by nitrogen dioxide radical (NO_2•), which is a decomposition product of peroxynitrous acid (Equation 2-2), as well because of its strong oxidizing potential (*46*). In contrast to some studies (*25*,*33*), the dehydrourate (with its structure depicted in Figure 1-2) is unlikely to be formed because it is antiaromatic molecule. Therefore, we propose that the intermediate of the second electron transfer from urate is diimine **5**. The diimine **5** is susceptible to nucleophilic addition and can rapidly react with nucleophile such as water or ammonia (*26*). Peroxynitrite anion has been reported to undergo nucleophilic addition in the reaction with diacetyl (*78*) and cyclicquinone (*79*). Moreover, our pH dependence experiments show that the radical formation was increased when pH was raised (Figure 2-4), and decreased when CO_2 was present (Figure 2-5). This result indicates that peroxynitrite anion is responsible for the production of radicals by reacting with an intermediate, initially formed from the oxidation of original urate. Taken together, we thus propose that peroxynitrite anion can react with diimine **5** to produce peroxo adduct **6**. After undergoing homolysis of the O-O bond (*78*), the peroxo adduct **6** decomposes to yield nitrite and radical intermediate **7**, which then rearranges to form carbonyl radical **8**. The carbonyl radical **8** can be converted to radial **9** by either losing carbon monoxide (CO) or reacting with O_2 and releasing carbon dioxide (CO_2). Another molecule of peroxynitrite anion may react with intermediate **10**, which is produced by reduction

of compound 9, to generate allantoin-peroxo adduct **11**. The multi-molar equivalent consumption of peroxynitrite leading to the radical formation was supported by our observation that the yield of radical formation was at maximum when a four-fold excess peroxynitrite over urate was used (Figure 2-3). By analogy similar to the degradation of **6**, triuretcarbonyl radical **13** is obtained. The β-cleavage of triuretcarbonyl radical **13** yields isocyanic acids and aminocarbonyl radical **14**, which is subsequently trapped by PBN (Figure 2-12).

Aside from being the intermediate for aminocarbonyl radical, triuretcarbonyl radical could be an intermediate candidate for the generation of triuret **15** as well (Figure 2-11). This hypothesis was supported by our observation that no triuret was observed when the reaction mixtures contained PBN. This indicates that PBN could quantitatively trapped the triuretaminocarbonyl radical, preventing the formation of triuret.

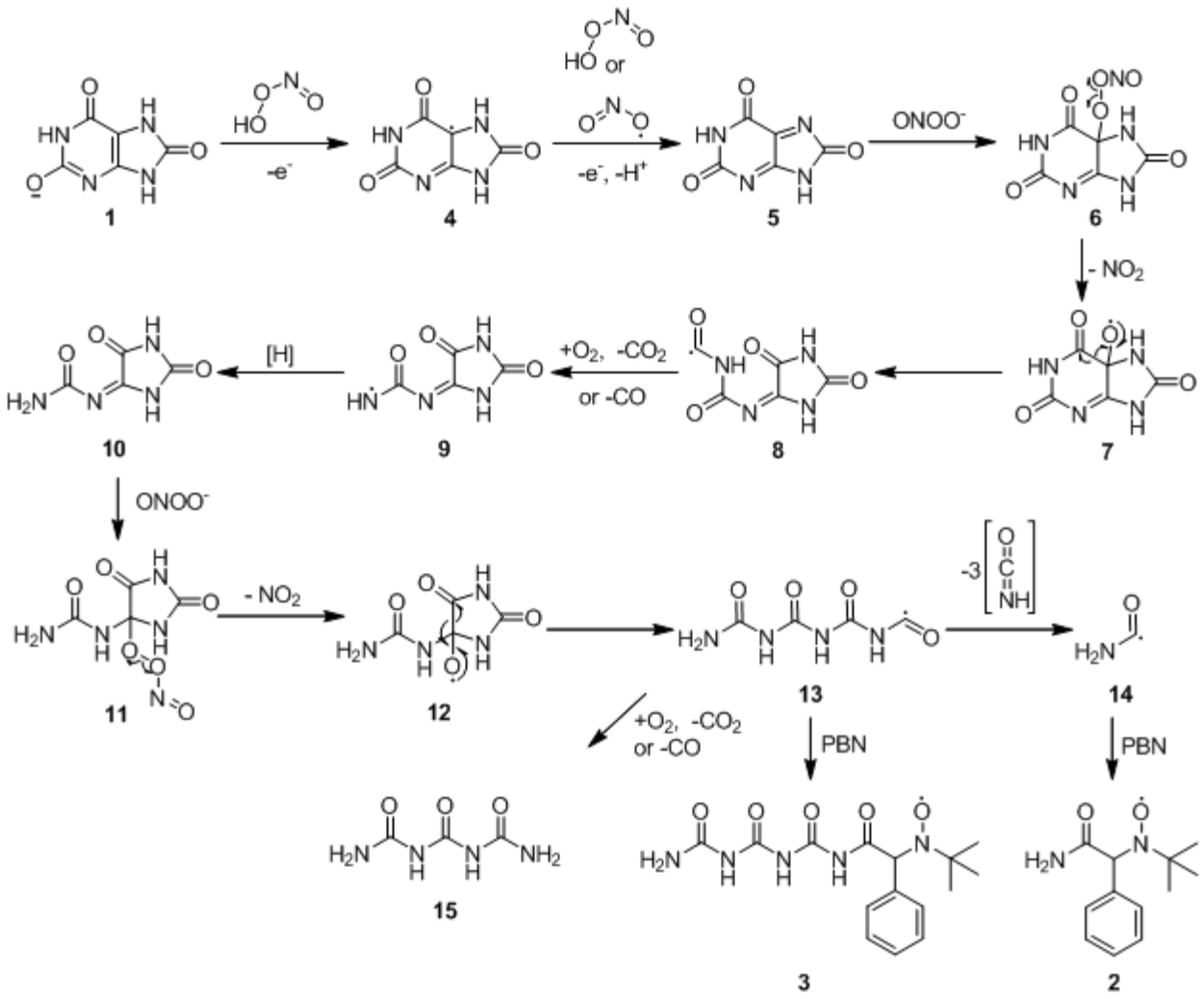

Figure 2-12. Proposed radical formation mechanism of the reaction between urate and peroxynitrite.

CHAPTER 3
REACTIONS OF PEROXYNITRITE WITH MONO-, DI-, AND TRI-METHYLURIC ACIDS STUDIED BY LIQUID CHROMATOGRAPHY-MASS SPECTROMETRY AND ELECTRON SPIN RESONANCE SPECTROSCOPY

Introduction

Uric acid is a purine degradation product from RNA, DNA and adenine nucleotides (*16*). Several isomers of methyluric acid are also commonly present *in vivo* and are derived from the metabolism of methylated purines such as caffeine, theobromine, theophylline, and plant methylxanthines (*80*).

Methyluric acids can attain significant concentrations in vivo, and have even been reported to cause kidney stones in subjects who are heavy coffee consumers (*81*). Indeed, Safranow and Machoy reported that methylated uric acids are found in all uric acid stones (*82*). Nevertheless, unlike the role of uric acid in quenching peroxynitrite mediated reactions, which is well established, less is known about the reaction of peroxynitrite with methyluric acids. In previous studies, depending on the reaction condition and the sources of the oxidants, the methylation at certain nitrogen positions in uric acid has been reported to affect the reactivity of uric acid (*83*,*84*). 1,3-Dimethyluric acid and 1,3,7-trimethyluric acid were found to have higher potency than uric acid to prevent lipid peroxidation in human erythrocyte membranes (*85*-*87*). However, when N-7 was methylated, the reactivity of uric acid toward the oxidation by 1,1-diphenyl-2-picrylhydrazyl (DPPH) radical was markedly decreased (*84*). The radicals derived from uric acid and its methyl derivatives upon photolysis in the presence of mild oxidants (not including peroxynitrite) have been investigated by ESR spectroscopy and calculation study (*88*). The radicals were proposed to be formed by hydrogen abstraction mechanism (*88*). The pK_a values of the corresponding N-methyluric acid radical-anions were determined to be in the range of 9.7-

11.2, and the intrinsic acidity of the N-H protons in both neutral and radical-anion forms was calculated to follow the order N1H < N9H < N3H (*88*).

We therefore examined the reactivity of various methyluric acids with peroxynitrite using liquid chromatography-mass spectrometry (LC-MS) and electron spin resonance (ESR) spectroscopy, a) to understand the reactivity of these biologically significant molecules with peroxynitrite and b) to test the hypothesis that methylation at N-7 might interfere with the oxidative reaction. This report shows the radical formations and reaction products generated from seven commercially available methyluric acids (Figure 3-1) upon reaction with peroxynitrite in phosphate buffer pH 7.4. The radicals formed from these reactions were investigated by ESR spin trapping method, using PBN as the spin trapping agent, and the reaction products were identified by LC-MS. In an attempt to probe the intermediates in these reactions we have incorporated methanol into the reaction mixtures to investigate if methanol could trap any intermediates generated during the course of the reactions, which were monitored by LC-MS.

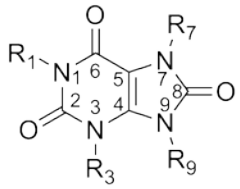

1

a: R_1, R_3, R_7, R_9 = H; **b:** R_1 = CH_3; R_3, R_7, R_9 = H;
c: R_1, R_3, R_7 = H; R_9 = CH_3; **d:** R_1, R_3 = CH_3; R_7, R_9 = H;
e: R_1, R_7 = CH_3; R_3, R_9 = H; **f:** R_1, R_9 = CH_3; R_3, R_7 = H;
g: R_1, R_9 = H; R_3, R_7 = CH_3; **h:** R_1, R_3, R_7 = CH_3; R_9 = H.

Figure 3-1. Structures of uric acid, monomethyluric acid, dimethyluric acid, and trimethyluric acid

Materials and Methods

Chemicals. Shown in Figure 3-1 are the different methylated uric acid compounds used. Uric acid (UA, **1a**), 1,3-dimethyluric acid (1,3-DiMeUA, **1d**) and 9-methyluric acid (9-MeUA,

1c) were purchased from Sigma. 1-Methyluric acid (1-MeUA, **1b**), 1,7-dimethyluric acid (1,7-DiMeUA, **1e**), 1,9-dimethyluric acid (1,9-DiMeUA, **1f**), 3,7-dimethyluric acid (3,7-DiMeUA, **1g**), and 1,3,7-trimethyluric acid (1,3,7-TriMeUA, **1h**) were purchased from Fluka. The d_4-methanol was purchased from Cambridge Isotopes. Distilled, deionized water (metal ion free) and EDTA (500 mM) were purchased from Gibco. Peroxynitrite, used in the experiments containing methanol, was purchased from Cayman Chemical. For the experiments conducted in phosphate buffer, peroxynitrite was synthesized following the method reported by Uppu and Pryor (*76*). The peroxynitrite concentration was measured spectrophotometrically at 302 nm (ε = 1670 M^{-1} cm^{-1}). To ensure the same reactivity, both sources of peroxynitrite reacted with uric acid in the same reaction conditions; the same reaction products, determined by LC-MS, were obtained.

ESR Spin Trapping Experiments. 100 mM stock solutions of uric acid (**1a**) and selected methyl derivatives of uric acids; namely, 1-methyluric acid (**1b**), 9-methyluric acid (**1c**), 1,3-dimethyluric acid (**1d**), 1,7-dimethyluric acid (**1e**), 1,9-dimethyluric acid (**1f**), 3,7-dimethyluric acid (**1g**), and 1,3,7-trimethyluric acid (**1h**) were prepared in 0.3 M potassium hydroxide. The reaction mixtures, conducted in 0.3 M potassium phosphate buffer at pH 7.4, contained the final concentration of 3 mM urate (or its analogues), 30 mM N-tert-Butyl-α-phenylnitrone (PBN), 0.1 mM DTPA, and 9 mM peroxynitrite. Then, the reaction mixture was transferred into a quartz capillary of approximately 1×2 mm ID×OD for ESR measurement. After two minutes, the ESR spectrum was recorded at room temperature using a commercial Bruker Elexsys E580 spectrometer, employing Bruker's high-Q cavity (ER 4123SHQE). Spectral parameters were typically: 100 kHz modulation frequency, 1 G modulation amplitude, 20 mW microwave power, 9.87 GHz microwave frequency, 82 ms time constant, and 164 ms conversion time/point.

Product Identification of the Reactions Conducted in Phosphate Buffer. Each reaction sample, conducted in 0.5 M phosphate buffer pH 7.4, contained the final concentration of 10 mM uric acid (or its methyl analogues), 0.1 M DTPA and 30 mM peroxynitrite. Then, the reaction mixtures were placed on ice, transferred to LC-MS vials on ice, and stored at 4°C to await LC-MS analysis.

The reaction mixtures were analyzed by LC-MS in the positive fullscan (both negative and positive) mode using electrospray ionization (ESI) method. This enabled us to detect the positive ions (mass range *m/z*: 50.0-900.0) as well as the fragmentation pattern of each intermediate, or product. The TSQ Quantum Discovery mass spectrometer (ThermoFinnigan, San Jose, CA, USA) and a ThermoFinnigan Surveyor liquid chromatography system (ThermoFinnigan, San Jose, CA, USA) was equipped with a Phenominex Luna C18 column (250x4.6 mm). To minimize the decomposition of labile intermediates, samples were kept cold until analysis. The mobile phases included 5mM NH_4OAc/0.1% AcOH and methanol (as gradient). Typical HPLC analyses were carried out in a gradient elution mode, using an aqueous mobile phase A (5 mmol/L ammonium acetate and 0.1% by volume of AcOH in water) and MeOH as organic mobile phase B. Mobile phase flow was 0.6 mL/min and the injection volume was 10 μL. The HPLC run time was 16 min and the gradient used was as follows: the gradient began at 85% A. The composition was linearly ramped to 10% A over the next 9 min and remained constant for 3 min, and reversed to the original composition of 85% A over 2 min, after which it was kept constant for 2 min to reequilibrate the column.

In the Quantum Discovery mass spectrometer, nitrogen was used as both the sheath (40 psi) and the auxiliary (15 units) gas. The spray voltage was 4000 V. The heated capillary temperature was maintained at 300 °C. The collision pressure was 1.5×10^{-3} Torr. The operation

of the LC-MS and data analyses was performed using the ThermoFinnigan Xcalibur 1.4 software.

Product Identification of the Reactions Conducted in Methanol. Each reaction sample contained the final concentration of 10 mM uric acid (or its methyl analogues) and 10 mM peroxynitrite in a mixed solvent of 50% alcohol (methanol or d_4-methanol) and 50% aqueous phosphate buffer solution at pH 7.4. Uric acid, or its methyluric acid powder, was added to alcohol/aqueous solution. Under this condition, uric acid only partially dissolved. However, after one equivalent of peroxynitrite was added to the reaction mixture, agitated, and allowed to incubate at room temperature for 3 min, uric acid dissolved completely as the reaction proceeded. Then, the reaction mixtures were placed on ice, transferred to LC-MS vials on ice, and stored at -80°C to await LC-MS analysis.

The reaction mixtures were analyzed by LC-MS in the fullscan (both positive and negative), tandem mass spectrometry (MS/MS), and single reaction monitoring (SRM) modes, using the atmospheric pressure chemical ionization (APCI) method. In addition, some samples were further analyzed using the electrospray ionization (ESI) method. This enabled us to detect both positive and negative ions, as well as the fragmentation pattern of each intermediate or product. The LC-MS analyses were performed using a Finnigan triple quadrupole mass spectrometer model TSQ 7000 and an Agilent quaternary pump HPLC model 1100, equipped with a Phenominex Luna C18 column (either 150 or 250x4.6 mm). To minimize the decomposition of labile intermediates, samples were kept cold until analysis. The mobile phases, used in the LC separation of the uric acid reaction products, included NH_4OAc/AcOH and methanol (as gradient), formic acid/methanol gradient, or NH_4OAc/AcOH/acetonitrile gradient. Typical HPLC analyses were carried out in a gradient elution mode using an aqueous mobile

phase A (5 mmol/L ammonium acetate and 0.1% by volume of AcOH in water) and MeOH as organic mobile phase B. Mobile phase flow was 0.6 mL/min. Two typical HPLC gradients used are as follows:

Gradient 1 (10 min HPLC run): the gradient began at 90% A. The composition was linearly ramped to 75% A over the next 9 min, then remained constant for 0.5 min, and then reversed to the original composition of 90% A over 0.5 min.

Gradient 2 (16 min HPLC run): the gradient began at 95% A. The composition was linearly ramped to 80% A over the next 9 min and to 10% A over the next 3 min, then remained constant for 2 min, and reversed to the original composition of 95% A over 1 min, after which it was kept constant for 1 min to reequilibrate the column.

Evaluation of the molecular weight and fragmentation patterns of the intermediates and products was performed using the mass spectrometer after the compounds had been separated on the LC column. The mobile phase flow was 0.6 mL/min, and the injection volume was 20 μL. Uric acid concentrations were determined in SRM mode using an APCI source in the negative mode. For uric acid, reactions were monitored at the m/z 166.9→95.9 and 166.9→123.9 using 25V. In the TSQ 7000 instrument, nitrogen was used as both the sheath (80 psi) and auxiliary (10 units) gases. In the APCI mode, the vaporizer was kept at 500°C, and the heated capillary temperature was maintained at 200°C. The corona current was set to 3 kA by applying approximately 4 kV to the corona needle. The second quadrupole was used as a collision chamber with argon as a collision gas at a pressure around 2.5×10^{-3} Torr. The LC-MS/MS ran on Xcalibur software, which is a flexible Windows NT PC-based data acquisition system that allowed complete instrument control. The operations of the LC-MS and data analyses were performed using the ThermoFinnigan Xcalibur software.

In addition to the fullscan LC-MS analyses, MS/MS experiments, at 15 and 25 V, were also conducted for M+1 ions (m/z 230.9, 245, 259), the mass corresponding to the uric acid (and its mono-, di-, and tri-methyl isomers) glycol dimethyl ethers.

Results

Electron Spin Resonance Spin Trapping. At pH 7.4, the ESR spectra obtained from the reactions of urate and its analogues with peroxynitrite are shown in Figure 3-2.

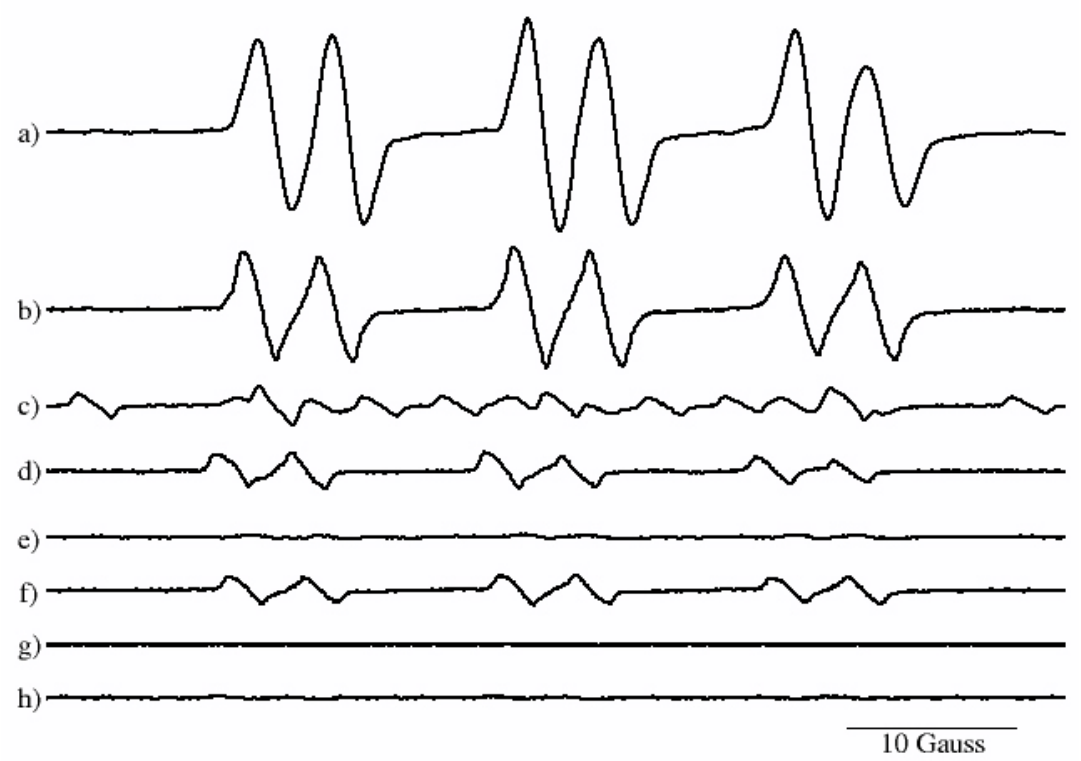

Figure 3-2. ESR spectra of the PBN-radical adducts from the reaction between uric acid and its methyl derivatives with peroxynitrite. The reaction mixture contained 3 mM uric acid or its analogues, 0.1 mM DTPA, 30 mM PBN and 9 mM peroxynitrite in 0.3 M phosphate buffer pH 7.4. (a) uric acid **1a**, (b) 1-methyluric acid **1b**, (c) 9-methyluric acid **1c**, (d) 1,3-dimethyluric acid **1d**, (e) 1,7-dimethyluric acid **1e**, (f) 1,9-dimethyluric acid **1f**, (g) 3,7-dimethyluric acid **1g**, (h) 1,3,7-trimethyluric acid **1h**.

The reaction between urate **1a** and peroxynitrite resulted in a six-line ESR spectrum with the hyperfine coupling constants: a(N) = 15.7 G, and a(H) = 4.3 G (Table 3-1). All methylated uric acids that gave ESR signals displayed similar hyperfine coupling constants, ranging from 4.2-4.4 G for a(H) and 15.7-16.0 G for a(N). These are close to the observed value from the uric

acid reaction, indicating that methylurates were converted to radicals, which are similar to the radicals produced by urate. In addition, the ESR spectrum obtained from 9-methyluric acid **1c** was composed of a mixture of two spectra. These spectra were characterized by a six-line and a nine-line ESR spectrum, with the hyperfine coupling constants: a(N) = 15.9 G, a(H) = 4.2 G and a(N) = 16.8 G, a(H) = 10.6 G, respectively. The latter showed a characteristic hyperfine structure of the hydrogen-PBN radical adduct.

Table 3-1. Hyperfine coupling constants a (Gauss) of PBN-radical adducts from the reaction between uric acid and methylated uric acids with peroxynitrite at pH 7.4, and their relative ESR intensities compared to uric acid.

Radicals from compound	a(H)	a(N)	ESR Intensity (arb. unit.) Relative to Uric acid[a]
UA (1a)	4.3	15.7	1.00
1-MeUA (1b)	4.4	15.9	0.61
9-MeUA (1c)	4.2	15.9	0.09
9-MeUA (1c) (H-adduct)	10.6	16.8	N/A
1,3-DiMeUA (1d)	4.4	16.0	0.18
1,7-DiMeUA (1e)	N/A	N/A	N/A
1,9-DiMeUA (1f)	4.3	15.9	0.14
3,7-DiMeUA (1g)	N/A	N/A	N/A
1,3,7-TriMeUA (1h)	N/A	N/A	N/A

[a] Carbon-based radical adducts

To compare the relative radical formation quantity, the measured ESR intensities corresponded to the first PBN-radical adduct peak. Methyluric acid **1b** formed radical adducts that were approximately 60% of that observed with uric acid (Table 3-1). The radicals derived from urate **1c, 1d,** and **1f** exhibited much lower ESR intensity than **1a**, but still showed a noticeable number of radical adducts formed. However, the generations of radical adducts from **1e**, **1g** and **1h** ($R_7 = CH_3$) were barely detectable, and their ESR intensities were too low to be accurately measured.

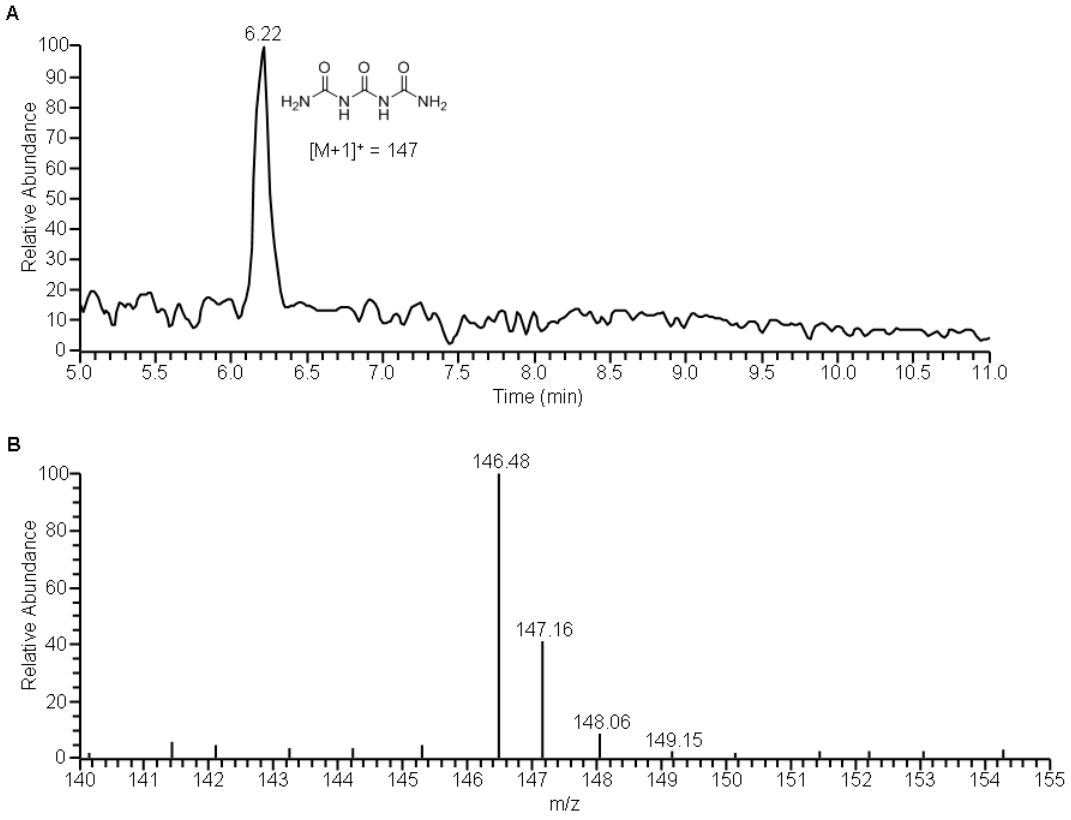

Figure 3-3. LC-MS study of the reaction between uric acid and peroxynitrite in phosphate buffer pH 7.4. (A) LC chromatogram obtained from the incubation of 10 mM urate, 0.1 mM DTPA anf 30 mM peroxynitrite in 0.5 M phosphate buffer pH 7.4. (B) Electrospray mass spectrum of triuret conducted in positive mode.

Liquid Chromatography-Mass Spectrometry Analysis of the Reactions Conducted in Phosphate Buffer. Under positive mode, the fullscan LC-MS analysis of the reaction between urate and peroxynitrite in phosphate buffer pH 7.4 showed a trace of mass peak of m/z 147 (Figure 3-3), which was consistent with triuret **2a** (Figure 3-4). We did not find other common urate oxidation products such as allantoin or alloxan in our reactions. With other methylated uric acid analogues, we observed the mass peaks at 161, 175, and 189 (Figure A-1 to A-7), which were attributed to monomethyltriurets **2b**;**2c**, dimethyltriurets **2d**;**2e**;**2f**;**2g**, and trimethyltriurets **2h**, respectively. This indicates that the reactions of methylated uric acid derivatives upon oxidation by peroxynitrite underwent similar oxidation mechanism like urate.

Liquid Chromatography-Mass Spectrometry Analysis of the Reactions Conducted in Methanol. Analyzed by LC-MS, each of the urate and seven methylurates individually reacted with peroxynitrite, producing various products, which are summarized in Table 3-2, and their structures are displayed in Figure 3-4.

Each reaction proceeded to various extents (Table 3-2), which depended on the methylation position. The percent conversion of each reaction was obtained by measuring the peak area of the untreated starting material and comparing with the peak area of the standard solution of the starting material. When N-3 was methylated, a low percent completion was obtained (22-35%), while the reaction of urate and 1-methylurate proceeded to 100 % completion. In addition to methylation at N-3, having methyl groups on N-7 or N-9 also decreased the percent conversion.

The LC trace and mass spectra obtained from the interaction between uric acid (**1a**) and peroxynitrite in methanol are shown as examples in Figure 3-5 (see Appendix B for full data set of other methylated uric acids).The fullscan MS spectra exhibited two products corresponding to the fragments of m/z 231, which is attributed to uric acid glycol dimethyl ether **3a**, and m/z 173, which is consistent with allantoin derivative **5a** (Figure 3-4).

Table 3-2. Reaction percent conversions and product yields of uric acids with one equivalent of peroxynitrite based on LC-MS analysis of the reaction products.

Compound	Conversion (%)	Products (% Yield)						
		3	4	5	6	7	8	9
UA (**1a**)	100	53.1	-	44.4	-	-	-	-
1-MeUA (**1b**)	100	74.7	-	25.1	-	-	-	-
9-MeUA (**1c**)	62	32.8	-	8.5	-	6.3 (i)	-	10.6
1,3-DiMeUA (**1d**)	30.4	2.3	-	10.4	-	4.7(ii)	-	-
1,7-DiMeUA (**1e**)	72.4	37.4	-	-	19.9	-	11.9	-
1,9-DiMeUA (**1f**)	52	36.0	0.5	9.3	-	6.2 (i)	-	-
3,7-DiMeUA (**1g**)	35	-	3.0	10.6	10.5	-	-	-
1,3,7-TriMeUA (**1h**)	22.8	-	-	2.4	13.3	-	-	-

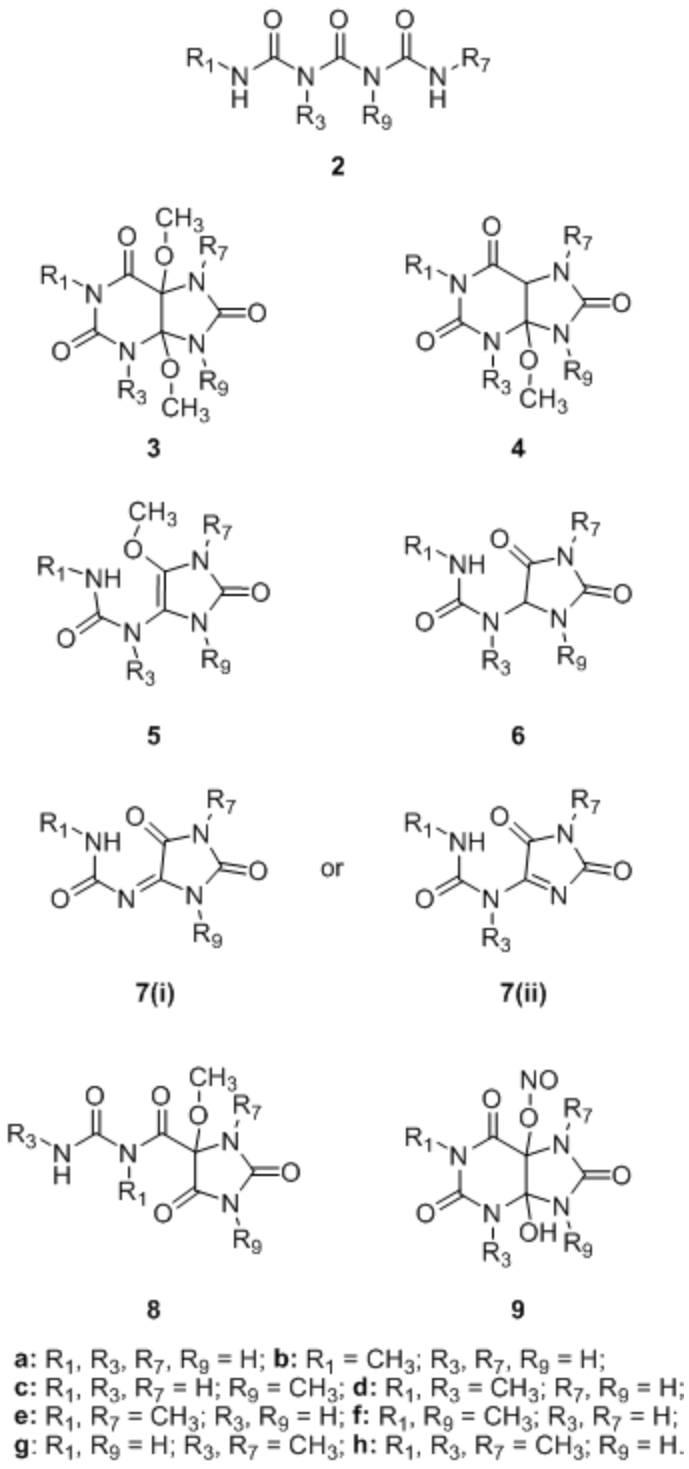

Figure 3-4. Proposed structures of the reaction products obtained from the reaction between uric acid (or various methylated uric acid analogues) and peroxynitrite.

The presence of methoxy groups in both products **3a** and **5a** is evidenced by using d_4-methanol to substitute non-labeled methanol. The ions at m/z 176 corresponding to d_3-methoxy

compound **5a**, and m/z 237 corresponding to di-d_3-methoxy adduct **3a** were observed (Figure 3-6). The losses of methanol molecules (MW 32) exhibited in MS/MS fragmentation analysis (Figure 3-7) further supported the proposed structure of the uric acid glycol dimethyl ether **3a**. Similar fragmentation patterns were also found in the MS/MS experiment of the corresponding uric acid glycol di-d_3-methyl ether **3a** (Figure 3-8).

Similar products found in the urate-peroxynitrite reaction were observed in the reactions of other methylated uric acid analogues treated with peroxynitrite as well. The fullscan MS spectra obtained from the reaction mixtures of monomethylurate **1b** and **1c** displayed the quasi ions at m/z 245, which were attributed to the methyluric acid glycol dimethyl ether **3b** and **3c** (Figure 3-4), respectively. In the case of dimethylurate **1d**, **1e**, and **1f**, the fragments of m/z 259 were observed and identified as the dimethyluric acid glycol dimethyl ether; **3d**, **3e**, and **3f** (Figure 3-4), respectively. Using the same analogy as conducted in urate reaction, the identifications of these dimethyl ethers **3** were confirmed by conducting isotope-labeled experiments using d_4-methanol and performing MS/MS analysis. In the presence of d_4-methanol, the fragments of m/z 251; and 265 were found in the reactions of monomethylated urates **1b**, **1c**, and dimethylated urates **1d**, **1e**, **1f**, respectively. Furthermore, the fragmentation analyses from MS/MS studies of ions m/z 251 and 265 exhibited a similar pattern (APPENDIX C) as observed in the MS/MS spectrum of dimethyl ether **3a** (Figure 3-7 and 3-8). These results indicate that two methoxy groups are present in compounds with fragment ions of m/z 245 and 259, which were consistent with dimethyl ether adducts **3**. We did not observe the dimethyl ether adducts **3** when dimethylurate **1g** and trimethylurate **1h** were used as reactants. However, in the reaction mixture of dimethylurate **1g**, we detected a mono-methoxy adduct **4g** (m/z 229) as a minor product. A small quantity (0.5%) of **4f** was found in the reaction mixture of dimethylurate **1f**.

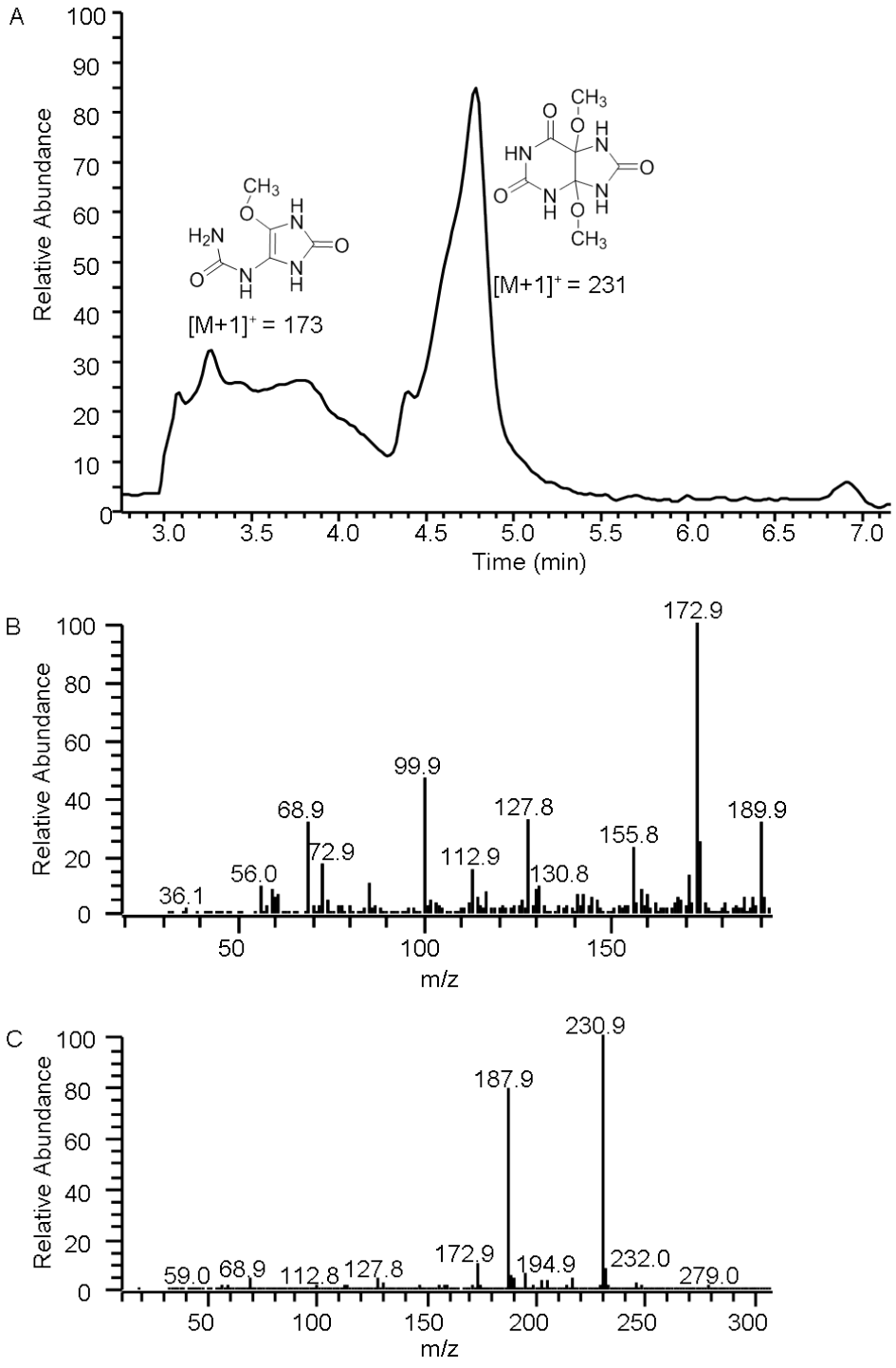

Figure 3-5. LC-MS study of the reaction between uric acid and peroxynitrite in the presence of methanol. (A) The fullscan LC chromatogram obtained from the reaction of 10 mM urate treated with 10 mM peroxynitrite in 50% methanol and 50% aqueous phosphate buffer solution at pH 7.4. The first peak was monitored at m/z 172.9 (B), corresponding to allantoin derivative **5a**. The second peak was monitored at m/z 230.9 (C), corresponding to uric acid glycol dimethyl ether **3a**.

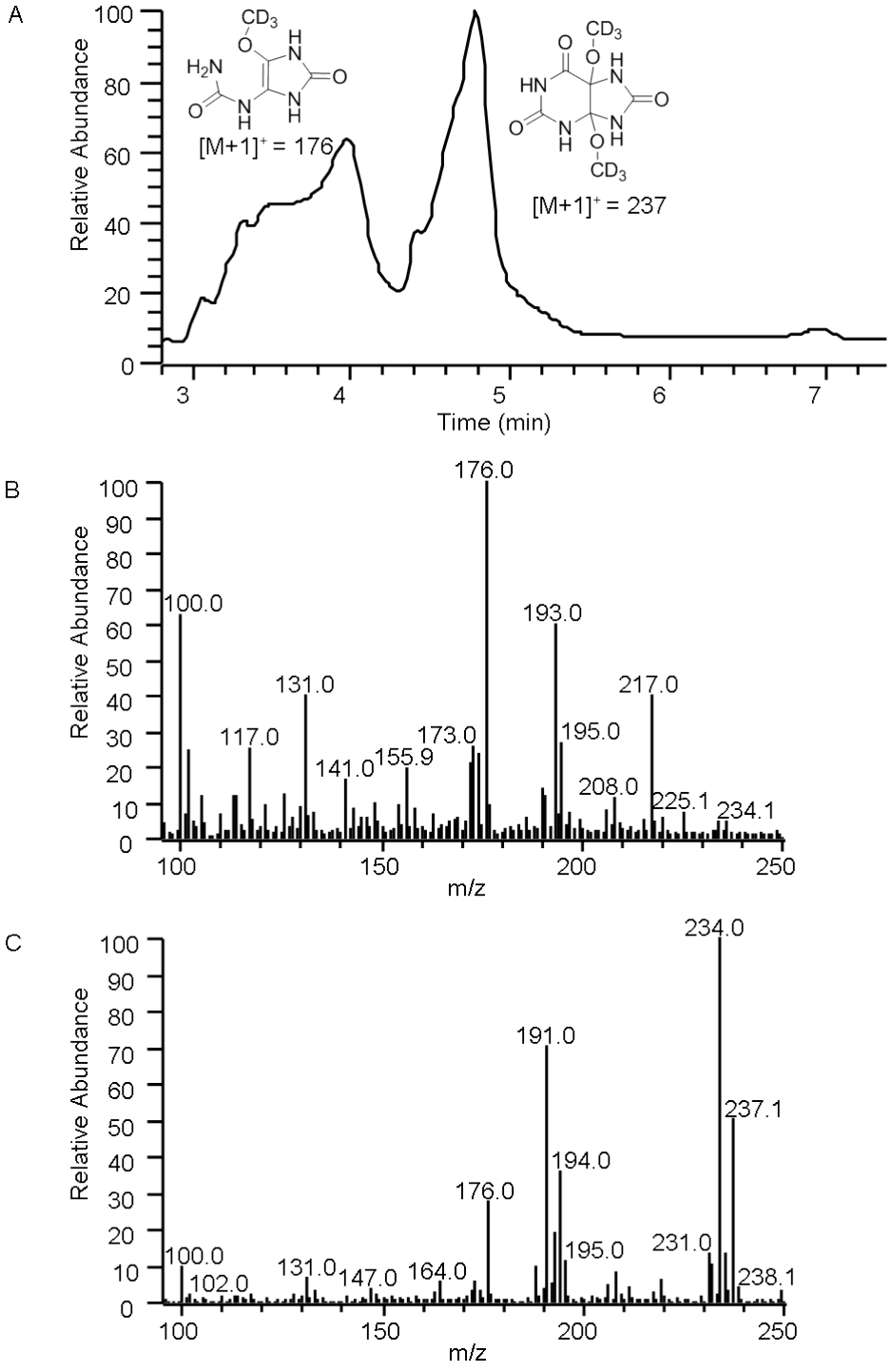

Figure 3-6. LC-MS study of the reaction between uric acid and peroxynitrite in the presence of d_4-methanol. (A) The fullscan LC chromatogram obtained from the reaction of 10 mM urate treated with 10 mM peroxynitrite in 50% d_4-methanol and 50% aqueous phosphate buffer solution at pH 7.4. The first peak was monitored at m/z 176.0 (B), corresponding to d_3-methoxy-allantoin derivative **5a**. The second peak was monitored at m/z 237 (C), corresponding to uric acid glycol di-d_3-methyl ether **3a**.

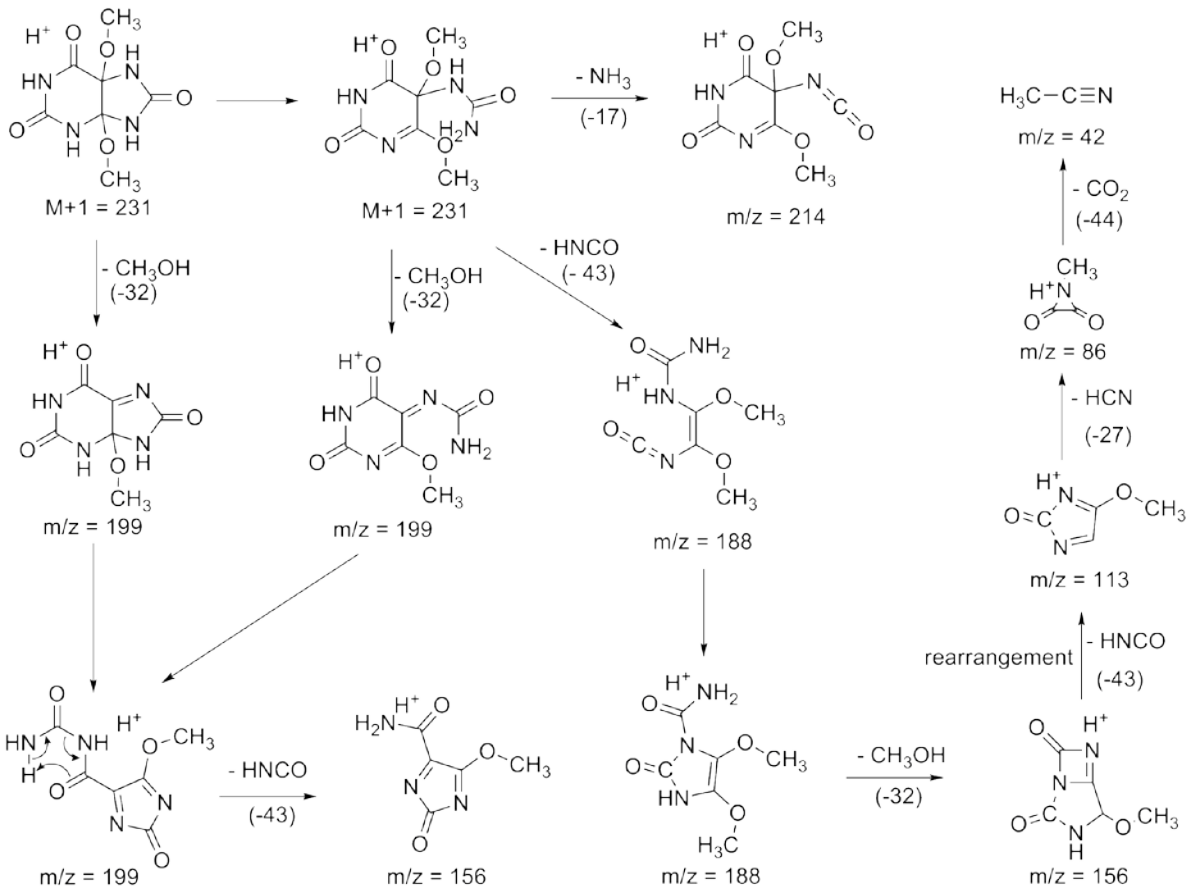

Figure 3-7. The fragmentation pattern of uric acid glycol dimethyl ether **3a**.

In addition to dimethyl ethers **3**, allantoin derivatives **5** (Figure 3-4) were observed in most reaction mixtures as well (except **1e**). We identified the structures of methoxy allantoin-like products **5** based on the quasi ions at m/z 187 from methylurate **1b** and **1c**, m/z 201 from dimethylurate **1d**, **1e**, **1f**, and **1g**, and m/z 215 from trimethylurate **1h**. The presence of the methoxy group, derived from solvent methanol, was confirmed by using d_4-methanol. Indeed, the expected ions at m/z 190, 204, and 218 were detected. In addition to these allantoin derivatives **5**, methylallantoin derivatives **6** (Figure 3-4), interpreted from m/z 187, and m/z 201, were observed when $R_7 = CH_3$; however, when $R_7 = H$ (except **1a** and **1b**), the dehydroallantoins **7**, corresponding to m/z 171 from methylurate **1c** and m/z 185 from dimethylurate **1d** and **1f**, were obtained.

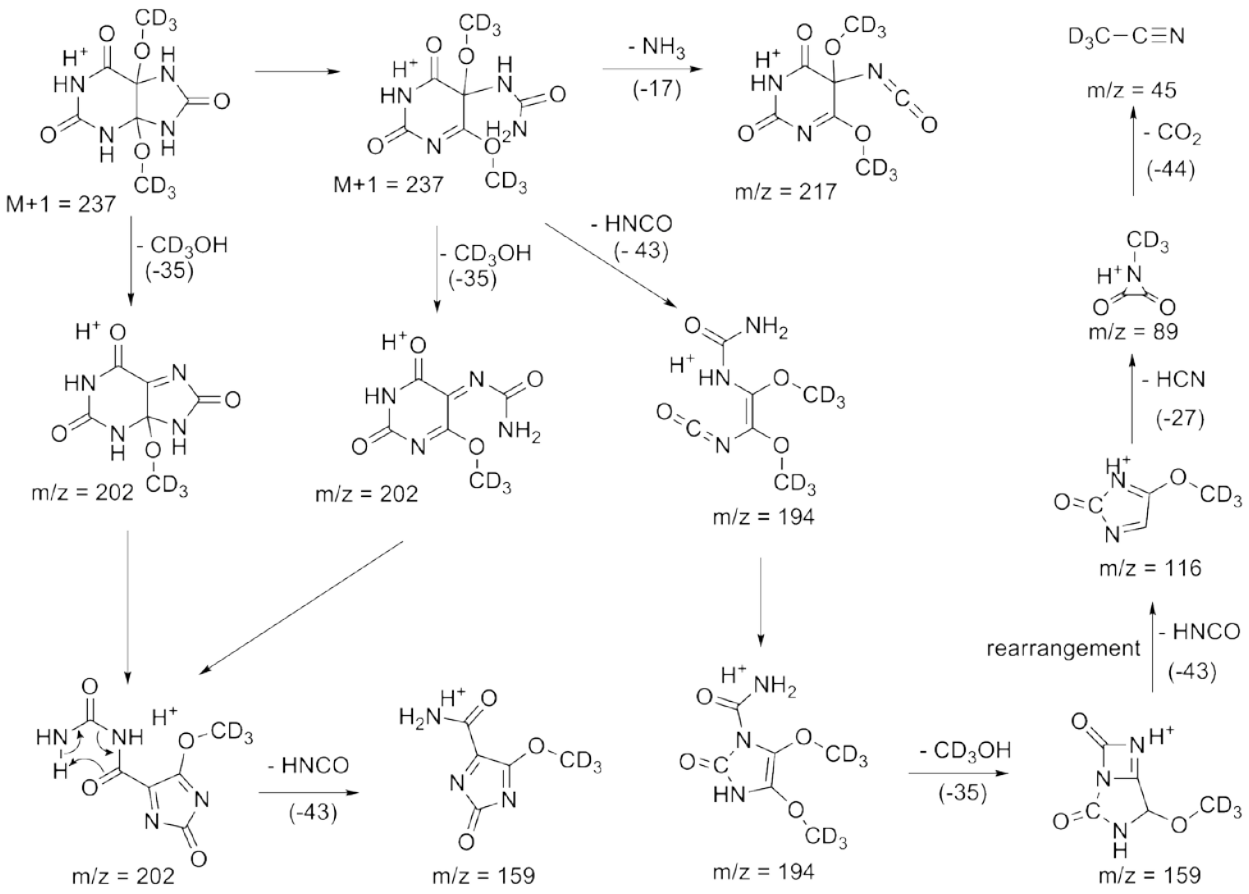

Figure 3-8. The fragmentation pattern of uric acid glycol di-d_3-methyl ether **3a**.

In addition to diadduct **3e** and allantoin derivatives **5e** and **6e**, LC-MS analysis of 1,7-dimethyluric acid **1e** exhibited m/z 245, which was tentatively identified as methyl ether **8e**. We also found a trace of an ion at m/z 246, which was identified as adduct **9c**—the addition product of peroxinitrous acid to 9-methylurate **1c**. We did not find the same intermediate in other reactions. Other minor products were found in some of the reactions, and their proposed structures are illustrated in Appendix B.

One of the puzzling aspects of our study was the identification of multiple isomers of some of the compounds in the LC-MS analysis. For example, four isomers of dimethyl ether **3b** were identified (Figure B-1), and the MS/MS data of the four isomers were identical. These isomers comprised tautomers—including an amide form and an imidic acid form. In solution, where

tautomerization is possible, the chemical equilibrium of the tautomers is reached quickly (Figure 3-9). As long as the hydrogen exchange is relatively slow, the tautomers may be separated by HPLC and LC-MS. Several examples of such separations have been reported (*89*). Formation of such tautomers could explain other compounds in this study exhibiting isomer formation.

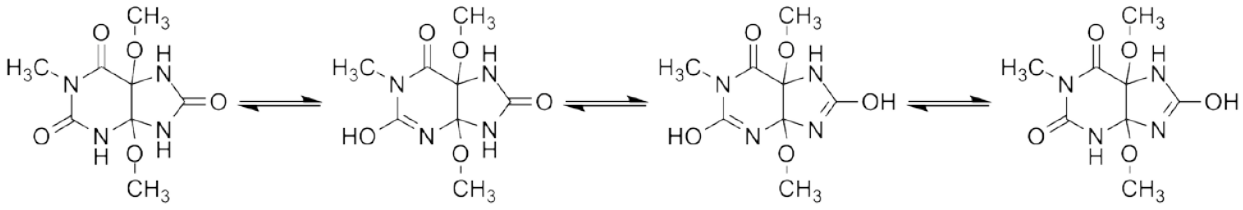

2b

Figure 3-9. Example of Tautomerization of compound 2b.

Discussion

These studies were initiated to determine the significance of the N-H group at various positions, and to determine the reactive intermediates and products formed from their reactions with peroxynitrite. In addition, we wanted to understand the mechanistic interaction of methyluric acids with peroxynitrite as these molecules are ubiquitous in the body.

Reactions in Phosphate Buffer. The methyl groups, methylated on various nitrogen position, were hypothesized to alter the course of radical adduct formation. The results indeed showed a difference when a certain hydrogen of ureide nitrogen was replaced by a methyl group. As shown in Figure 3-2, the intense six-line ESR spectra were observed only if N-7 was not methylated. With methylation at N-7, the production of radical adduct was greatly diminished (Figure 3-2). Moreover, not only methylation at N-7, but methylation at N-9 (**1c**, **1f**) and N-3 (**1d**) also reduced the radical formations. This data indicated that the methyl group on N-7 and either on N-3 or N-9 positions of uric acid has a great impact on the reactivity of urate with peroxynitrite.

The LC-MS analysis suggested that all methylated uric acid analogues reacted with peroxynitrite and formed methylated triuret derivatives as major products. As described in Chapter 2, we hypothesized that triuret, a product generated from the oxidation of urate by peroxynitrite, could be produced from the triuretcarbonyl radical. It is possible that methylated triurets **2** derived from N-7 methylated uric acids could be produced from their corresponding methylated triuretcarbonyl radicals as well. But these radicals may not be trapped by PBN because of the steric hindrance between the methyl group of triuret moiety and the phenyl group of PBN (Figure 3-10). As a result, there was no detected ESR signal in the reactions of N-7 methyl derivatives.

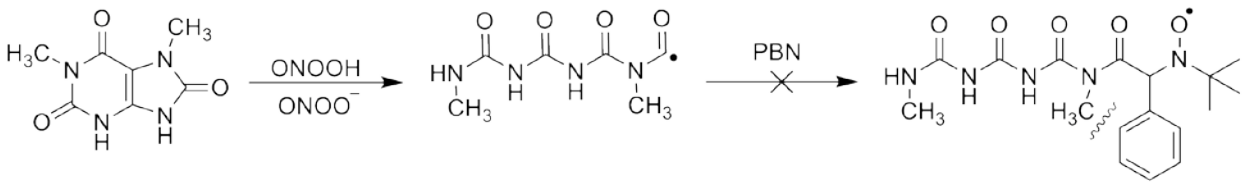

Figure 3-10. The steric hindrance between the methyl group of triuret moiety and the phenyl group of PBN prevents the PBN-radical adduct formation.

Reactions in Methanol. In the presence of methanol, our study documents that all methyluric acids react with peroxynitrite as determined by mass spectrometry, with different degree of conversions, depending on the position and extent of substitution (UA=MeUA > DiMeUA > TriMeUA). Replacing hydrogen with a methyl group at N-3, N-7, or N-9 retarded the reactions, giving relatively lower percent conversion. These studies suggest that the C4-C5 bond is the reaction center, and we speculate that methylation at N-3, N-7, or N-9 that are adjacent to C4-C5 bond may control the stability of the intermediates, resulting to different degree of conversions.

The addition of alcohols to the C4 and C5 position, forming dimethyl ether **3**, and the formation of alkylated allantoin analogues (compound **5** and **6**) suggested that an intermediate

that can rapidly react with methanol and water may be produced. We propose that the reactive intermediate **12** is formed (Figure 3-11 and 3-12), presumably via the electron transfer mechanism similar to the mechanism proposed for the oxidation of urate by peroxynitrite as described in Figure 2-12. Moreover, we proposed that there are two possible structures of intermediate **12**, **12(i)** and **12(ii)**, depending upon the methylation position.

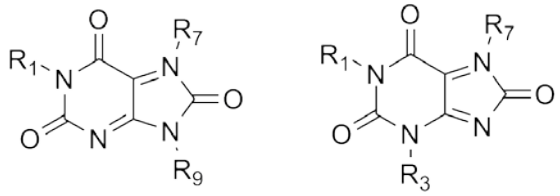

12(i) **12(ii)**

As reported in the study of the intrinsic acidity of uric acid and its derivatives by Telo (*88*), the N-H proton at N-3 is the most acidic one followed by the N-H proton at N-9. When N-3 is not methylated (i.e., in the case of **1a**, **1b**, **1c**, **1e**, and **1f**), the N3H proton is deprotonated to produce anion form of compound **1a**, **1b**, **1c**, **1e**, and **1f** (Figure 3-11). The oxidation of these anion compounds by peroxynitrous acid will give intermediates **12(i)** (Figure 3-11). While, in the case of **1d**, **1g**, **and 1h** where N-3 is methylated, the deprotonation occurs at N9H (Figure 3-12). After oxidized by peroxynitrous acid, the anion forms of **1d**, **1g**, **and 1h** are converted to intermediates **12(ii)**. The formation of **12(ii)** is however highly unfavorable because the compound **12(ii)** is antiaromatic. Consequently, this could be the reason why we observed very low percent conversion in the oxidation of **1d**, **1g**, **and 1h**, which contain a methyl group at N-3.

We speculated that intermediate **12** can undergo nucleophilic addition with methanol to form product **3** and **5**, and with water to generate methylated allantoin derivatives **6** (Figure 3-11 and 3-12). It is possible that allantoin derivatives **6** could be oxidized by peroxynitrous acid to produce the oxidized form of the corresponding allantoins **7**. However, we had a LC-MS result showing that no product was formed from the reaction between allantoin **6a** and peroxynitrite.

Nevertheless, this result may not be the case with these methylated allantoins **6**. In addition to the oxidation of compound **6**, product **7** can be generated from the process initiated by the nucleophilic addition of peroxynitrite to intermediate **12** as well (Figure 3-11 and 3-12). By the same analogy described in Chapter 2 (Figure 2-12), one would expect the formation of methylated triurets in these reactions. Although we did not observe any methylated triuret products in these reactions that contained methanol, this argument may still be valid because based on our proposed mechanism in Figure 2-12, four mole of peroxynitrite is required to form triuret. However, in the reaction condition that we performed, we have used only one equivalent of peroxynitrite. This may be the factor that controls the progress of the reaction. Furthermore, we have shown that the oxidation of uric acid **1a** and 1-methyluric acid **1b** with one equivalent of peroxynitrite went to completion Table 3-2. These results suggested that the second electron transfer from urate radical **10** could be initiated by nitrogen dioxide radical ($NO_2^{\bullet}$) (Figure 3-11 and 3-12). Moreover, the existence of urate radical **10** is evidenced by the formation of product **4** because the only way that C-5 could form a covalent bond with hydrogen would be by a radical process.

Beside the products that derived from intermediates **12**, we also detected compound **9c**, which is the adduct of 9-methylurate and peroxynitrous acid. A similar product to compound **9,** has been proposed in the reaction between peroxynitrite and deoxyguanosine, and characterized as 4,5-Dihyrdo-5-hydroxy-4-(nitrosooxy)-deoxyguanosine (*90*,*91*).

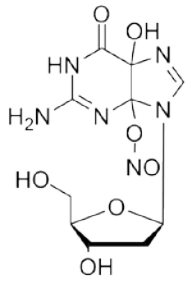

4,5-Dihyrdo-5-hydroxy-4-(nitrosooxy)-deoxyguanosine

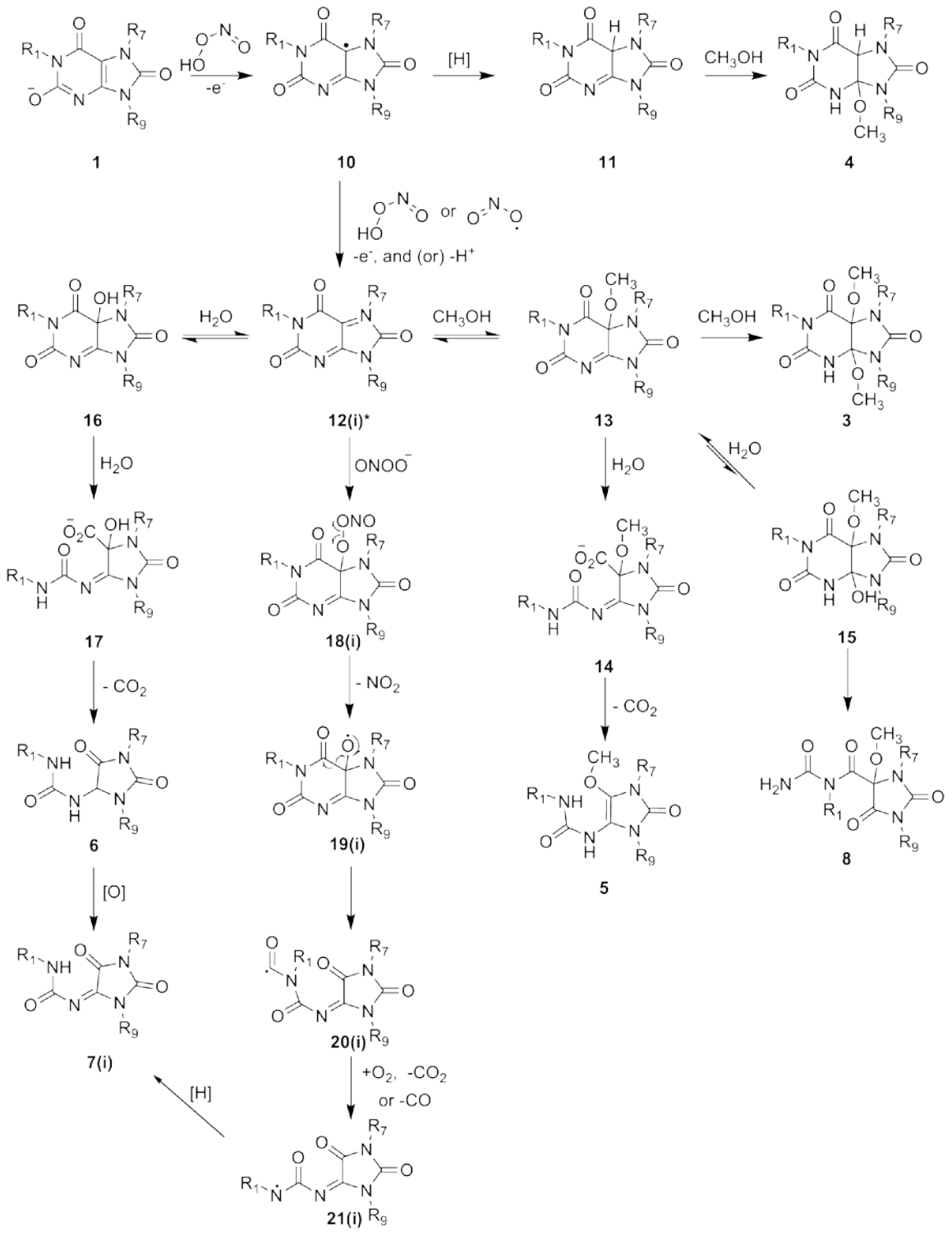

Figure 3-11. The proposed mechanism of the reaction between urate **1a** or methylurate derivatives **1b**, **1c**, **1e**, **1f** and peroxynitrite, leading to the formation of various products. *Intermediates **12(i)** contain a positive charge at N-7 if N-7 is methylated.

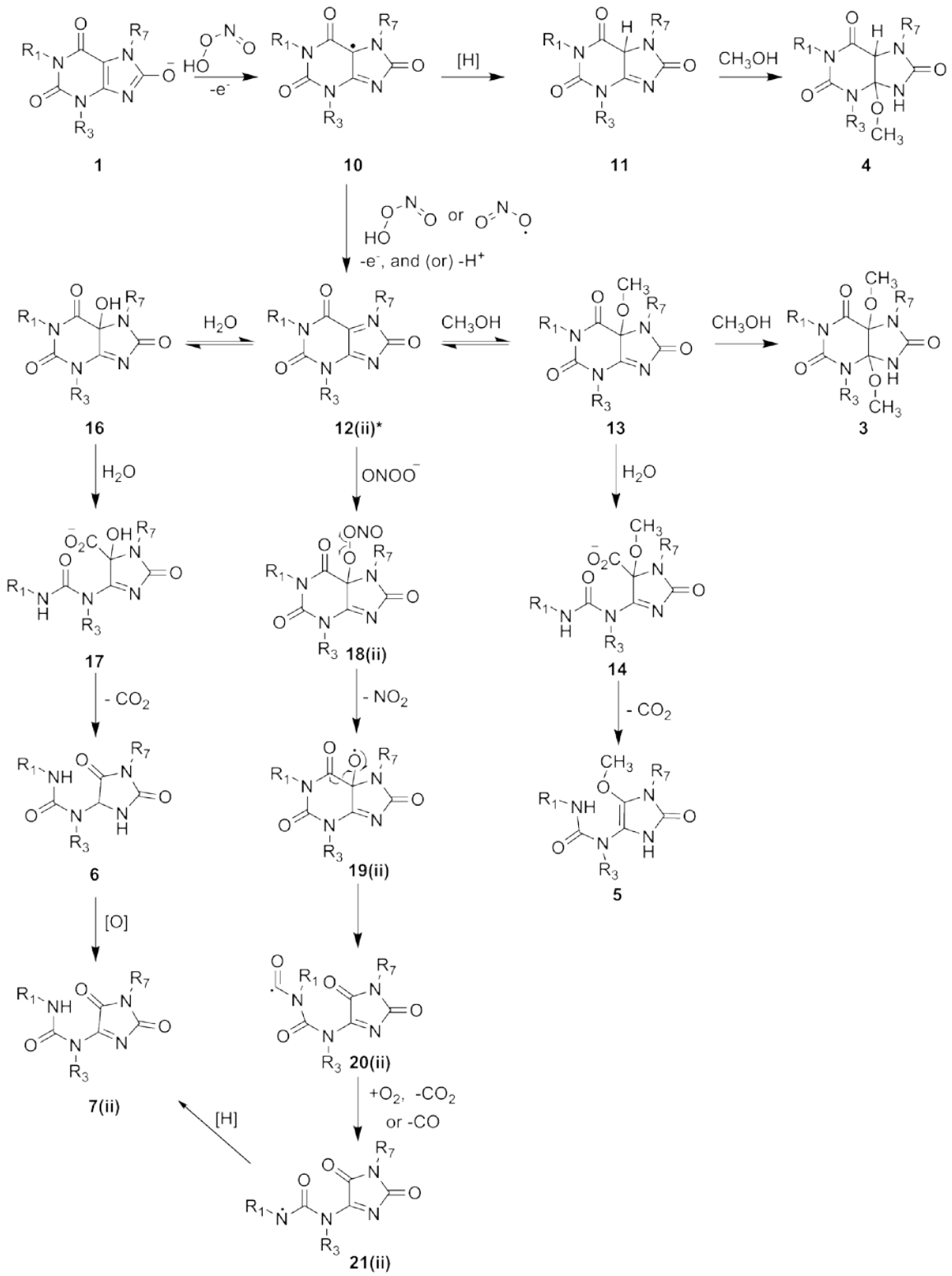

Figure 3-12. The proposed mechanism of the reaction between methylurate derivatives **1d**, **1g**, **1h** and peroxynitrite, leading to the formation of various products. *Intermediates **12(ii)** contain a positive charge at N-7 if N-7 is methylated.

In our study, among the eight tested reactions, only the reaction of **1c** yielded the proposed adduct **9c**. Its proposed formation was initiated by a single electron transfer from uric acid to peroxynitrite. Peroxynitrite then dissociates to the nitrogen dioxide (NO_2•) and the hydroxide anion ($^-$OH) which adds to the urate free radical, generating adduct **9c** (Figure 3-13, route A).

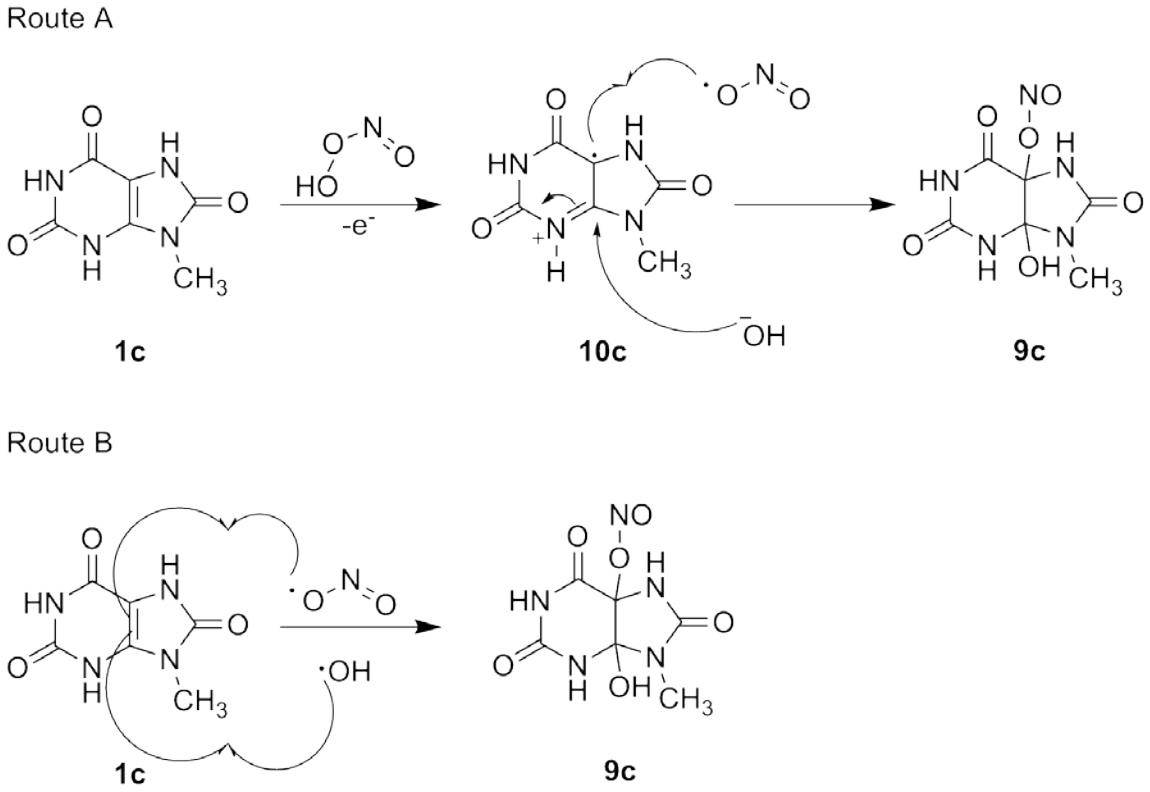

Figure 3-13. The proposed mechanism of the formation of 9-methylurate-peroxynitrite adduct **8c**.

Alternatively, the formation of intermediate **9c** could also be obtained by the addition of hydroxyl (HO•) and nitrogen dioxide (NO_2•) free radicals, which are the decomposition products from the homolytic cleavage of peroxynitrous acid (Equation 3-2), across the C4-C5 bond (*92-94*) (Figure 3-13, route B).

$$ONOO^- + H^+ \rightleftharpoons ONOOH \quad (3\text{-}1)$$

$$ONOOH \longrightarrow [ONO^{\bullet}\cdot{}^{\bullet}OH] \longrightarrow {}^{\bullet}OH + NO_2^{\bullet} \quad (3\text{-}2)$$

However, the formation of the two radicals according to equation 3-2 is still debated (*46*). Moreover, our ESR spin trapping experiments did not show any formation of the hydroxyl radical. Therefore we believe that the formation of adduct **9c** by the addition of hydroxyl ($HO^{\bullet}$) and nitrogen dioxide ($NO_2^{\bullet}$) free radicals pathway (Figure 3-13, route B) is less feasible than the proposed mechanism depicted in Figure 3-13, route A. Nevertheless, the reason why we did not observe this adduct in other methyl-urate derivatives is unknown. Because of the complexity of these reactions, the mechanistic study of these reactions deserves further consideration.

CHAPTER 4
ESR SPIN TRAPPING OF THE REACTION BETWEEN URIC ACID AND PEROXYNITRITE: THE HYDROGEN ADDUCT

Introduction

Previously, we reported the trapping of the carbon-centered radicals from the reaction between uric acid and peroxynitrite under phosphate buffer pH 7.4. In an attempt to understand the in depth chemistry of the radical formation, we have employed the ESR spin trapping experiment to investigate the generation of the free radicals from the reaction between uric acid and peroxynitrite at various chemical conditions. Under a certain circumstance, we surprisingly found a nine-line ESR spectrum, corresponding to the trapping of a hydrogen atom when PBN was used as a spin trapping agent. This intriguing finding led us to study, in more detail, the production of the hydrogen adduct (H-adduct). In this report, the factors that could affect the forming of H-adduct and the mechanism of its formation will be discussed.

Materials and Methods

Chemicals. Uric acid was purchased from Sigma. Diethylenetriaminepentaacetic- acid (DTPA) was purchased from Fluka. N-*tert*-butyl-α-phenylnitrone (PBN) and α-(4-Pyridyl 1-oxide)-N-tert-butylnitrone (POBN) were obtained from Alexis Biochemicals. Peroxynitrite was synthesized following the method reported by Uppu and Pryor (*76*). The peroxynitrite concentration was measured spectrophotometrically at 302 nm ($\varepsilon = 1670\ M^{-1}\ cm^{-1}$).

pH Dependence Experiments on Urate-Peroxynitrite Reactions. The ESR spin trapping of the reaction between uric acid and peroxynitrite at various pHs was performed by using 0.1 M Tris-buffer with a range of pH 7.4-9.0. PBN was used as a spin trapping agent. The reaction mixtures contained: 1.5 mM uric acid, 15 mM PBN, 0.1 mM DTPA, and 6 mM peroxynitrite in 0.1 M Tris-buffer.

Effect of Spin Trapping Agents on the Hydrogen Adduct Formation. The effect of the spin trapping agent on the formation of the hydrogen adduct was performed in 0.3 M potassium phosphate buffer pH 7.4 or 0.3 M KOH. The reaction mixtures contained: 3 mM urate, 30 mM PBN or POBN, 0.1 mM DTPA, and 9 mM peroxynitrite.

Electron Spin Resonance Parameters. The reaction mixture was transferred into a quartz capillary of approximately 1×2 mm ID×OD for ESR measurement. After two minutes, the ESR spectrum was recorded at room temperature, using a commercial Bruker Elexsys E580 spectrometer, employing Bruker's high-Q cavity (ER 4123SHQE). Spectral parameters were typically: 100 kHz modulation frequency, 1 G or 0.2 G modulation amplitude, 20 mW microwave power, 9.87 GHz microwave frequency, 82 ms time constant, and 164 conversion time/point.

Results

pH Dependence Studies on Urate-Peroxynitrite Reactions. By using Tris-buffer, the six-line ESR spectrum was the only observed ESR signal at pH 7.4-8.0. The ESR intensity of this six-line spectrum was increased when we raised the pH form 7.4 to 8.0, and started to decrease when the pH was raised to pH 8.5. At pH 9.0, the ESR spectrum exhibited an overlapping between a six-line and a nine-line ESR (Figure 4-1). On the other hand, the ESR spectrum obtained from pH 9 was derived from a mixture of a two trapped radical species. The six-line ESR spectrum corresponded to the trapping of carbon-centered radical by PBN, while the nine-line ESR spectra with relative intensities (1:2:1:1:2:1:1:2:1) displayed a characteristic spectrum of the hydrogen-PBN adduct with the hyperfine splitting a(H) = 10.68 G and a(N) = 16.64 G.

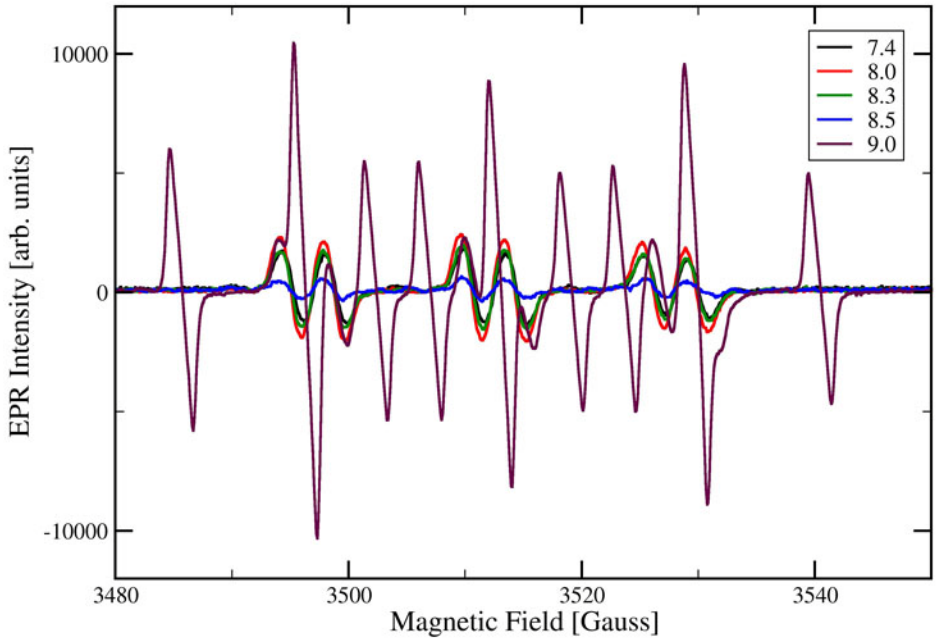

Figure 4-1. The pH dependence study of the urate-peroxynitrite reaction in Tris-buffer. The ESR spectra obtained from the spin trapping experiment of the reaction between 1.5 mM urate and 6 mM peroxynitrite in the presence of 15 mM PBN and 0.1 mM DTPA in 0.1 M Tris-buffer at pH ranging from 7.4-9.0.

Electron Spin Resonance Spin Trapping by PBN and POBN. The hydrogen adduct formation has been detected recently when POBN, another nitrone spin trapping agent, was used (*95*). This prompted us to investigate whether we would obtained the same result when POBN was used as a spin trapping agent under the same reaction condition as we performed with PBN. In phosphate buffer at pH 7.4, the ESR spin trapping by PBN exhibited a six-line ESR spectrum corresponding to the trapping of the carbon-based radical, which is the only observed product from the oxidation of urate by peroxynitrite (Figure 4-2), while spin trapping by POBN displayed a mixture of two radical species, a six-line and a nine-line spectrum (Figure 4-3). The nine-line ESR spectrum belonged to the H-POBN adduct and has a much higher ESR intensity than the six-line ESR spectrum which is consistent with the carbon-based radical adduct.

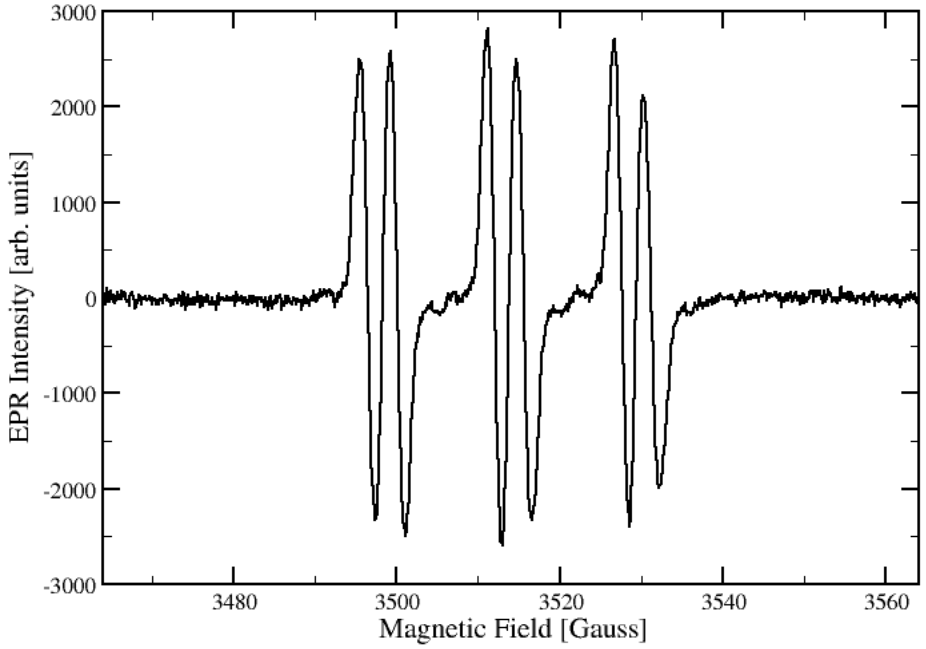

Figure 4-2. ESR spectrum of the PBN-radical adduct at pH 7.4 obtained from the spin trapping experiment of the reaction between 3 mM urate and 9 mM peroxynitrite in the presence of 30 mM PBN and 0.1 mM DTPA in 0.3 M phosphate buffer pH 7.4.

As described earlier, the pH study exhibited the formation of H-adduct at basic condition (pH 9.0). We thus performed the spin trapping experiment under very basic condition, by replacing phosphate buffer with 0.3 M KOH, to investigate whether basic condition could promote the formation of the H-adduct. The final pH of the solution mixture averaged around pH 12. Indeed, we observed the H-adduct from both spin trapping agents, PBN and POBN at this pH. The ESR spectrum obtained from PBN exhibited a six-line ESR spectrum, corresponding to the carbon-centered radical adduct, overlapped with a nine-line ESR spectrum, corresponding to the H-adduct (Figure 4-4). With POBN, only the nine-line ESR spectrum, which was consistent with the H-adduct, was observed, and its ESR intensity was relatively much higher than PBN (Figure 4-5).

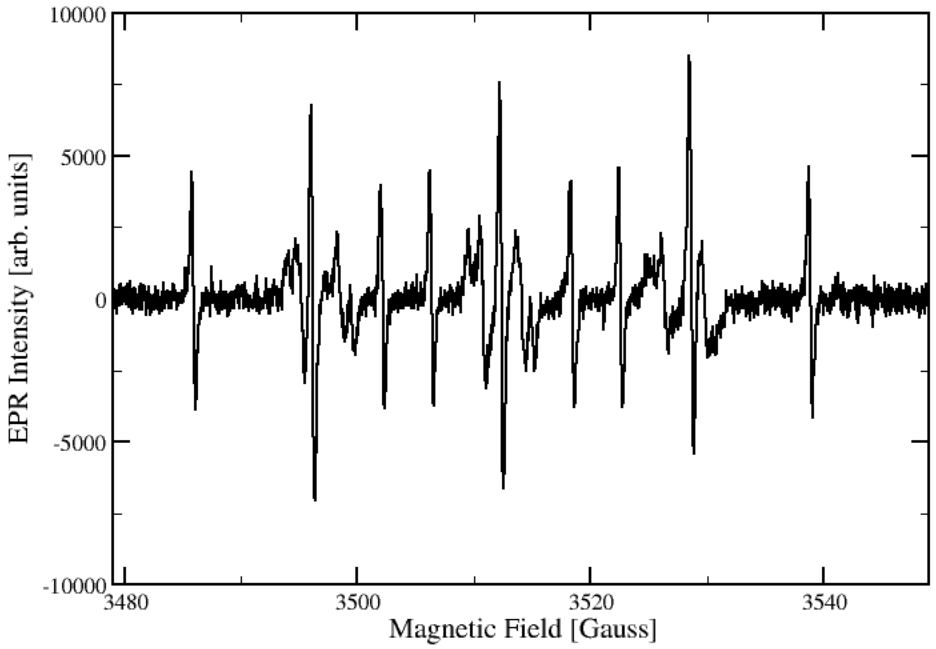

Figure 4-3. ESR spectrum of the POBN-radical adduct at pH 7.4 obtained from the spin trapping experiment of the reaction between 3 mM urate and 9 mM peroxynitrite in the presence of 30 mM POBN and 0.1 mM DTPA in 0.3 M phosphate buffer pH 7.4.

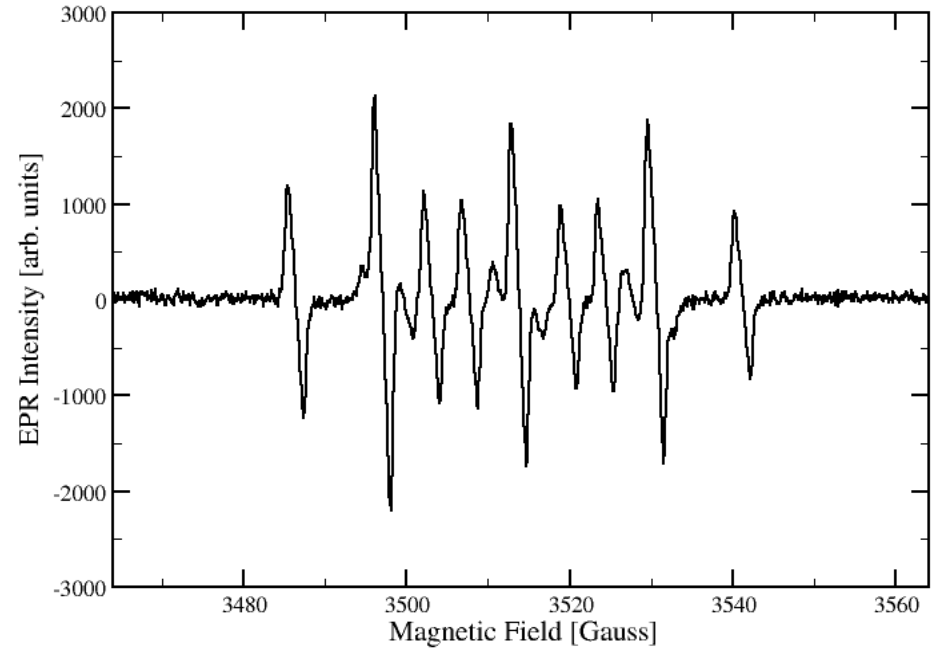

Figure 4-4. ESR spectrum of the PBN-radical adduct at pH 12 obtained from the spin trapping experiment of the reaction between 3 mM urate and 9 mM peroxynitrite in the presence of 30 mM PBN and 0.1 mM DTPA in 0.3 M KOH.

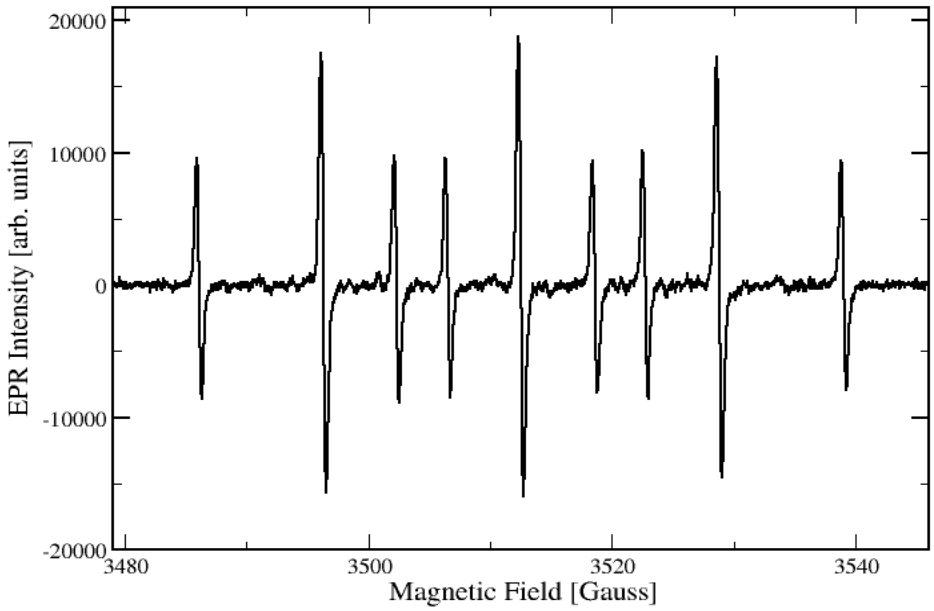

Figure 4-5. ESR spectrum of the POBN-radical adduct at pH 12 obtained from the spin trapping experiment of the reaction between 3 mM urate and 9 mM peroxynitrite in the presence of 30 mM POBN and 0.1 mM DTPA in 0.3 M KOH.

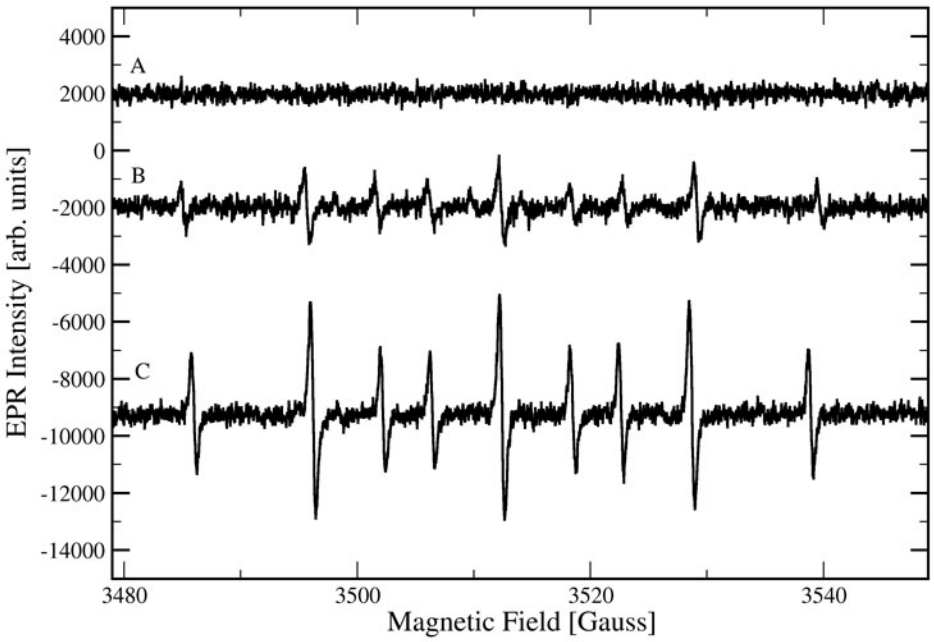

Figure 4-6. ESR spectra of the control reactions (without uric acid). (A) the ESR spectrum obtained from the spin trapping experiment of the reaction contained 30 mM PBN, 0.1 mM DTPA, and 9 mM peroxynitrite in 0.3 M phosphate buffer pH 7.4. (B) the ESR spectrum obtained from the spin trapping experiment of the reaction contained 30 mM PBN, 0.1 mM DTPA, and 9 mM peroxynitrite in 0.3 M KOH. (C) the ESR spectrum obtained from the spin trapping experiment of the reaction contained 30 mM POBN, 0.1 mM DTPA, and 9 mM peroxynitrite in 0.3 M KOH.

Interestingly, in the control reaction without uric acid, conducted in 0.3 M KOH, the PBN-H adduct was also observed with less intensity than the reaction containing uric acid (Figure 4-6). This indicates that the PBN-H adduct was not only derived from uric acid; however, the presence of uric acid amplified the formation of H-adduct. Beside PBN, POBN-H adduct was detected in the control reaction without uric acid as well, and its ESR intensity was even higher than PBN-H. These results indicate that the formation of the H-adduct depends on the type of the spin trapping agent.

Discussion

Recently, hydrogen adducts were identified in the peroxynitrite-mediated oxidation of tetrahydrobiopterin by using spin trap, POBN (*95*).

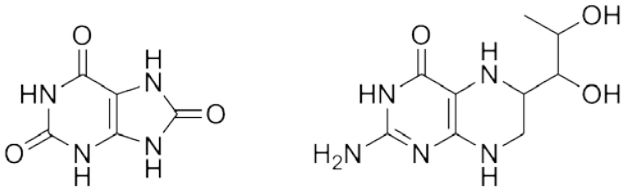

The authors reported a mixture of two spin trapped components: a six-line spectrum corresponding to a carbon-centered radical and a nine-line spectrum resulting from an H-atom trapped by POBN. It was proposed that peroxynitrite promoted a homolytic cleavage of a N-H bond of tetrahydrobiopterin, yielding a hydrogen radical, which could further react with POBN. We speculated that even though a hydrogen atom can be generated, it is unlikely that the hydrogen atom would survive long enough to be captured by the spin trap POBN.

We postulated that hydrogen adducts may be formed by an electron transfer mechanism. Under basic condition, the electron transfer between PBN and a reducing agent could be favored as depicted in Equation 4-1.

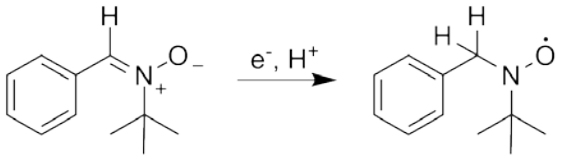

PBN PBN-H adduct (4-1)

But what could be the source of the electron? In our study, we discovered that peroxynitrite must be present in the reaction mixture in order to produce the H-adduct. Without it, the reaction mixture of urate and PBN did not yield any ESR signal. This indicates that the reaction between urate and peroxynitrite must take place and it may be one of the urate-derived intermediates that provide an electron to the spin trapping agent (Equation 4-2).

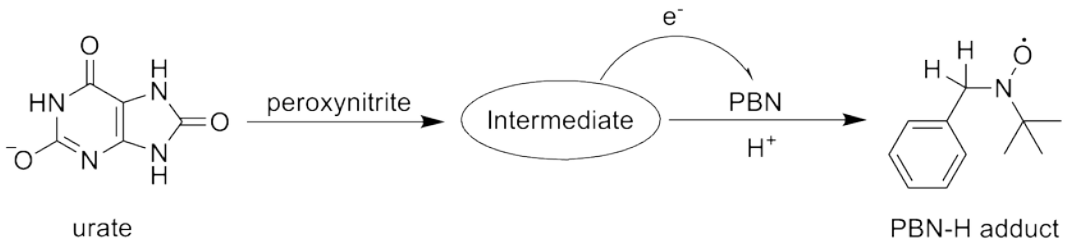

urate PBN-H adduct (4-2)

This proposed mechanism could not however explain the formation of the H-adduct in the control reaction that contained only the spin trapping agents and peroxynitrite. From this reaction (the reaction without urate), we observed the H-adduct formation (in both PBN and POBN) but its ESR intensity is much lower than the reaction that contained urate. Nevertheless, this observation indicates that uric acid is not necessary to be the only specie that can give up one electron to the spin trapping agents. However, it is unlikely that peroxynitrite can directly reduce PBN, due to the strong oxidant property of peroxynitrite (*45*). This led us to postulate that other species that could transfer an electron to spin trapping agents may be formed by a different mechanism called inverted spin trapping (*96-98*).

Inverted spin trapping is a process where the oxidation initially occurs at the spin trapping agent ([ST]) to form its radical cation ($[ST]^{+\bullet}$, followed by the reaction with nucleophile ($[Nu]^-$) such as water or hydroxide, and thus the radical adduct is formed (Equation 4-3).

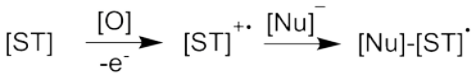

(4-3)

In basic condition without uric acid, peroxynitrite could potentially oxidize PBN (or POBN) to PBN radical cation, which is susceptible to a nucleophilic attack by hydroxide, forming a PBN-OH radical adduct (Figure 4-7). However, we did not detect the existence of this PBN-OH radical in our experiment. This is probably due to the instability of this radical adduct, which has been reported to be unstable by hydrolysis reaction with its half-life less than one second at a pH higher than 9.0 (*99*). The decomposition products of this process have been identified as *N-tert*-butylhydroaminoxyl and benzaldehye (Equation 4-4) (*99*).

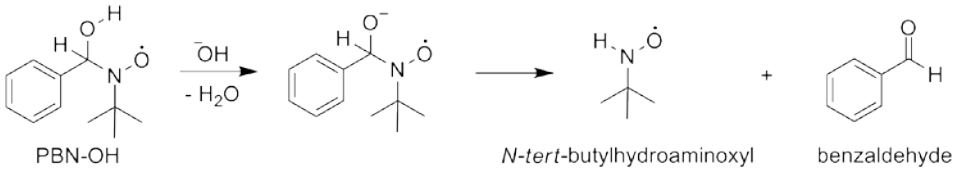

(4-4)

We hypothesize that it could be either PBN-OH radical adduct or *N-tert*-butylhydroaminoxyl that transfers an electron to PBN giving rise to the generation of the H-adduct (Figure 4-7).

The existence of inverted spin trapping in our condition is further supported by the observation that POBN yielded more H-adduct than PBN both in the presence or absence of uric acid. Comparing to PBN, one would predict that POBN may have less potential for oxidation than PBN because of the presence of another nitroxide (N→O) group, which can increase the electron withdrawing ability of POBN.

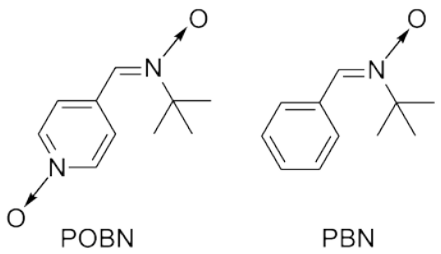

However, the electrochemical study of spin traps by McIntire et al. (*100*) discovered that in fact, PBN is harder to oxidize than POBN. This can be rationalized by the fact that the conjugation between the two nitroxide functions of POBN helps to stabilize the radical cation that is formed after oxidation. On the other hand, POBN radical cation exhibits the number of resonance structures more than PBN (Figure 4-8). As a consequence, POBN is more susceptible toward oxidation by peroxynitrite than PBN, causing more pronounced hydrogen adduct formation according to the inverted spin trapping scheme.

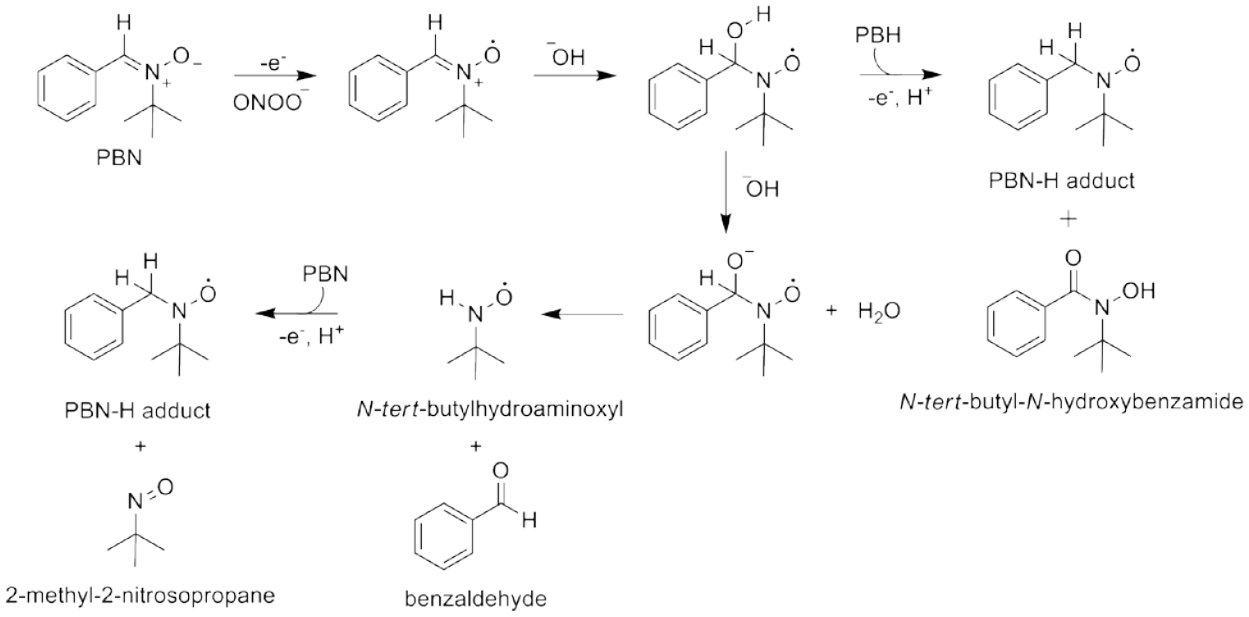

Figure 4-7. Mechanism scheme shows the possible pathway of the PBN-H adduct formation.

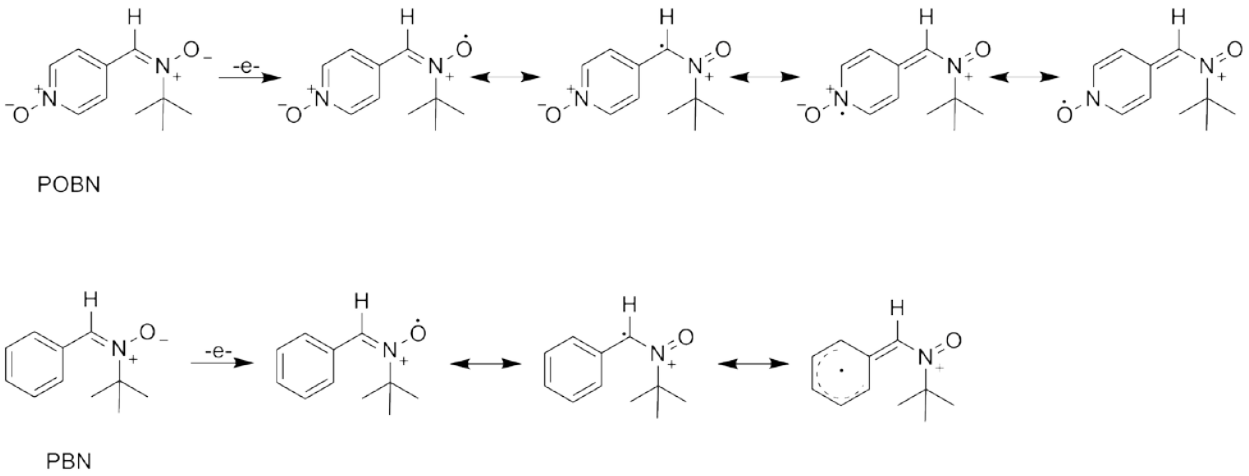

Figure 4-8. The resonance stabilization of POBN and PBN radical cations.

CHAPTER 5
CONCLUSIONS AND SUGGESTIONS FOR FUTURE WORK

Conclusions

By using ESR spin trapping coupled with LC-MS, we have discovered two urate-derived radicals trapped by a spin trap, PBN, from the peroxynitrite-mediated urate oxidation. The structures of the trapped radicals were characterized as the aminocarbonyl radical, which has previously been described (*36*), and the new finding radical—triuretcarbonyl radical, which we proposed to be the intermediate for the formations of aminocarbonyl radical and triuret. Observed by ESR, the radical formation was pH dependent and exhibited lower yield when CO_2 is present. These results indicate that peroxynitrite anion is responsible for the production of the urate-derived radicals. The generation of this radical intermediate may be responsible for the deleterious effect of urate in a biological system.

In addition to uric acid, we have extended our study to investigate the peroxynitrite-mediated oxidation with various methylated uric acid isomers. We have reported the first mass spectrometric analysis of these reactions. In phosphate buffer pH 7.4, the major products from these reactions were methyl triuret dervatives, which were proposed to be produced by radical processes as evidenced by ESR spin trapping results. Methylation at N-7 did not yield any ESR signal; however, the radicals may still be produced, but the formation of the radical adducts are not favored due to the steric effect (Figure 3-10). To trap the reaction intermediate, the reactions were purposely conducted in methanol. The extent of the reactions depended on the position and extent of the substitution (urate = methylurate > dimethylurate > trimethylurate). The administration of methanol resulting in the formation of dimethyl ethers **3** and allantoin derivatives **5** (Figure 3-4) indicated that diimine, a common intermediate found in various urate oxidation conditions, was formed (Figure 3-11 and 3-12). Methylation at N-3, N-7, and N-9

could all reduce the extent of the reaction as compared to the reaction with uric acid, suggesting that the C4-C5 bond of the uric acid scaffold is the initial reaction site. The ability of these methylated uric acid analogues, which exist in the human body, to quench peroxynitrite may prove to be important in their metabolism.

Under a very basic condition, the hydrogen adduct was formed as a major product from the reaction between uric acid and peroxynitrite studied by ESR spin trapping, and it could be observed even without urate. Without uric acid, its formation is proposed to undergo a non-traditional spin trapping process called inverted spin trapping mechanism, followed by the electron transfer between spin traps and the PBN-OH (or POBN-OH) adduct or its decomposition product. The H-adduct formation is amplified when uric acid and peroxynitrite are present. However, the exact nature of this amplification by urate is still unknown. Different yields of H-adducts obtained from various spin traps supported the inverted spin trapping mechanism and can be rationalized by the redox potential of the spin traps.

Suggestions for Future Work

It would be of interest to determine whether a urate radical resulting from one electron oxidation by peroxynitrite is actually formed. Although, the direct detection of a urate radical has been reported in various oxidizing conditions (*32,100,101*), the peroxynitrite-mediated oxidation of urate is still not known. To detect a very short-lived radical, one can use a rapid-mixing/continuous flow set-up coupled with ESR. This would allow enough accumulation of the free radicals to reach the ESR detection limit. It would also be of interest in terms of urate-peroxynitrite mechanism to determine if one of the oxygen of triuret is derived from peroxynitrite as proposed in Figure 2-12. One can synthesize peroxynitrite with ^{18}O isotope labeled. The oxygen attached to C-2 of triuret should be labeled (Equation 5-1).

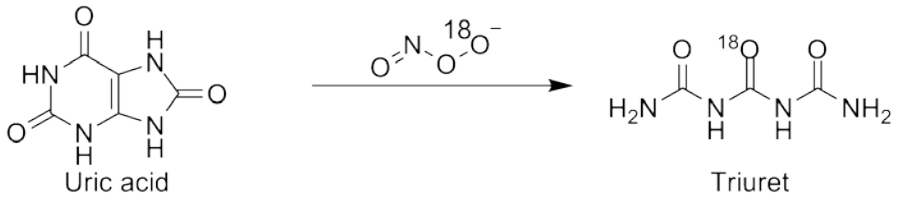

(5-1)

Based on the finding of the hydrogen adduct, it would be worthwhile to investigate the H-adduct formation in the presence of 1,1,1,3,3,3-hexafluoropropan-2-ol (HFP), which is a solvent reported to suppress the effect on the inverted spin trapping mechanism (*101*). If the H-adduct formation is indeed generated by inverted spin trapping mechanism, its yield should be decreased when HFP is present

Another interesting topic for uric acid chemistry is the complex formation between uric acid and transition metals. It has been shown that uric acid can form complexes with transition metal ions such as Cd(II) and Pb(II) (*102*). Little is known if transion metal ions can stabilize urate-derived radicals. Our preliminary results showed that an EPR signal was observed from the incubation of uric acid with peroxynitrite, in the presence of Cd(II) or Zn(II) (Appendix D).Unfortunately, we could not identify the structures of these complexes because of their poor solubility. It is necessary to investigate the method to purify these complexes for further structural characterization.

The oxidant-antioxidant paradox of uric acid is still a major interest among researchers. Therefore, the chemistry of uric acid, with oxidant like peroxynitrite, deserves further investigation to complete the jigsaw that is still missing from its mechanism scheme.

APPENDIX A
LC CHROMATOGRAMS AND ELECTROSPRAY MASS SPECTRA OBTAINED FROM THE REACTIONS OF VARIOUS METHYLATED URIC ACIDS WITH PEROXYNITRITE CONDUCTED IN PHOSPHATE BUFFER

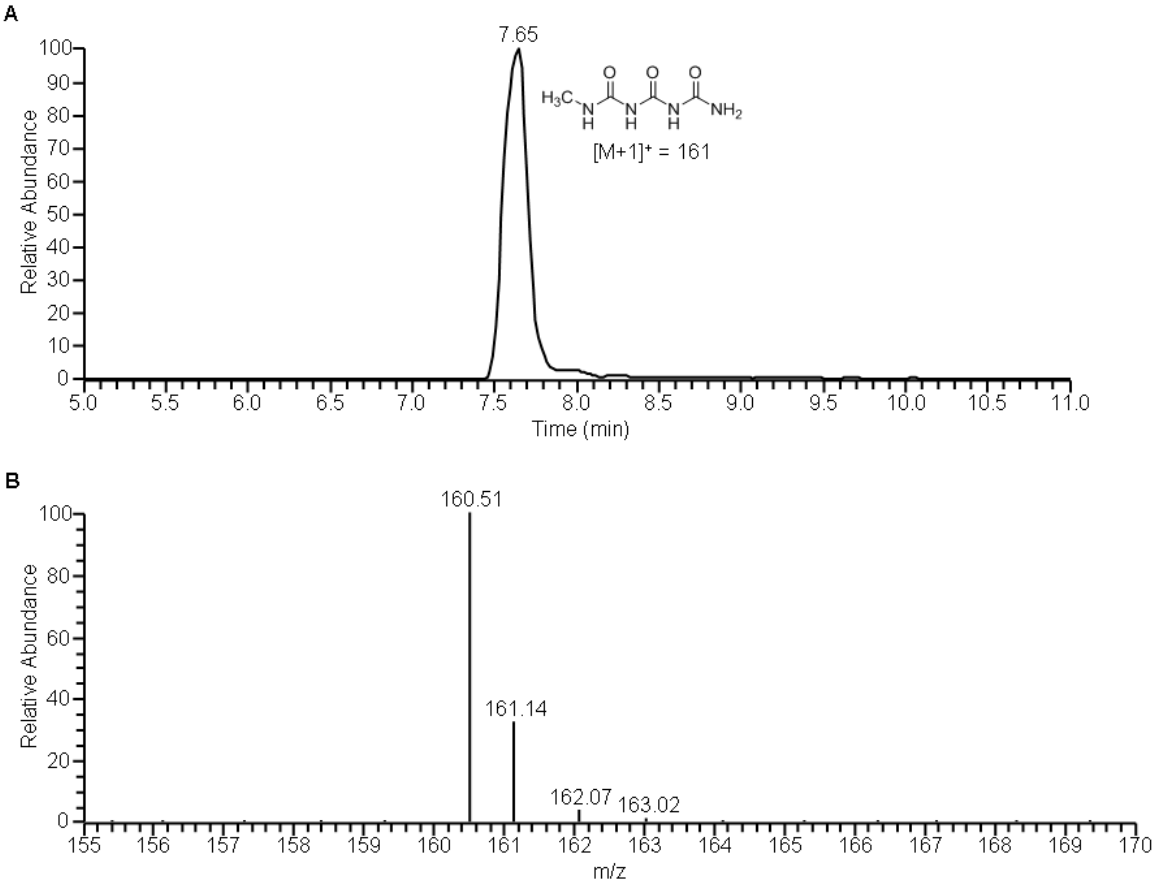

Figure A-1. LC-MS study of the reaction between 1-methyluric acid and peroxynitrite in phosphate buffer pH 7.4. (A) LC chromatogram obtained from the incubation of 10 mM 1-methylurate, 0.1 mM DTPA anf 30 mM peroxynitrite in 0.5 M phosphate buffer pH 7.4. (B) Electrospray mass spectrum of triuret conducted in positive mode.

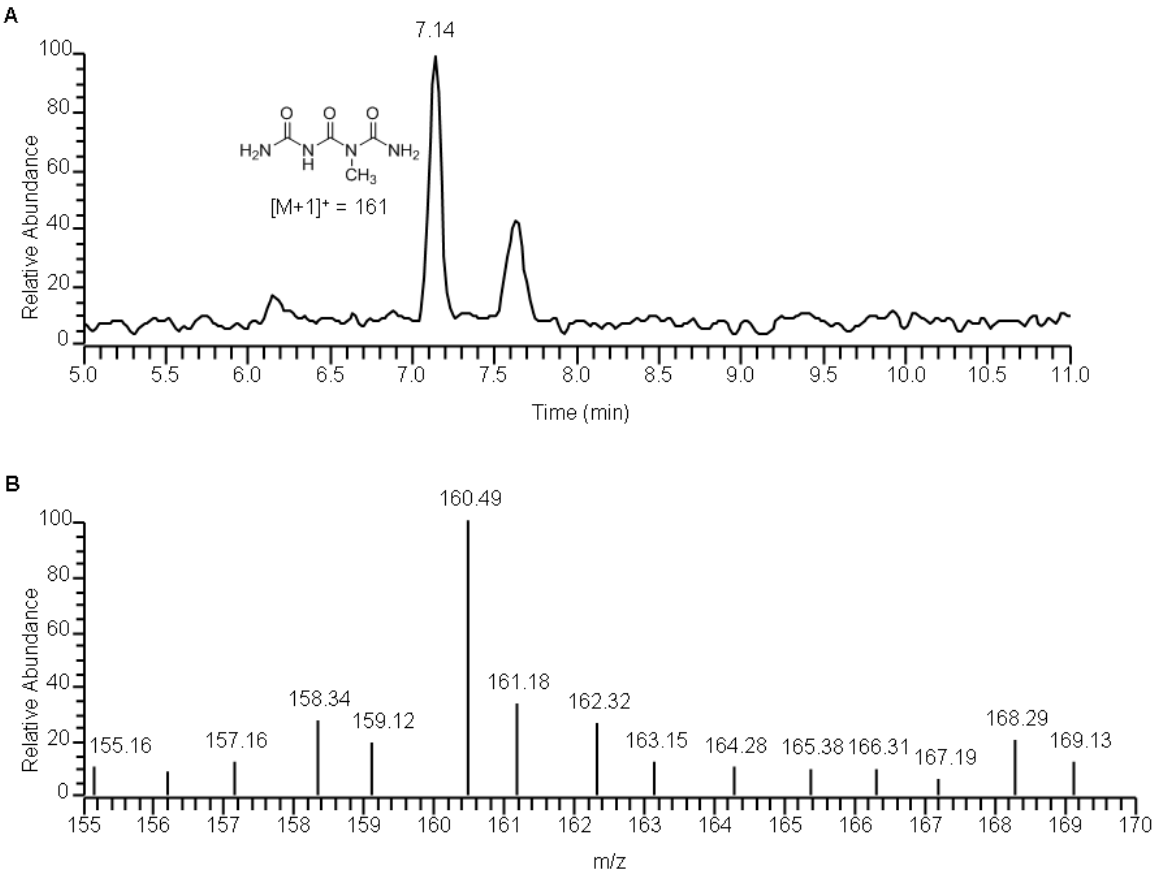

Figure A-2. LC-MS study of the reaction between 9-methyluric acid and peroxynitrite in phosphate buffer pH 7.4. (A) LC chromatogram obtained from the incubation of 10 mM 9-methylurate, 0.1 mM DTPA anf 30 mM peroxynitrite in 0.5 M phosphate buffer pH 7.4. (B) Electrospray mass spectrum of triuret conducted in positive mode.

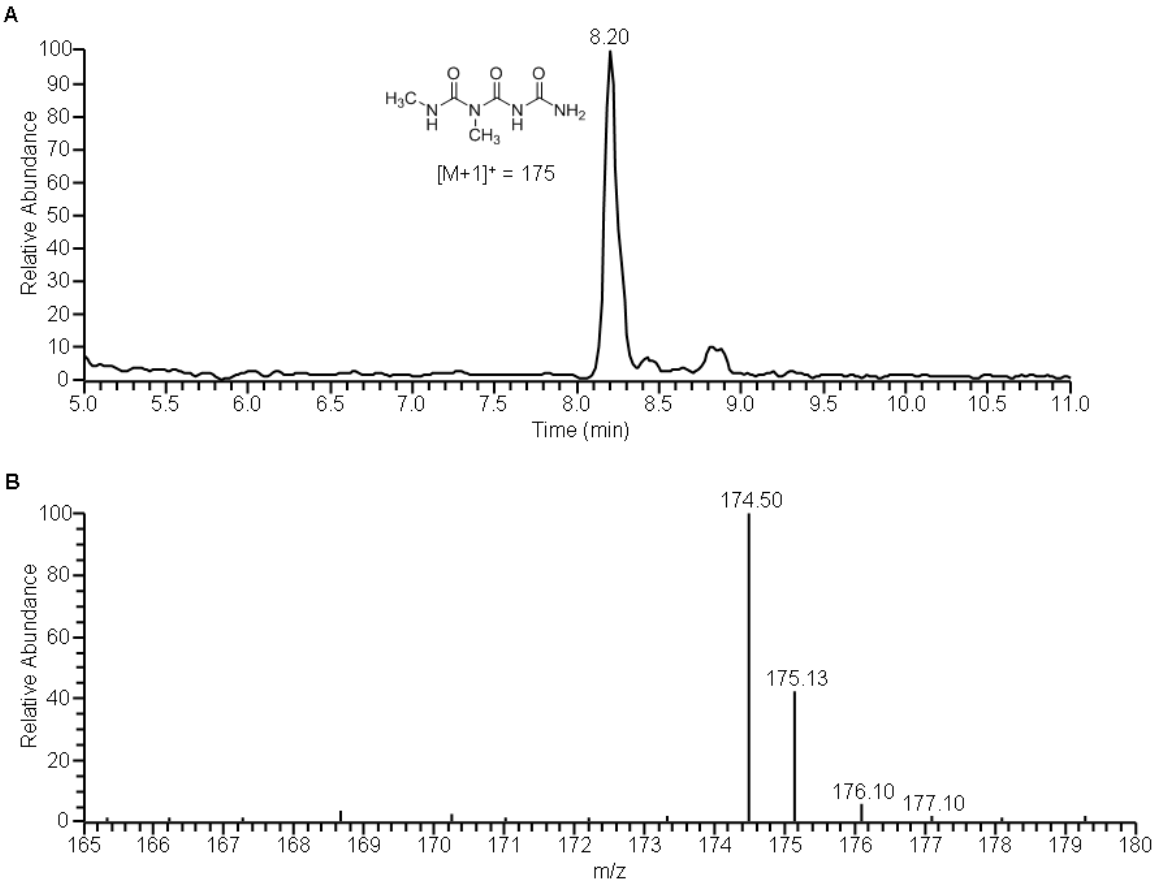

Figure A-3. LC-MS study of the reaction between 1,3-dimethyluric acid and peroxynitrite in phosphate buffer pH 7.4. (A) LC chromatogram obtained from the incubation of 10 mM 1,3-dimethylurate, 0.1 mM DTPA anf 30 mM peroxynitrite in 0.5 M phosphate buffer pH 7.4. (B) Electrospray mass spectrum of triuret conducted in positive mode.

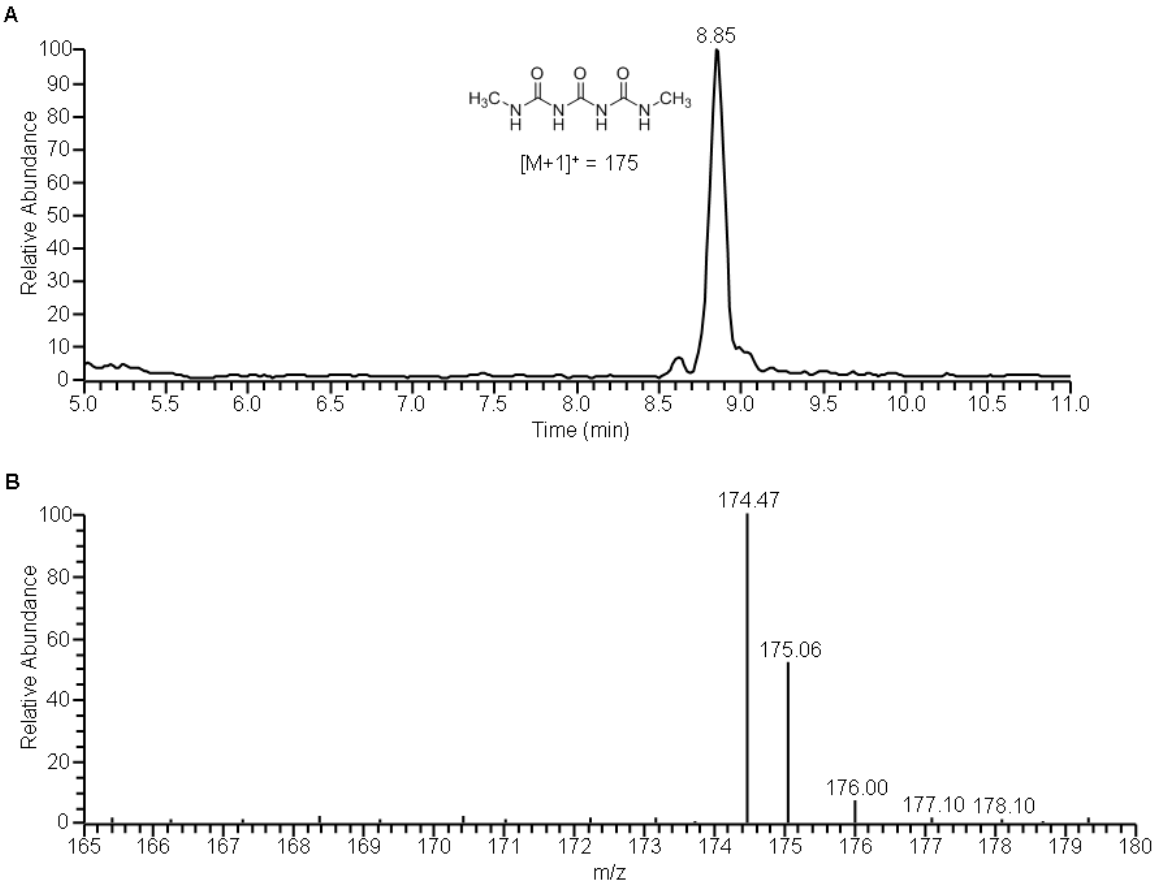

Figure A-4. LC-MS study of the reaction between 1,7-dimethyluric acid and peroxynitrite in phosphate buffer pH 7.4. (A) LC chromatogram obtained from the incubation of 10 mM 1,7-dimethylurate, 0.1 mM DTPA anf 30 mM peroxynitrite in 0.5 M phosphate buffer pH 7.4. (B) Electrospray mass spectrum of triuret conducted in positive mode.

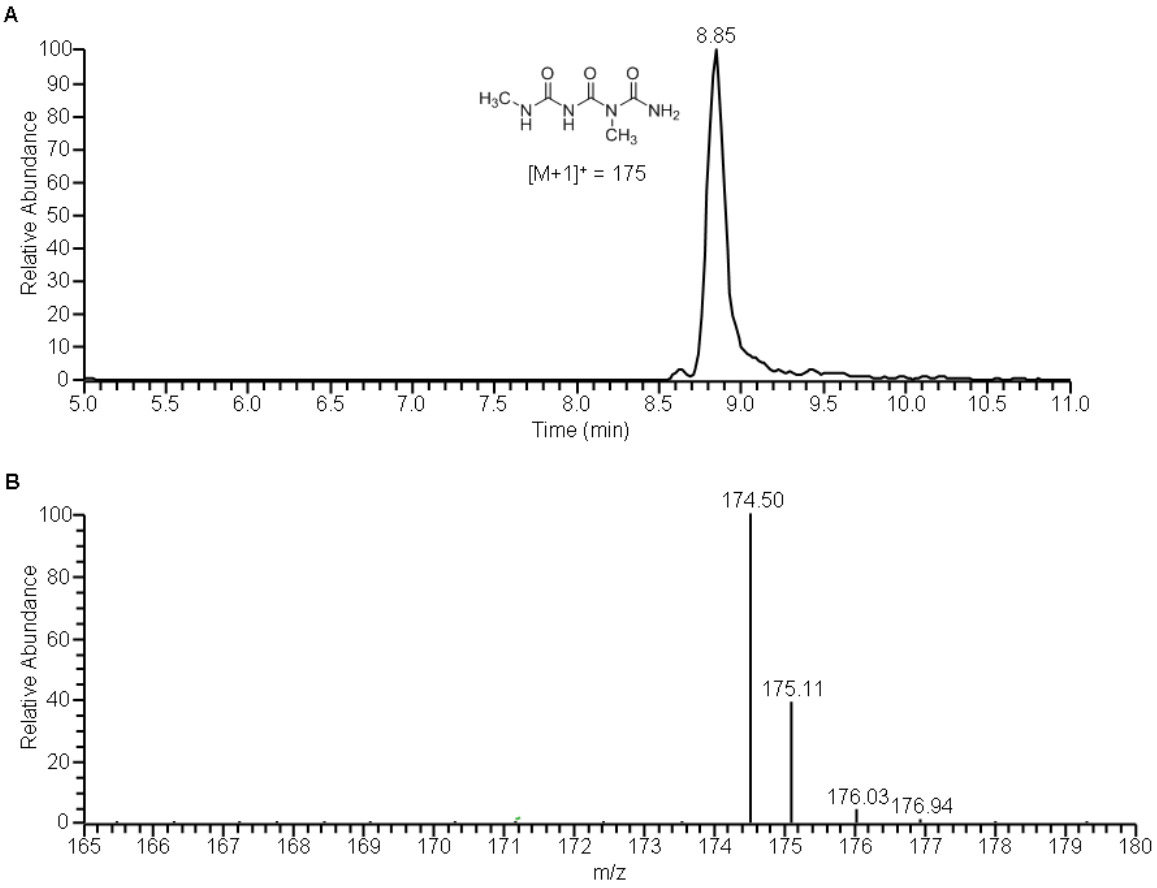

Figure A-5. LC-MS study of the reaction between 1,9-dimethyluric acid and peroxynitrite in phosphate buffer pH 7.4. (A) LC chromatogram obtained from the incubation of 10 mM 1,9-dimethylurate, 0.1 mM DTPA anf 30 mM peroxynitrite in 0.5 M phosphate buffer pH 7.4. (B) Electrospray mass spectrum of triuret conducted in positive mode.

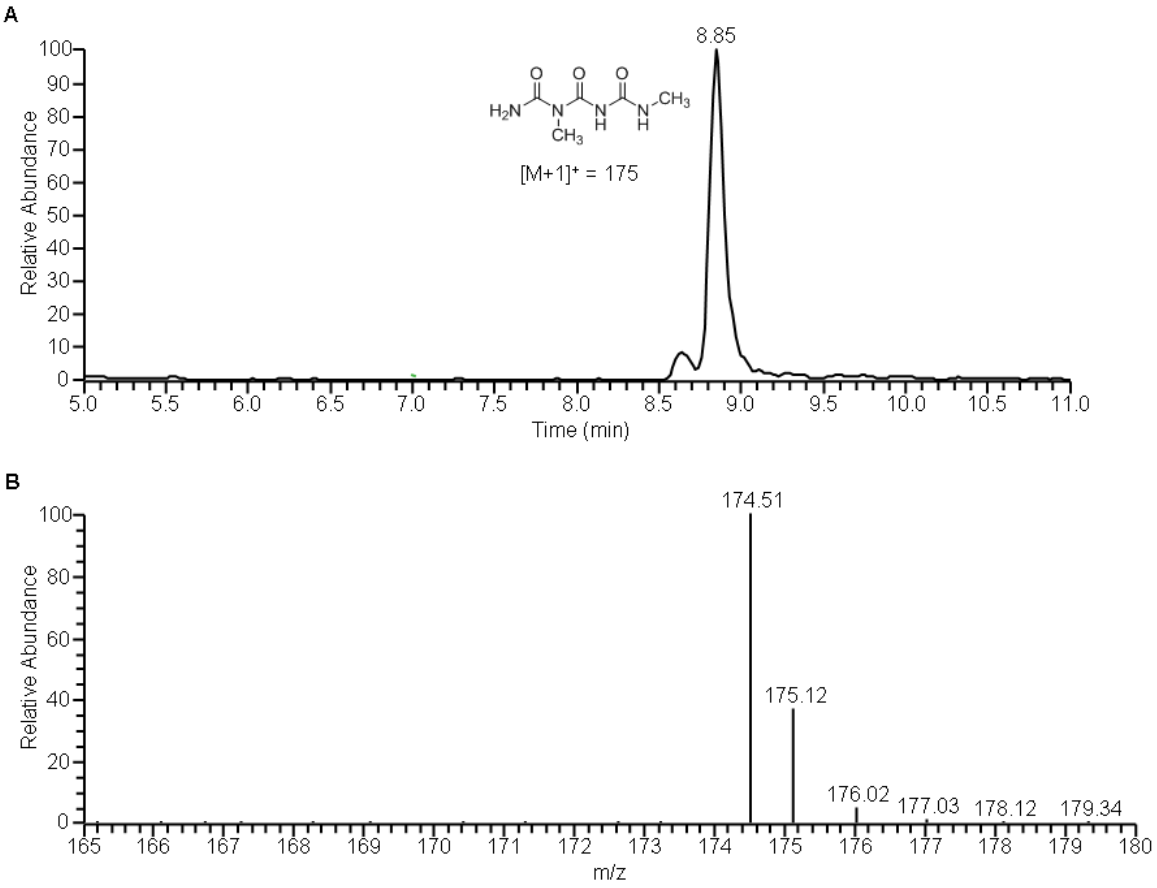

Figure A-6. LC-MS study of the reaction between 3,7-dimethyluric acid and peroxynitrite in phosphate buffer pH 7.4. (A) LC chromatogram obtained from the incubation of 10 mM 3,7-dimethylurate, 0.1 mM DTPA anf 30 mM peroxynitrite in 0.5 M phosphate buffer pH 7.4. (B) Electrospray mass spectrum of triuret conducted in positive mode.

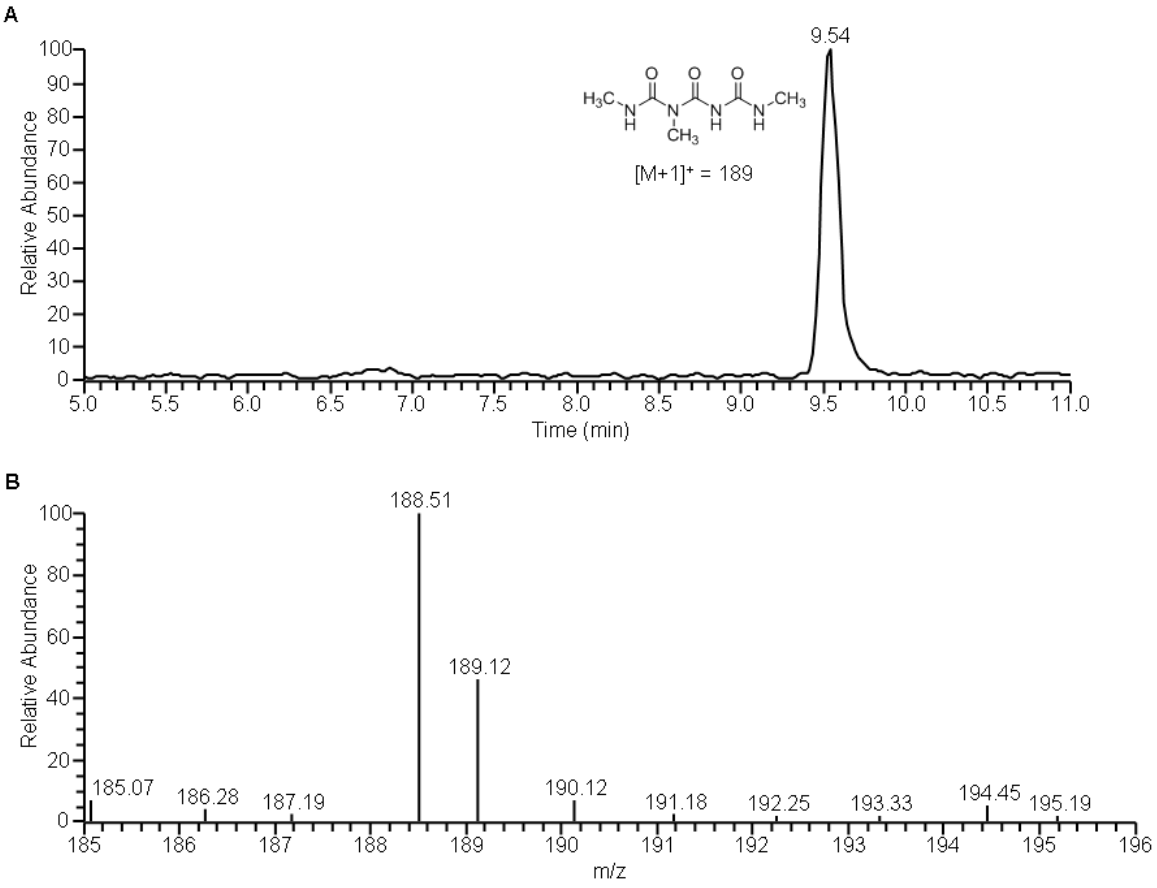

Figure A-7. LC-MS study of the reaction between 1,3,7-trimethyluric acid and peroxynitrite in phosphate buffer pH 7.4. (A) LC chromatogram obtained from the incubation of 10 mM 1,3,7-trimethylurate, 0.1 mM DTPA anf 30 mM peroxynitrite in 0.5 M phosphate buffer pH 7.4. (B) Electrospray mass spectrum of triuret conducted in positive mode.

APPENDIX B
LC CHROMATOGRAMS OBTAINED FROM THE REACTIONS OF VARIOUS METHYLATED URIC ACIDS WITH PEROXYNITRITE CONDUCTED IN METHANOL

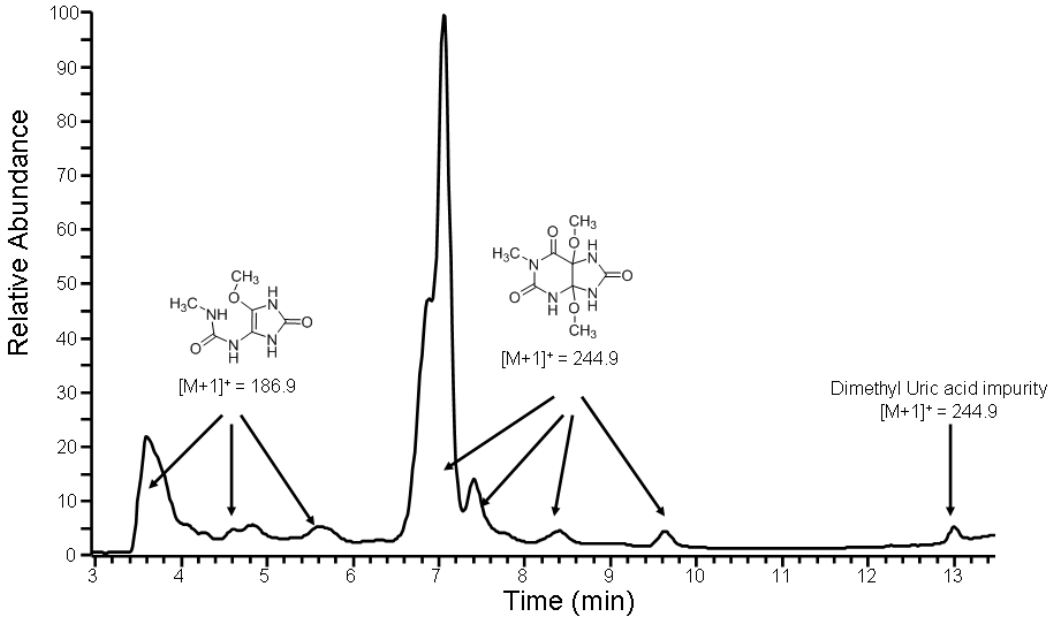

Figure B-1. LC chromatogram of 10 mM 1-methylurate treated with 10 mM peroxynitrite in 50% methanol and 50% aqueous phosphate buffer solution at pH 7.4.

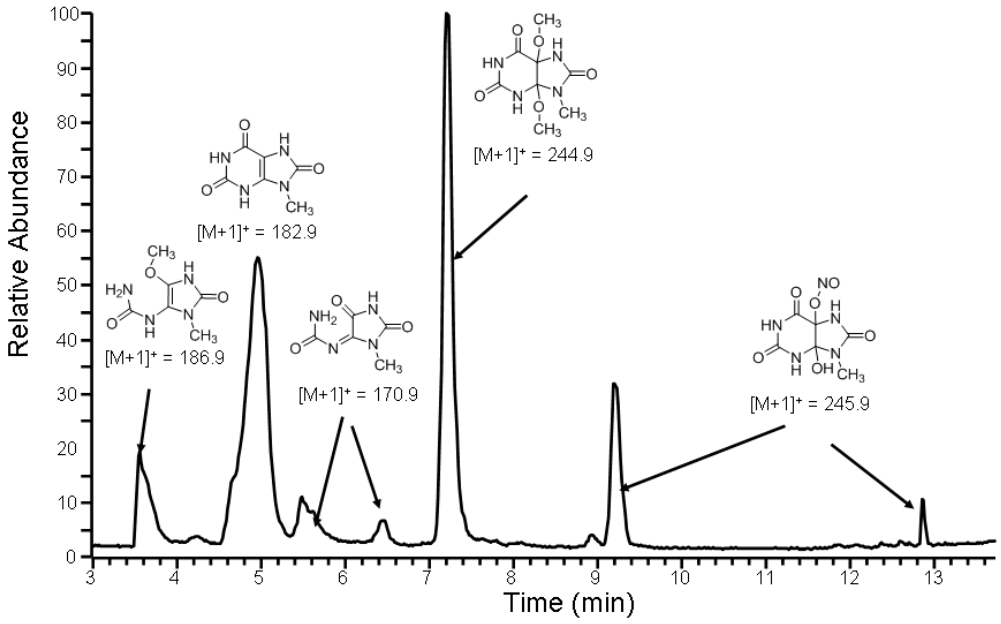

Figure B-2. LC chromatogram of 10 mM 9-methylurate treated with 10 mM peroxynitrite in 50% methanol and 50% aqueous phosphate buffer solution at pH 7.4.

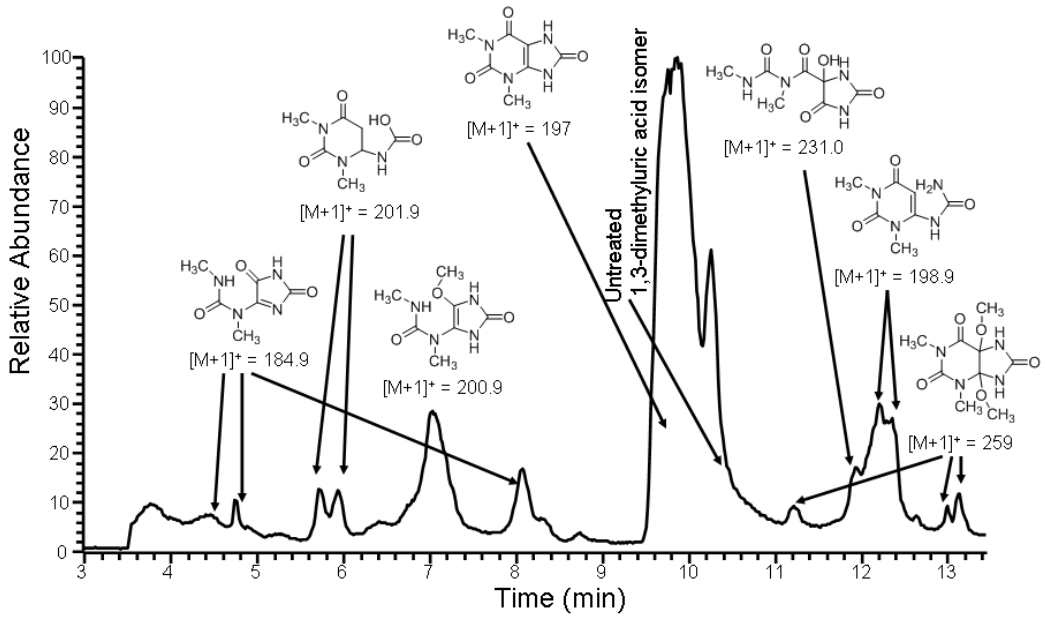

Figure B-3. LC chromatogram of 10 mM 1,3-dimethylurate treated with 10 mM peroxynitrite in 50% methanol and 50% aqueous phosphate buffer solution at pH 7.4.

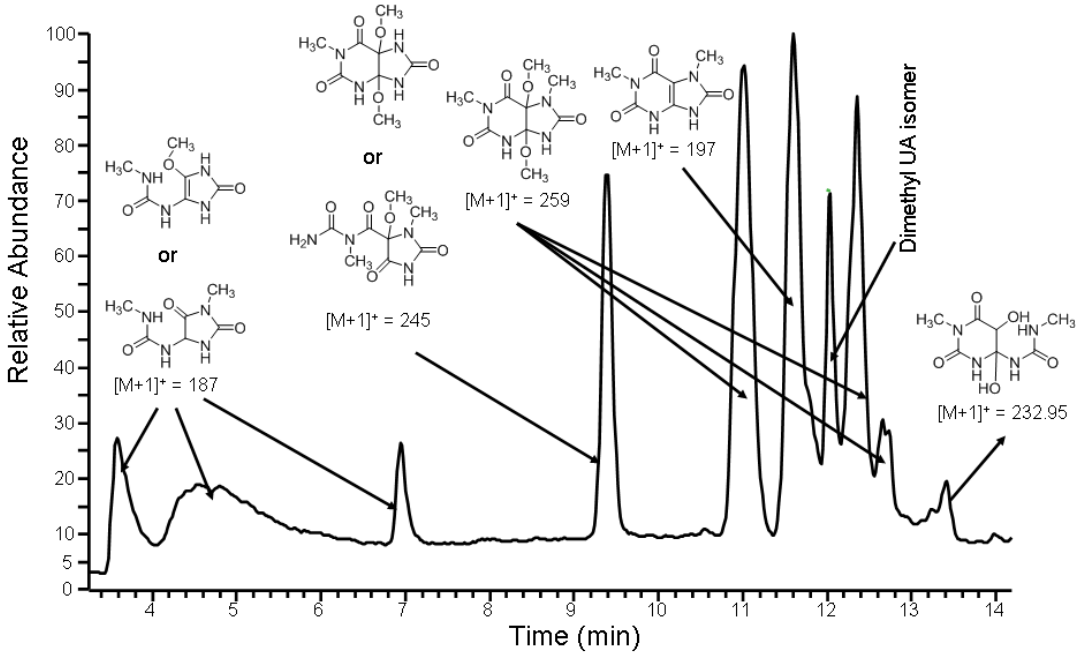

Figure B-4. LC chromatogram of 10 mM 1,7-dimethylurate treated with 10 mM peroxynitrite in 50% methanol and 50% aqueous phosphate buffer solution at pH 7.4.

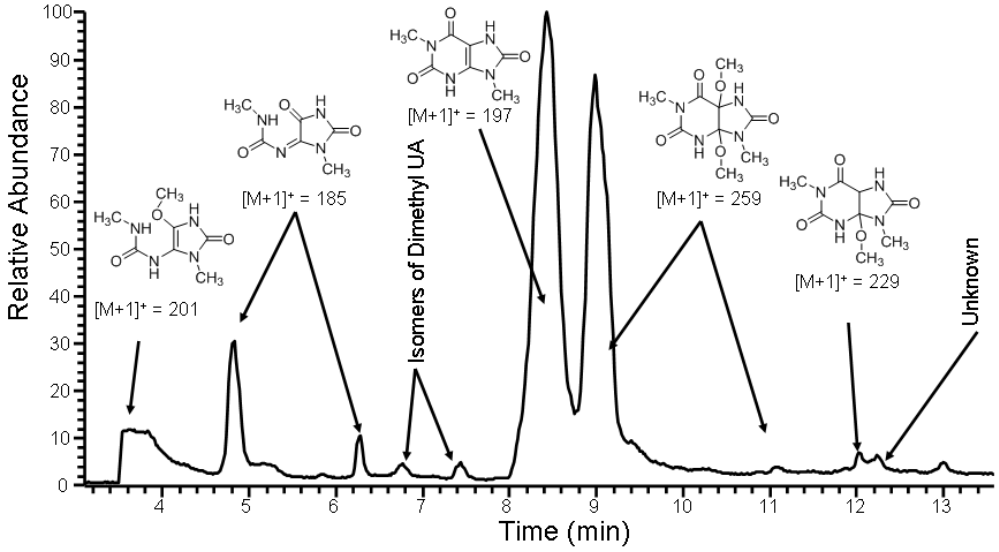

Figure B-5. LC chromatogram of 10 mM 1,9-dimethylurate treated with 10 mM peroxynitrite in 50% methanol and 50% aqueous phosphate buffer solution at pH 7.4.

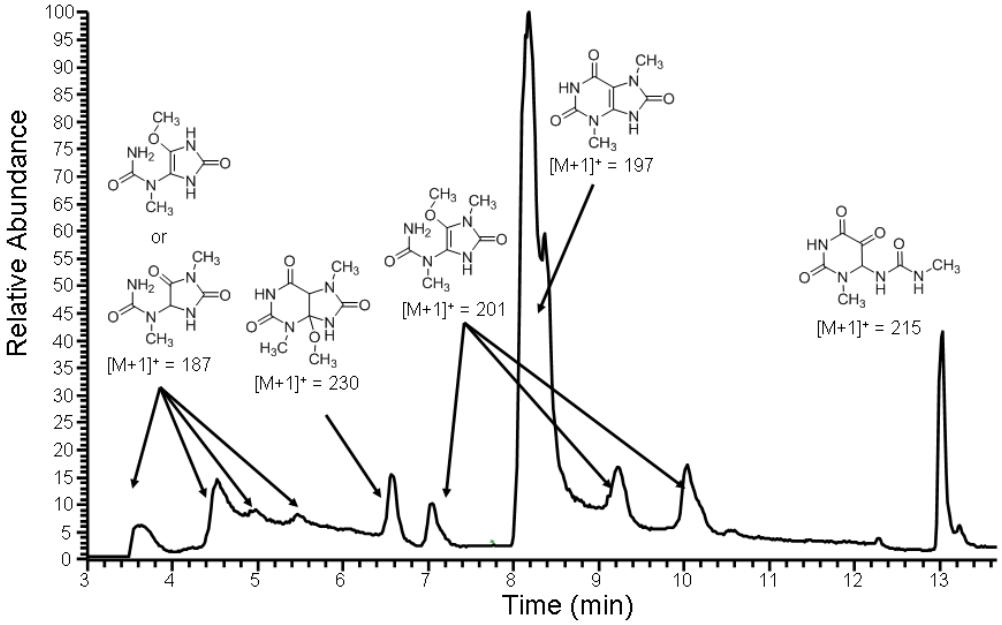

Figure B-6. LC chromatogram of 10 mM 3,7-dimethylurate treated with 10 mM peroxynitrite in 50% methanol and 50% aqueous phosphate buffer solution at pH 7.4.

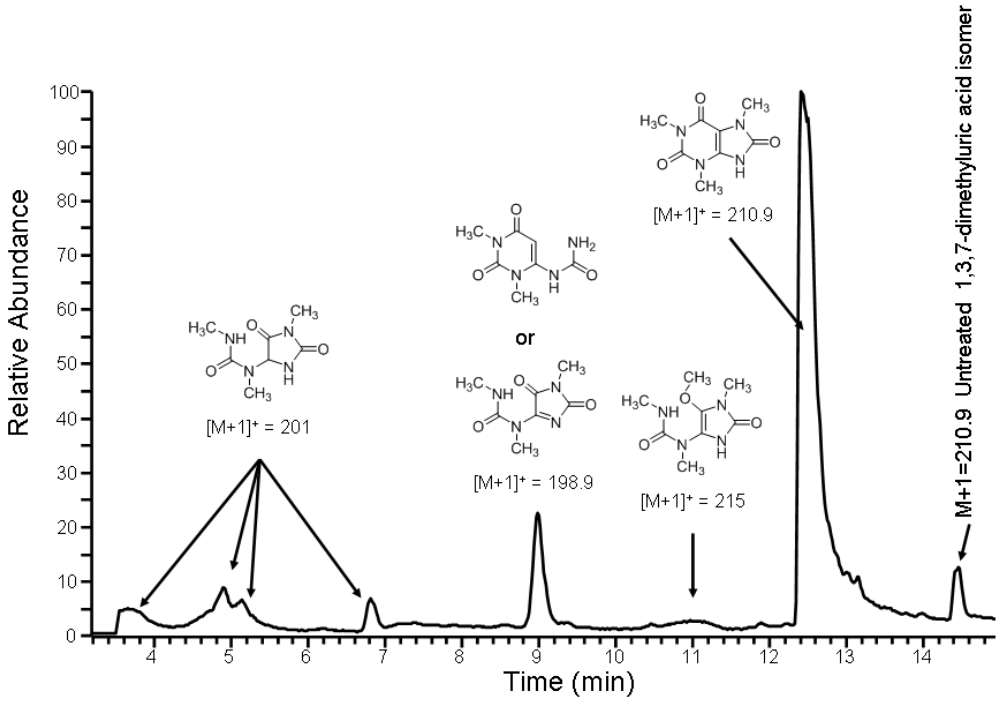

Figure B-7. LC chromatogram of 10 mM 1,3,7-trimethylurate treated with 10 mM peroxynitrite in 50% methanol and 50% aqueous phosphate buffer solution at pH 7.4.

APPENDIX C
FRAGMENTATION PATTERNS OF DIMETHOXYDEHYDROURIC ACIDS

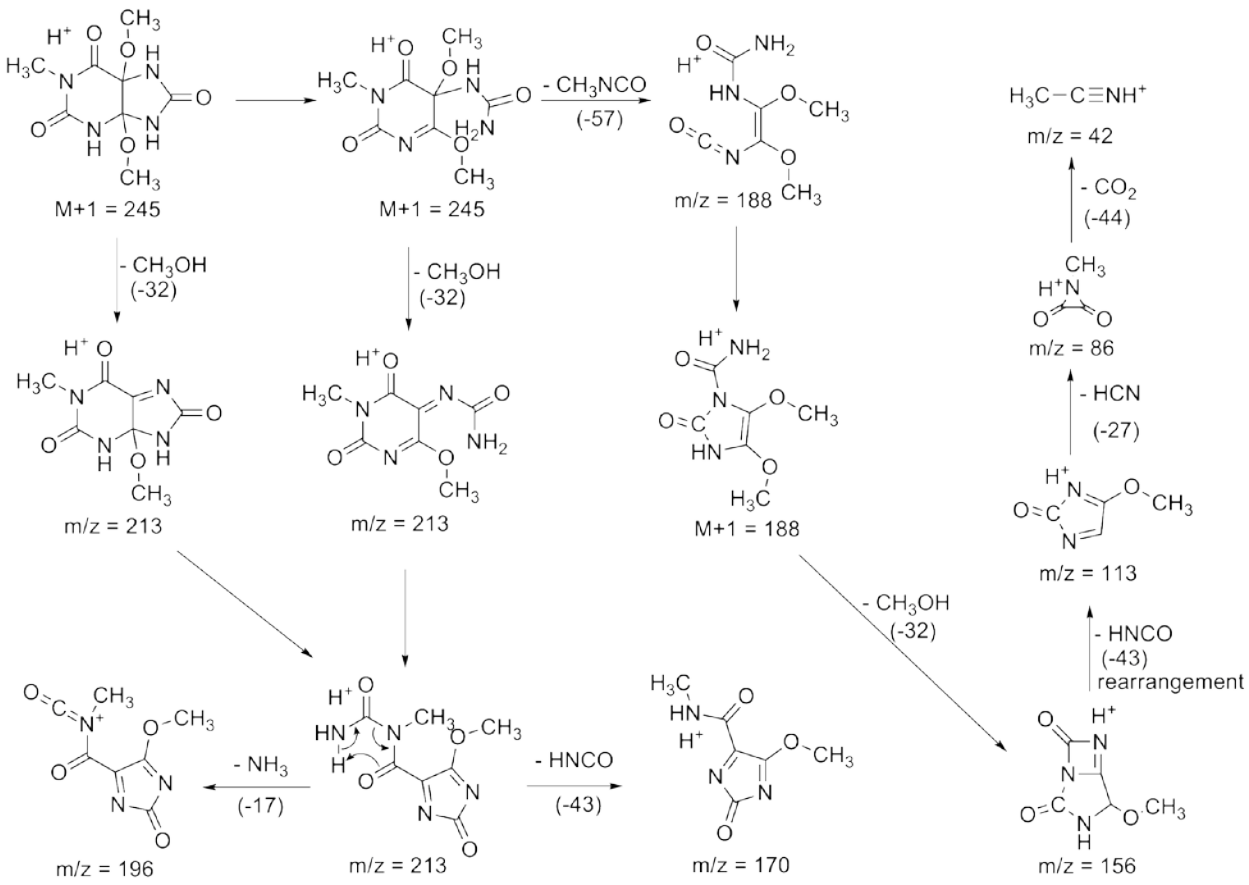

Figure C-1. Fragmentation pattern of 1-methyluric acid glycol dimethyl ether **3b**.

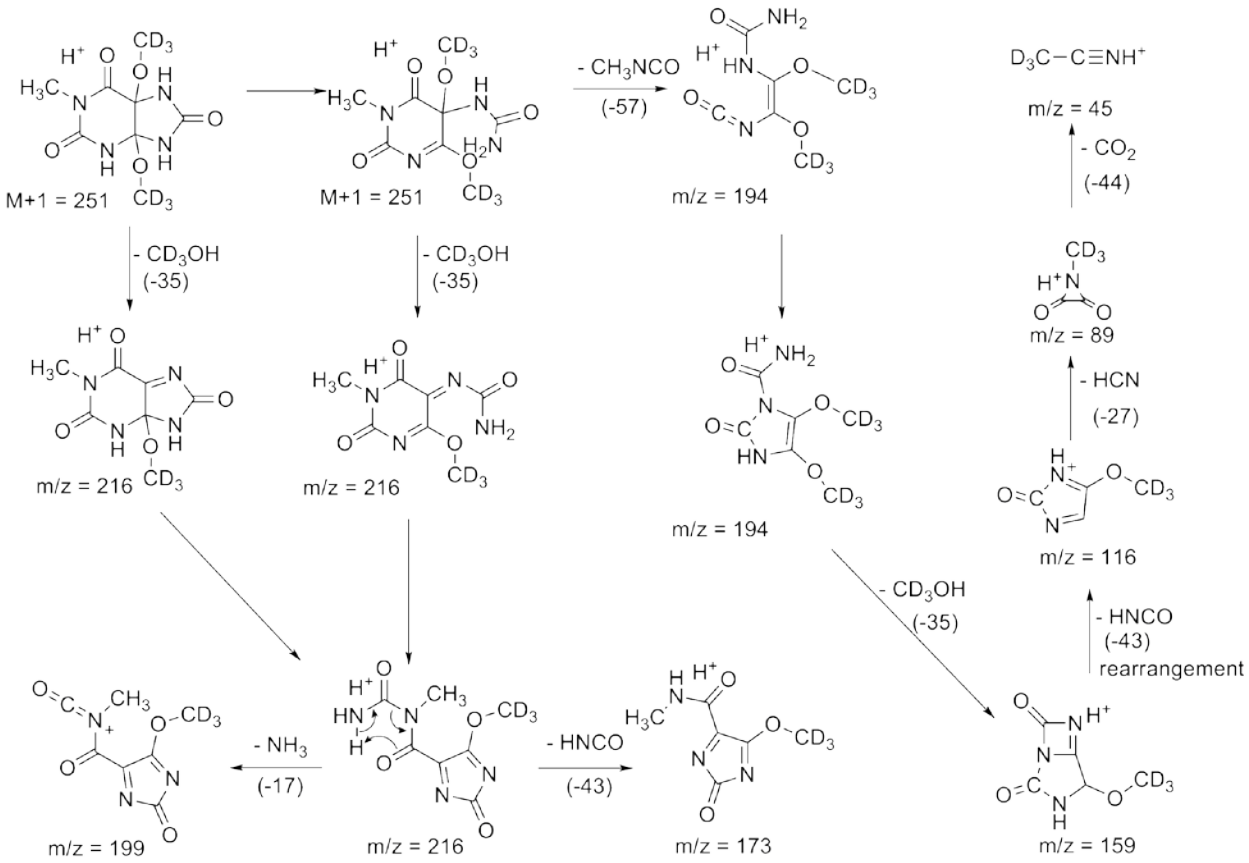

Figure C-2. Fragmentation pattern of 1-methyluric acid glycol di-d_3-methyl ether **3b**.

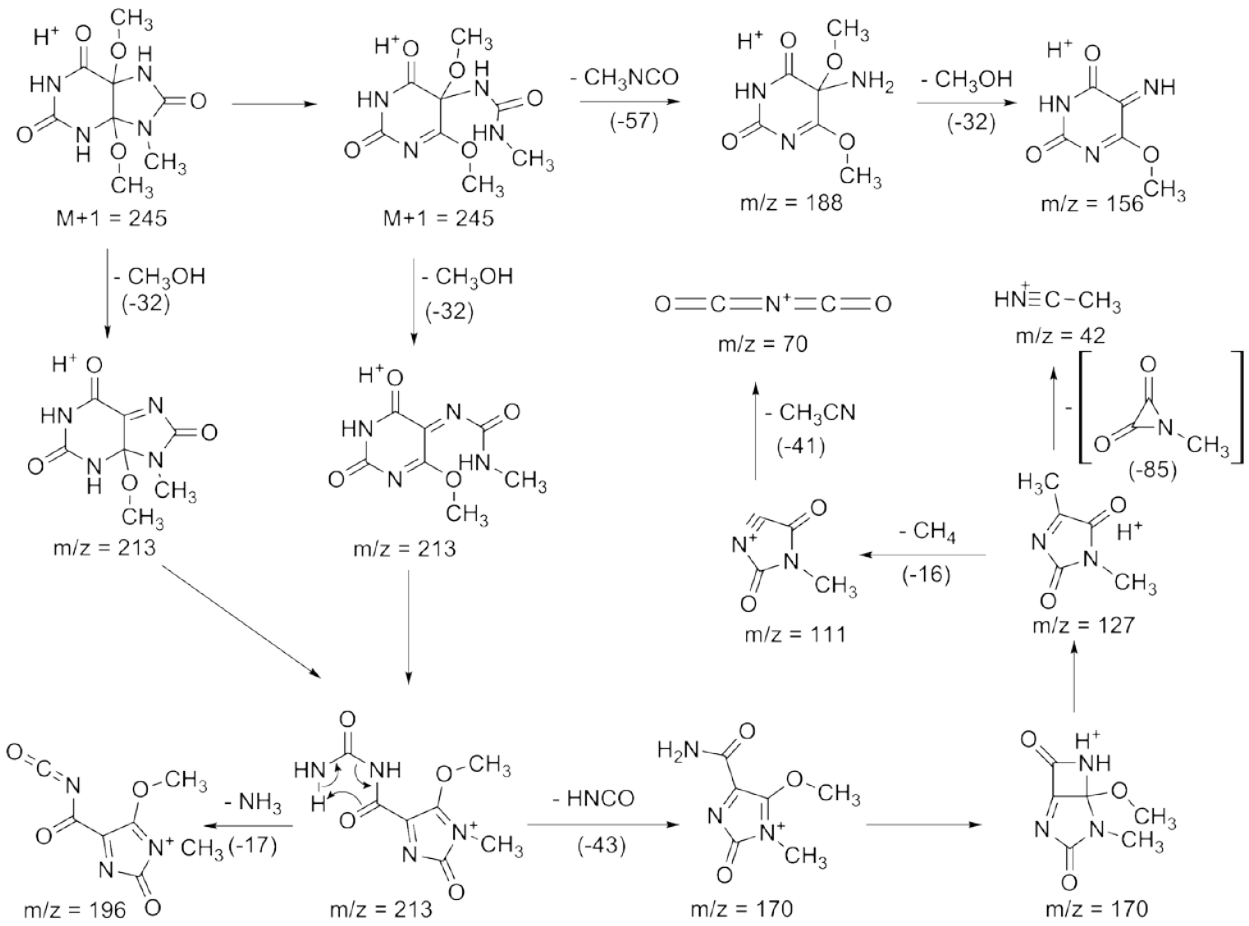

Figure C-3. Fragmentation pattern of 9-methyluric acid glycol dimethyl ether **3c**.

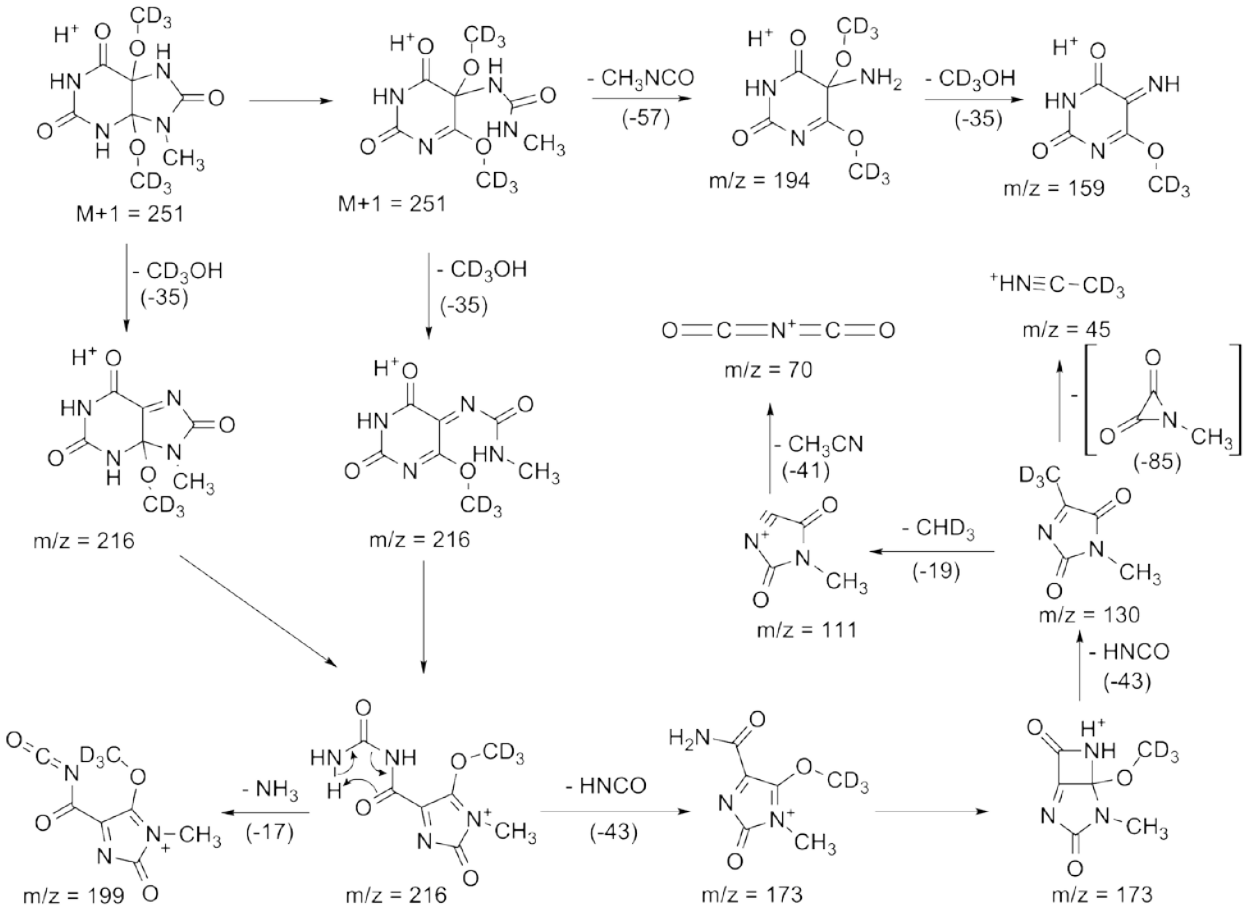

Figure C-4. Fragmentation pattern of 9-methyluric acid glycol di-d_3-methyl ether **3c**.

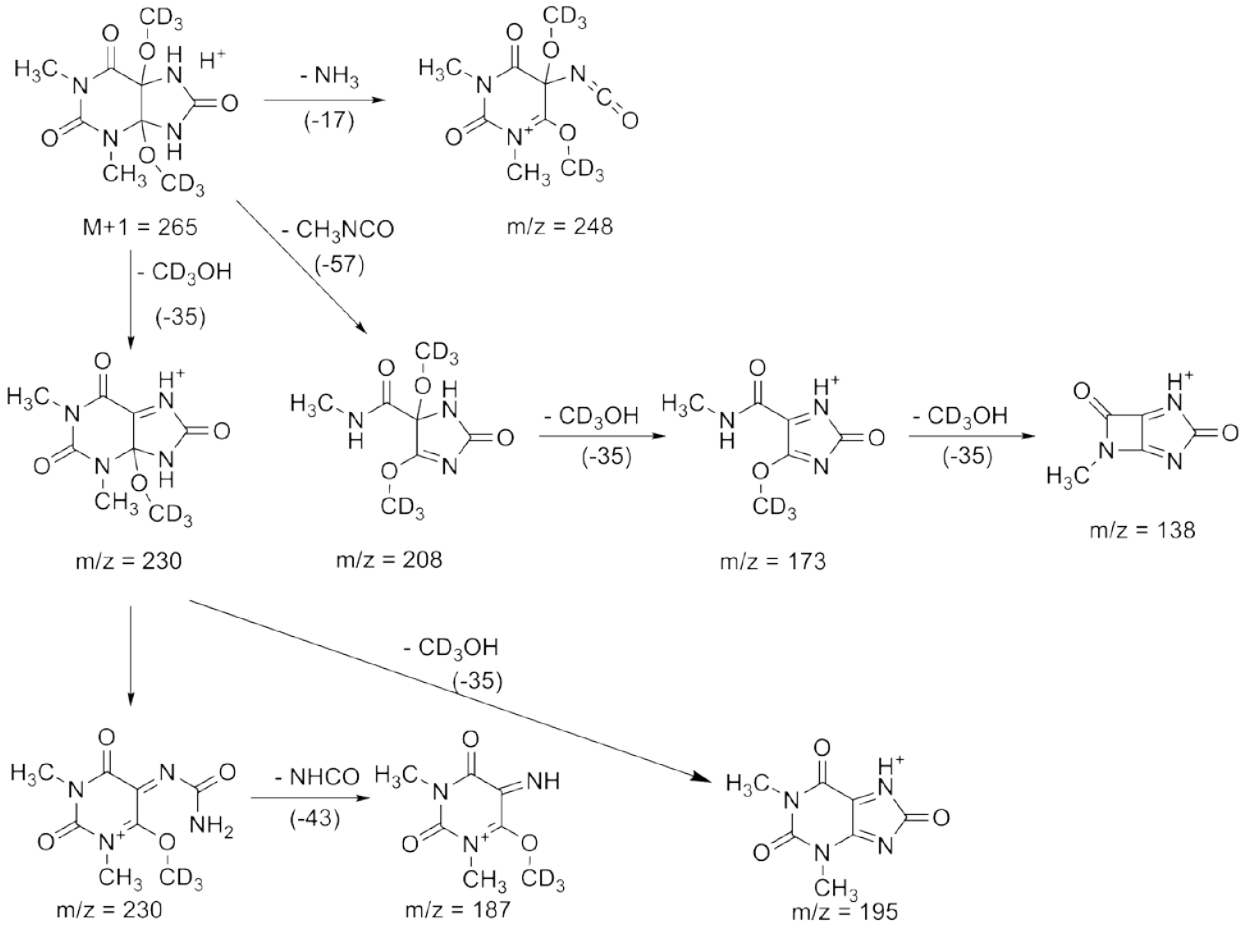

Figure C-5. Fragmentation pattern of 1,3-dimethyluric acid glycol di-d_3-methyl ether **3d**.

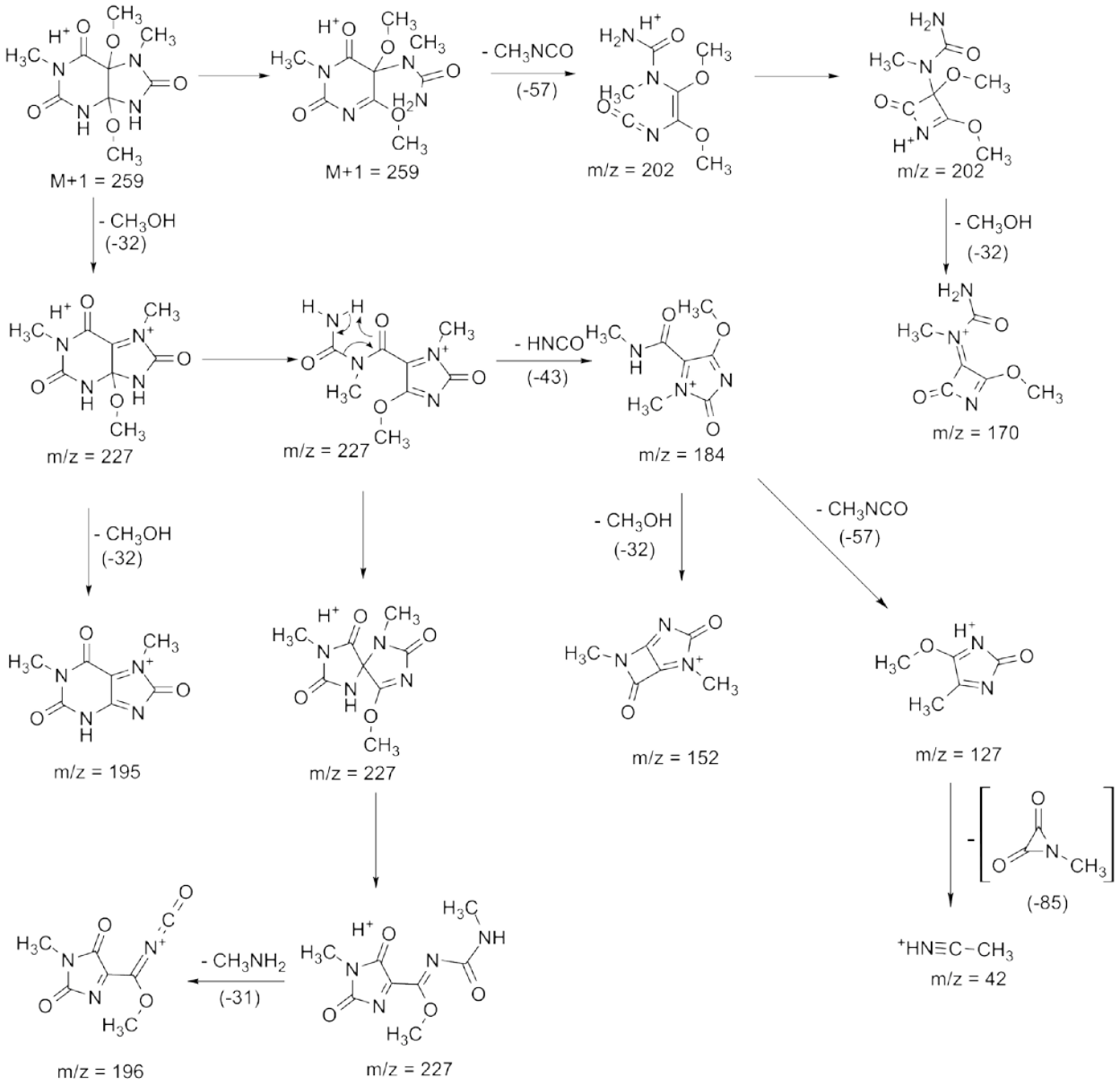

Figure C-6. Fragmentation pattern of 1,7-dimethyluric acid glycol dimethyl ether **3e**.

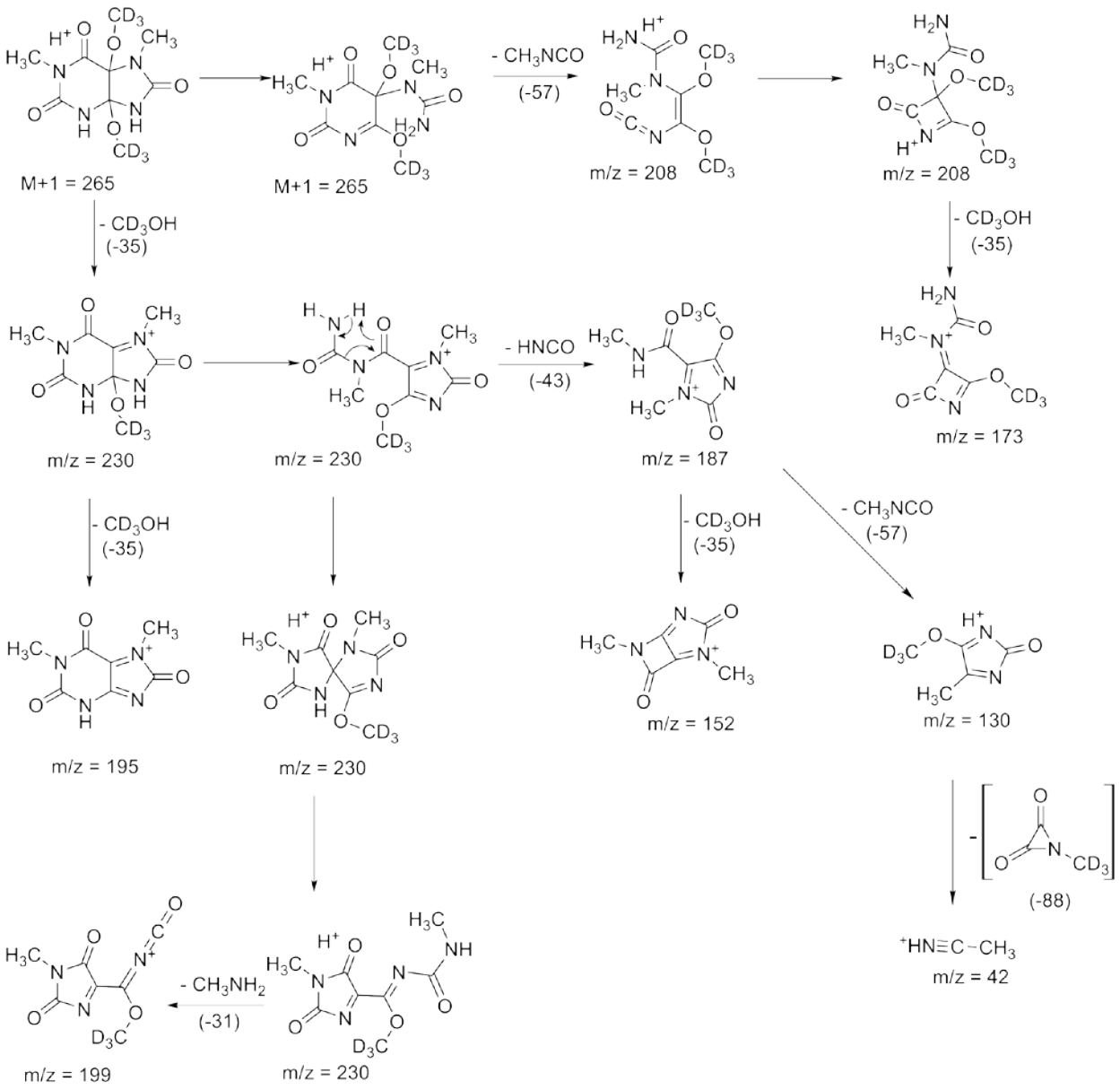

Figure C-7. Fragmentation pattern of 1,7-dimethyluric acid glycol di-d_3-methyl ether **3e**.

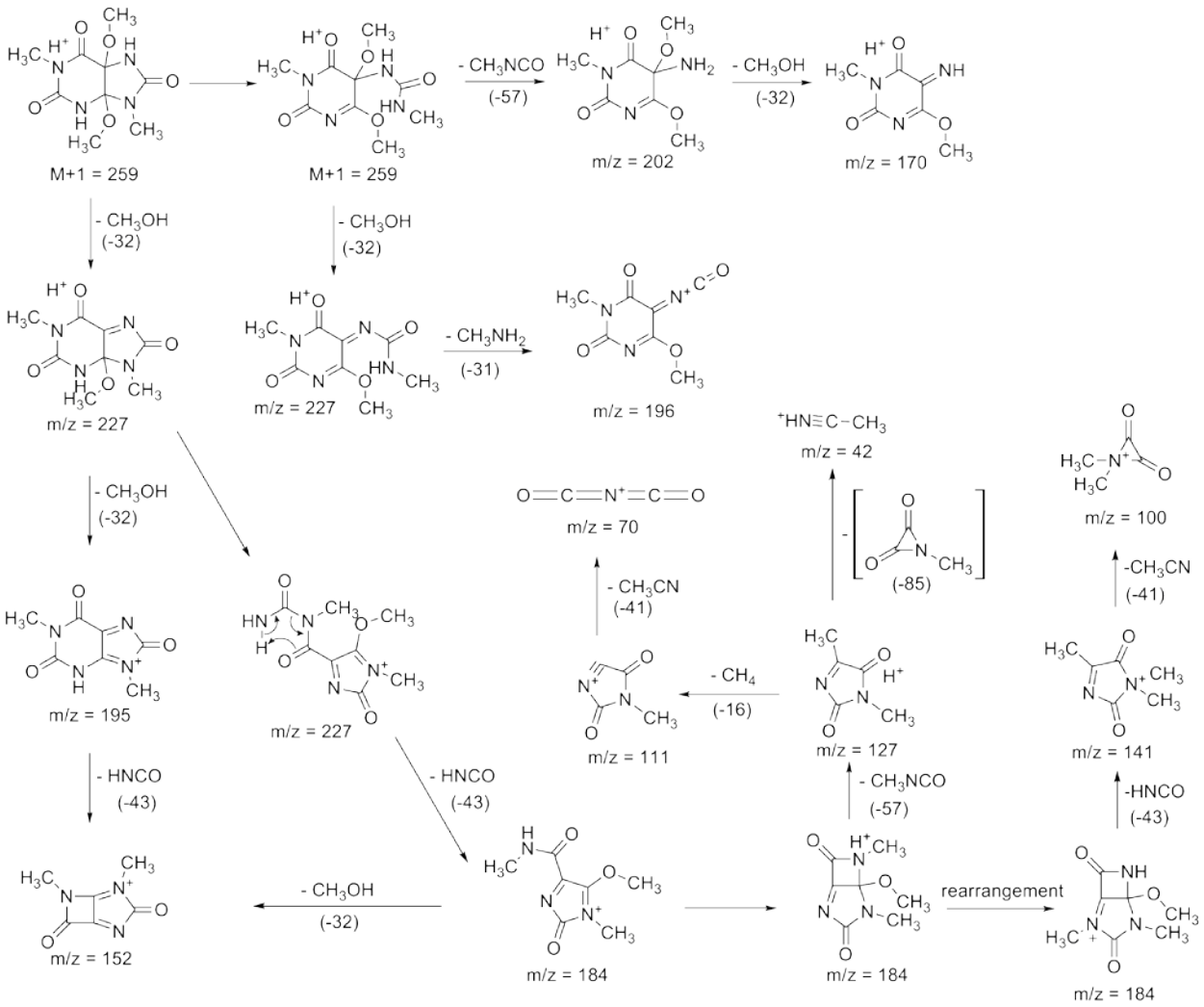

Figure C-8. Fragmentation pattern of 1,9-dimethyluric acid glycol dimethyl ether **3f**.

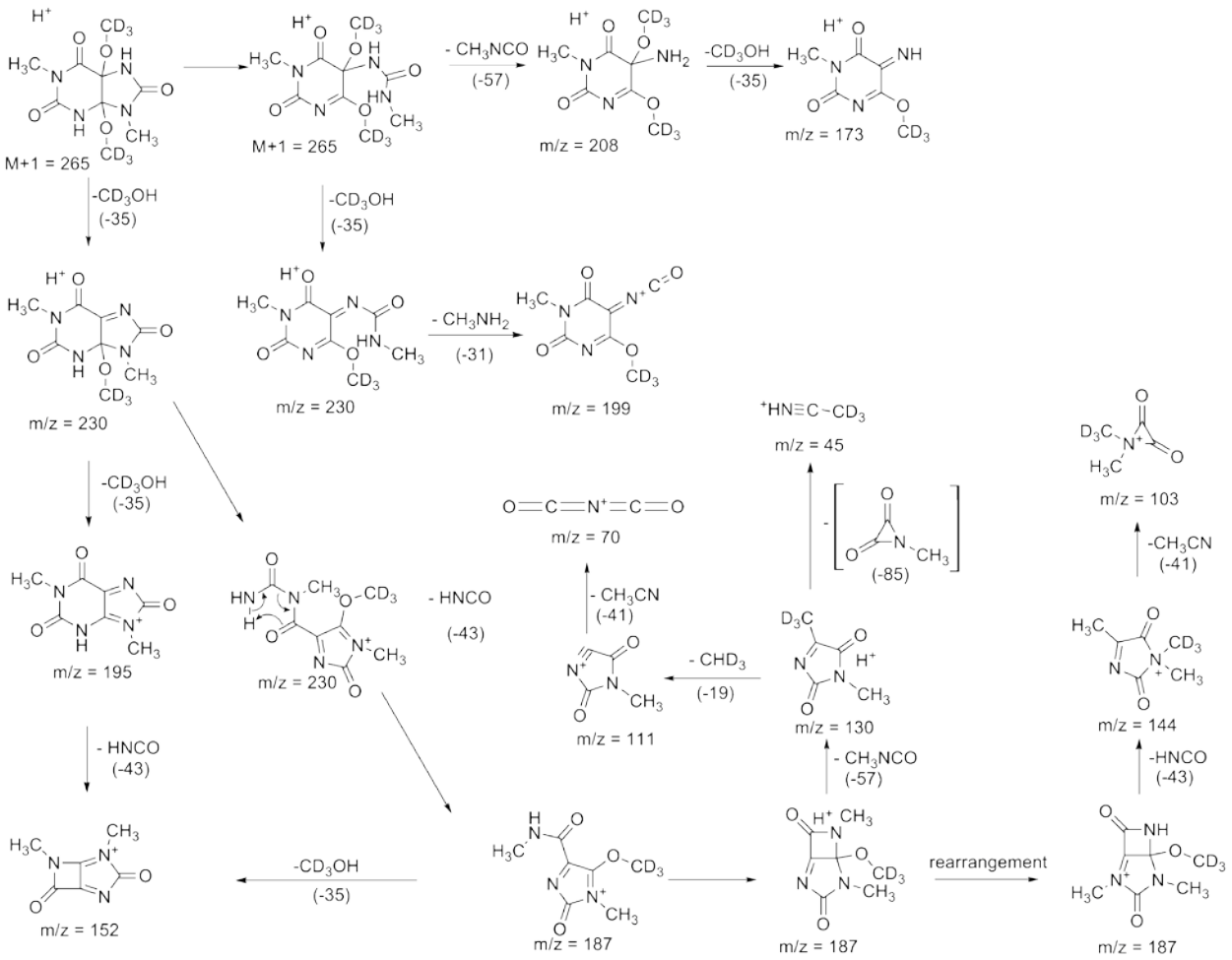

Figure C-9. Fragmentation pattern of 1,9-dimethyluric acid glycol di-d_3-methyl ether **3f**.

APPENDIX D
EFFECT OF DIVALENT METAL IONS ON THE REACTION BETWEEN URIC ACID AND PEROXYNITRITE

Introduction

We extended our study to investigate the effect of divalent metal ions on the stability of the urate derived radicals generated from the reaction between uric acid and peroxynitrite at pH 12. The nine divalent metal ions, Ca(II), Zn(II), Mg(II), Cu(II), Ni(II), Co(II), Fe(II), Cd(II) and Mn(II) were tested and monitored by X-band EPR.

Materials and Methods

Chemicals. Uric aid was purchased from Sigma. L-(+)-Ascorbic Acid was purchased from Fisher and isoamyl nitrite was purchased from Acros Organics. All of the divalent metals used were in the form of chloride salts and purchased from Fisher. Urate stock solutions were prepared with 0.3 M potassium hydroxide (100 mM urate). Peroxynitrite was synthesized according to Uppu and Pryor (*76*). The peroxynitrite stock solution concentration was measured spectrophotometrically at 302 nm ($\varepsilon = 1670\ M^{-1}\ cm^{-1}$)

Electron Paramagnetic Resonance Parameters. EPR spectra were recorded at room temperature using a Bruker Elexsys E580 spectrometer employing Bruker's high-Q cavity (model) and using quartz capillaries of approximately 1 mm ID. Spectral parameters were typically: 100 kHz modulation frequency, 1 G modulation amplitude, 2 mW microwave power, 9.87 GHz microwave frequency, 20.48 ms time constant and 81.92 conversion time/point. All spectra were recorded after the addition of peroxynitrite.

Reaction Mixtures. All reaction Mixtures contained a solution of 5 mM of urate and 25 mM of metal ions. Peroxynitrite was added to these solutions to 15 mM final concentration.

Results and Discussion

Of all the metal ions we tested. Only the reactions in the presence of Zn(II) and Cd(II) gave EPR signals. The precipitates were formed from both reactions. After filtration, it was clearly shown that the EPR signals came from the precipitates. As shown in Figure D-1, the Cd(II) spectrum consists of a single intense line at g = 2.0149, while the Zn(II) spectrum displays a similar line shape with g = 2.0124 (Figure D-2). Both g-values are consistent with carbon-centered radicals. Interestingly, when ascorbate was added to the reaction mixture, the EPR signal was diminished completely (Figure D-3) and the doublet EPR spectrum, corresponding to the ascorbyl radical, was formed. We postulated that the EPR spectra arose from the formation of the complexes between urate derived radicals, generated from the reaction between uric acid and peroxynitrite, and metal ions, Zn(II) and Cd(II). However, we still need to do additional experiments to identify the structures of these complexes.

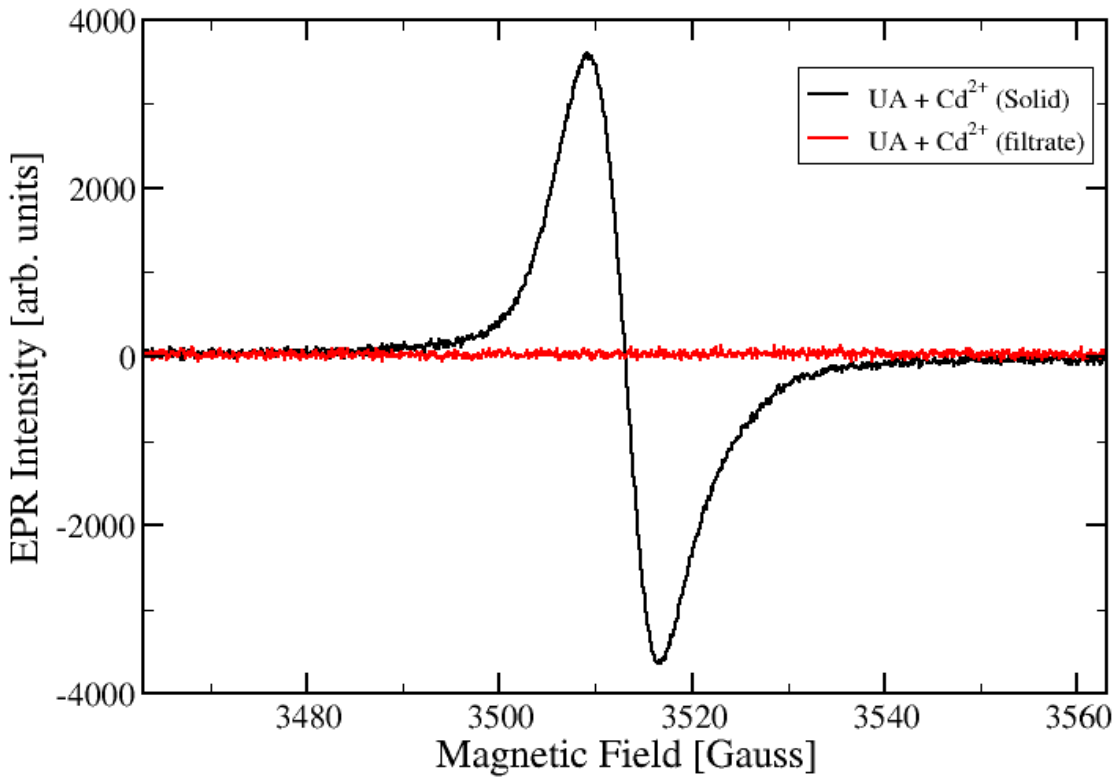

Figure D-1. EPR spectra of the urate-Cd(II) complex obtained by incubating uric acid (5 mM), $CdCl_2$ (25 mM) and peroxynitrite (PN) (15 mM) at room temperature at pH 12. The reaction mixture was filtered to separate the precipitate from the filtrate and monitored by EPR separately. Spectrometer settings: microwave power = 2 mW; modulation frequency = 100 kHz; modulation amplitude = 1 GHz; time constant = 20.48 ms; sweep time = 83.89 s; sweep width = 100 G; and receiver gain = 60 db.

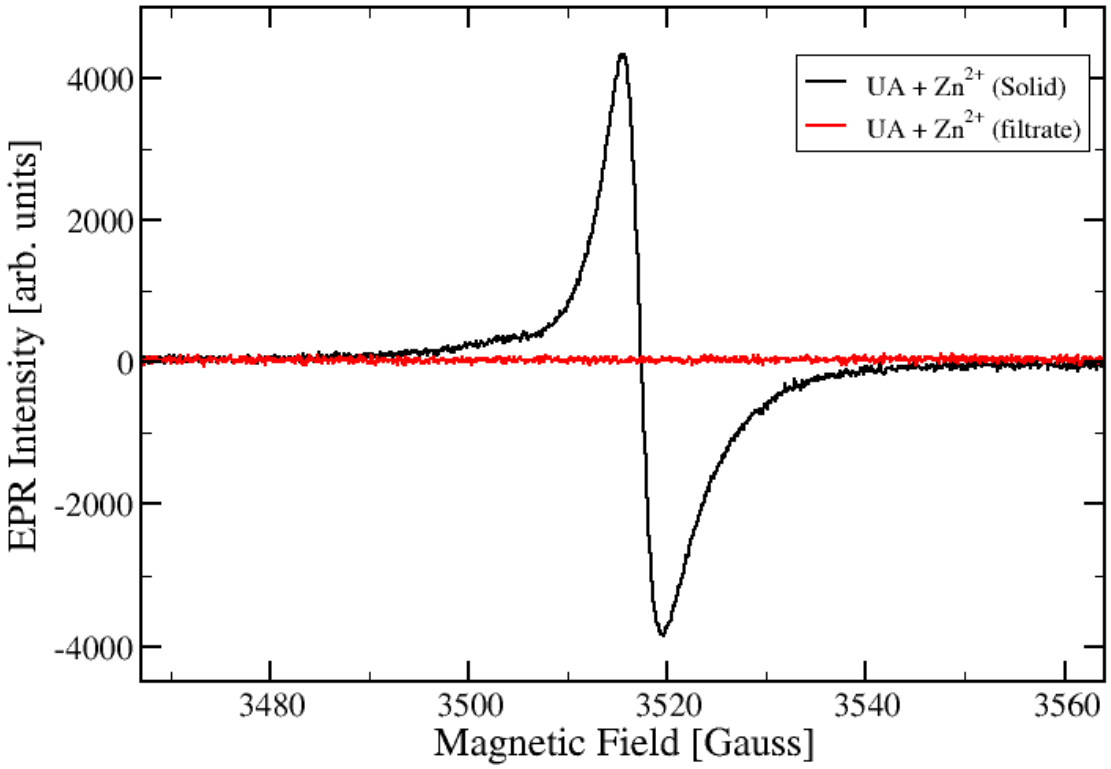

Figure D-2. EPR spectra urate-Zn(II) complex obtained by incubating uric acid (UA) (5 mM), $ZnCl_2$ (25 mM) and peroxynitrite (PN) (15 mM) at room temperature at pH 12. The reaction mixture was filtered to separate the precipitate from the filtrate and monitored by EPR separately. Spectrometer settings: microwave power = 2 mW; modulation frequency = 100 kHz; modulation amplitude = 1 GHz; time constant = 20.48 ms; sweep time = 83.89 s; sweep width = 100 G; and receiver gain = 60 db.

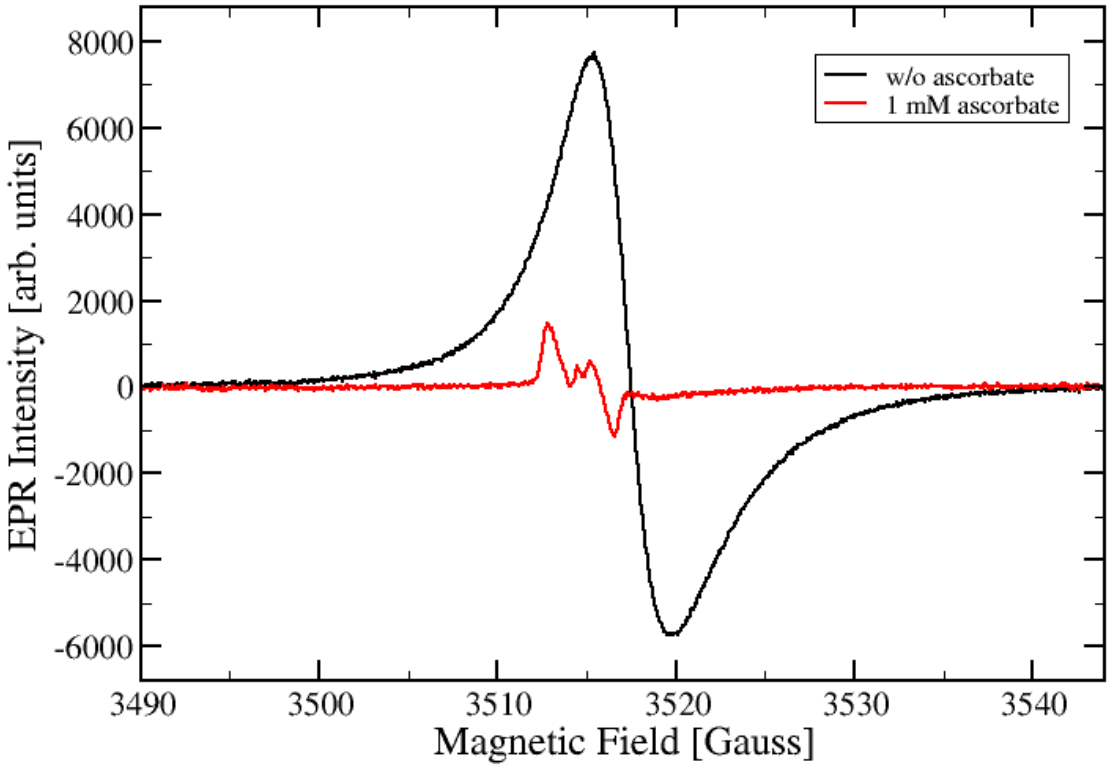

Figure D-3. Effect of ascorbate on the urate-Zn(II) complex formation. EPR spectra obtained by incubating urate (5mM), $ZnCl_2$ (25 mM) and peroxynitrite (PN) (15 mM) at room temperature at pH 12. An aliquot amount of the reaction mixture was withdrew to examine the stability of the radical complexes in the presence of ascorbate (1 mM) and monitored by EPR (–). Spectrometer settings: microwave power = 19.97 mW; modulation frequency = 100 kHz; modulation amplitude = 1 GHz; time constant = 20.48 ms; sweep time = 83.89 s; sweep width = 54 G; and receiver gain = 60 db.

LIST OF REFERENCES

1. Kopani, M., Celec, P., Danisovic, L., Michalka, P., and Biro, C. (2006) Oxidative stress and electron spin resonance. *Clin. Chim. Acta. 364*, 61-66.

2. Hardy, M., Ouari, O., Charles, L., Finet, J. P., Iacazio, G., Monnier, V., Rockenbauer, A., and Tordo, P. (2005) Synthesis and spin-trapping behavior of 5-ChEPMPO, a cholesteryl ester analogue of the spin trap DEPMPO. *J. Org. Chem. 70*, 10426-10433.

3. Finkel, T., and Holbrook, N. J. (2000) Oxidants, oxidative stress and the biology of ageing. *Nature. 408*, 239-247.

4. Beckman, K. B., and Ames, B. N. (1998) The free radical theory of aging matures. *Physiological Reviews. 78*, 547-581.

5. Xia, Y., Khatchikian, G., and Zweier, J. L. (1996) Adenosine deaminase inhibition prevents free radical-mediated injury in the postischemic heart. *J. Biol. Chem. 271*, 10096-10102.

6. Halliwell, B., and Chirico, S. (1993) Lipid-Peroxidation - Its Mechanism, Measurement, and Significance. *Am. J. Clin. Nutr. 57*, S715-S725.

7. Wiseman, H., and Halliwell, B. (1996) Damage to DNA by reactive oxygen and nitrogen species: Role in inflammatory disease and progression to cancer. *Biochem. J. 313*, 17-29.

8. Thornally, P. J. (1986) Theory and biological applications of the electron spin resonance technique of spin trapping. *Life Chemistry Reports*, 57-122

9. Buettner, G. R. (1987) Spin Trapping - Electron-Spin-Resonance Parameters of Spin Adducts. *Free Radical Biol. Med. 3*, 259-303.

10. Janzen, E. G., and BLACKBUR.BJ. (1968) Detection and Identification of Short-Lived Free Radicals by An Electron Spin Resonance Trapping Technique. *J. Am. Chem. Soc. 90*, 5909-&.

11. Janzen, E. G., and BLACKBUR.BJ. (1969) Detection and Identification of Short-Lived Free Radicals by Electron Spin Resonance Trapping Techniques (Spin Trapping) - Photolysis of Organolead, -Tin, and -Mercury Compounds. *J. Am. Chem. Soc. 91*, 4481-&.

12. Samuni, A., Samuni, A., and Swartz, H. M. (1989) The Cellular-Induced Decay of Dmpo Spin Adducts of .Oh and .O2-. *Free Rad. Biol. Med. 6*, 179-183.

13. Frejaville, C., Karoui, H., Tuccio, B., Lemoigne, F., Culcasi, M., Pietri, S., Lauricella, R., and Tordo, P. (1995) 5-(Diethoxyphosphoryl)-5-Methyl-1-Pyrroline N-Oxide - A New Efficient Phosphorylated Nitrone for the In-Vitro and In-Vivo Spin-Trapping of Oxygen-Centered Radicals. *J. Med. Chem. 38*, 258-265.

14. Olive, G., Mercier, A., Le Moigne, F., Rockenbauer, A., and Tordo, P. (2000) 2-Ethoxycarbonyl-2-methyl-3,4-dihydro-2H-pyrrole-1-oxide: evaluation of the spin trapping properties. *Free Rad. Biol. Med. 28*, 403-408.

15. Zhao, H. T., Joseph, J., Zhang, H., Karoui, H., and Kalyanaraman, B. (2001) Synthesis and biochemical applications of a solid cyclic nitrone spin trap: A relatively superior trap for detecting superoxide anions and glutathiyl radicals. *Free Rad. Biol. Med. 31*, 599-606.

16. Sautin, Y. Y., and Johnson, R. J. (2008) Uric acid: The oxidant-antioxidant paradox. *Nucleosides, Nucleotides Nucleic Acids. 27*, 608-619.

17. Wu, X. W., Muzny, D. M., Lee, C. C., and Caskey, C. T. (1992) Two independent mutational events in the loss of urate oxidase during hominoid evolution. *J. Mol. Evol. 34*, 78-84.

18. Johnson, R. J., Kang, D. H., Feig, D., Kivlighn, S., Kanellis, J., Watanabe, S., Tuttle, K. R., Rodriguez-Iturbe, B., Herrera-Acosta, J., and Mazzali, M. (2003) Is there a pathogenetic role for uric acid in hypertension and cardiovascular and renal disease? *Hypertension. 41*, 1183-1190.

19. Becker, B. F. (1993) Towards the Physiological-Function of Uric-Acid. *Free Radical Biol. Med. 14*, 615-631.

20. Bagnati, M., Perugini, C., Cau, C., Bordone, R., Albano, E., and Bellomo, G. (1999) When and why a water-soluble antioxidant becomes pro-oxidant during copper-induced low-density lipoprotein oxidation: a study using uric acid. *Biochem. J. 340*, 143-152.

21. Smith, C. M., Rovamo, L. M., and Raivio, K. O. (1977) Fructose-Induced Adenine-Nucleotide Catabolism in Isolated Rat Hepatocytes. *Can. J. Biochem. 55*, 1237-1240.

22. Friedl, H. P., Till, G. O., Trentz, O., and Ward, P. A. (1991) Role of Oxygen Radicals in Tourniquet-Related Ischemia-Reperfusion Injury of Human Patients. *Klinische Wochenschrift. 69*, 1109-1112.

23. Ames, B. N., Cathcart, R., Schwiers, E., and Hochstein, P. (1981) Uric-Acid Provides An Antioxidant Defense in Humans Against Oxidant-Caused and Radical-Caused Aging and Cancer - A Hypothesis. *Proc. Natl. Acad. Sci. U. S. A. 78*, 6858-6862.

24. Kuzkaya, N., Weissmann, N., Harrison, D. G., and Dikalov, S. (2005) Interactions of peroxynitrite with uric acid in the presence of ascorbate and thiols: Implications for uncoupling endothelial nitric oxide synthase. *Biochem. Pharmacol. 70*, 343-354.

25. Robinson, K. M., Morre, J. T., and Beckman, J. S. (2004) Triuret: a novel product of peroxynitrite-mediated oxidation of urate. *Arch. Biochem. Biophys. 423*, 213-217.

26. Volk, K. J., Yost, R. A., and Brajtertoth, A. (1989) Online Electrochemistry Thermospray Tandem Mass-Spectrometry As A New Approach to the Study of Redox Reactions - the Oxidation of Uric-Acid. *Anal. Chem. 61*, 1709-1717.

27. Whiteman, M., and Halliwell, B. (1996) Protection against peroxynitrite-dependent tyrosine nitration and alpha 1-antiproteinase inactivation by ascorbic acid. A comparison with other biological antioxidants. *Free Radical Res. 25*, 275-283.

28. Squadrito, G. L., Cueto, R., Splenser, A. E., Valavanidis, A., Zhang, H. W., Uppu, R. M., and Pryor, W. A. (2000) Reaction of uric acid with peroxynitrite and implications for the mechanism of neuroprotection by uric acid. *Arch. Biochem. Biophys. 376*, 333-337.

29. Kand'ar, R., Zakova, P., and Muzakova, V. (2006) Monitoring of antioxidant properties of uric acid in humans for a consideration measuring of levels of allantoin in plasma by liquid chromatography. *Clin. Chim. Acta. 365*, 249-256.

30. Howell, R. R., and Wyngaarden, J. B. (1960) Mechanism of Peroxidation of Uric Acids by Hemoproteins. *J. Biol. Chem. 235*, 3544-3550.

31. Mazzali, M., Hughes, J., Kim, Y. G., Jefferson, J. A., Kang, D. H., Gordon, K. L., Lan, H. Y., Kivlighn, S., and Johnson, R. J. (2001) Elevated uric acid increases blood pressure in the rat by a novel crystal-independent mechanism. *Hypertension. 38*, 1101-1106.

32. Maples, K. R., and Mason, R. P. (1988) Free-Radical Metabolite of Uric-Acid. *J. Biol. Chem. 263*, 1709-1712.

33. Kahn, K., Serfozo, P., and Tipton, P. A. (1997) Identification of the true product of the urate oxidase reaction. *J. Am. Chem. Soc. 119*, 5435-5442.

34. Kahn, K., and Tipton, P. A. (1998) Spectroscopic characterization of intermediates in the urate oxidase reaction. *Biochemistry. 37*, 11651-11659.

35. Goyal, R. N., Brajtertoth, A., Dryhurst, G., and Nguyen, N. T. (1982) A Comparison of the Peroxidase-Catalyzed and Electrochemical Oxidation of Uric-Acid. *Bioelectrochem. Bioenerg. 9*, 39-60.

36. Santos, C. X. C., Anjos, E. I., and Augusto, O. (1999) Uric acid oxidation by peroxynitrite: Multiple reactions, free radical formation, and amplification of lipid oxidation. *Arch. Biochem. Biophys. 372*, 285-294.

37. Aruoma, O. I., and Halliwell, B. (1989) Inactivation of Alpha-Antiproteinase by Hydroxyl Radicals - the Effect of Uric-Acid. *FEBS Lett. 244*, 76-80.

38. Kittridge, K. J., and Willson, R. L. (1984) Uric-Acid Substantially Enhances the Free Radical-Induced Inactivation of Alcohol-Dehydrogenase. *FEBS Lett. 170*, 162-164.

39. Sanguinetti, S. M., Batthyany, C., Trostchansky, A., Botti, H., Lopez, G. I., Wikinski, R. L. W., Rubbo, H., and Schreier, L. E. (2004) Nitric oxide inhibits prooxidant actions of uric acid during copper-mediated LDL oxidation. *Arch. Biochem. Biophys. 423*, 302-308.

40. Plumb, R. C., Tantayanon, R., Libby, M., and Xu, W. W. (1989) Chemical-Model for Viking Biology Experiments - Implications for the Composition of the Martian Regolith. *Nature. 338*, 633-635.

41. Kobayashi, K., Miki, M., and Tagawa, S. (1995) Pulse-Radiolysis Study of the Reaction of Nitric-Oxide with Superoxide. *J. Chem. Soc., Dalton Trans.*, 2885-2889.

42. Huie, R. E., and Padmaja, S. (1993) The Reaction of No with Superoxide. *Free Radical Res. Commun. 18*, 195-199.

43. Goldstein, S., and Czapski, G. (1995) The Reaction of No-Center-Dot with O-2(Center-Dot-) and Ho2-Center-Dot - A Pulse-Radiolysis Study. *Free Radical Biol. Med. 19*, 505-510.

44. Pacher, P., Beckman, J. S., and Liaudet, L. (2007) Nitric oxide and peroxynitrite in health and disease. *Physiological Reviews. 87*, 315-424.

45. Koppenol, W. H., Moreno, J. J., Pryor, W. A., Ischiropoulos, H., and Beckman, J. S. (1992) Peroxynitrite, A Cloaked Oxidant Formed by Nitric-Oxide and Superoxide. *Chem. Res. Toxicol. 5*, 834-842.

46. Kissner, R., Nauser, T., Kurz, C., and Koppenol, W. H. (2003) Peroxynitrous acid - Where is the hydroxyl radical? *Iubmb Life. 55*, 567-572.

47. Kissner, R., Nauser, T., Bugnon, P., Lye, P. G., and Koppenol, W. H. (1997) Formation and properties of peroxynitrite as studied by laser flash photolysis, high-pressure stopped-flow technique, and pulse radiolysis. *Chem. Res. Toxicol. 10*, 1285-1292.

48. Tsai, J. H. M., Harrison, J. G., Martin, J. C., Hamilton, T. P., vanderWoerd, M., Jablonsky, M. J., and Beckman, J. S. (1994) Role of Conformation of Peroxynitrite Anion (Onoo-) in Its Stability and Toxicity. *J. Am. Chem. Soc. 116*, 4115-4116.

49. Tsai, H. H., Hamilton, T. P., Tsai, J. H. M., vanderWoerd, M., Harrison, J. G., Jablonsky, M. J., Beckman, J. S., and Koppenol, W. H. (1996) Ab initio and NMR study of peroxynitrite and peroxynitrous acid: Important biological oxidants. *J. Phys. Chem. 100*, 15087-15095.

50. Lymar, S. V., and Hurst, J. K. (1998) CO2-catalyzed one-electron oxidations by peroxynitrite: Properties of the reactive intermediate. *Inorg. Chem. 37*, 294-301.

51. Uppu, R. M., Squadrito, G. L., and Pryor, W. A. (1996) Acceleration of peroxynitrite oxidations by carbon dioxide. *Arch. Biochem. Biophys. 327*, 335-343.

52. Uppu, R. M., Winston, G. W., and Pryor, W. A. (1997) Reactions of peroxynitrite with aldehydes as probes for the reactive intermediates responsible for biological nitration. *Chem. Res. Toxicol. 10*, 1331-1337.

53. Yang, D., Tang, Y. C., Chen, J., Wang, X. C., Bartberger, M. D., Houk, K. N., and Olson, L. (1999) Ketone-catalyzed decomposition of peroxynitrite via dioxirane intermediates. *J. Am. Chem. Soc. 121*, 11976-11983.

54. Masumoto, H., and Sies, H. (1996) The reaction of ebselen with peroxynitrite. *Chem. Res. Toxicol. 9*, 262-267.

55. Koppenol, W. H., and Kissner, R. (1998) Can O = NOOH undergo homolysis? *Chem. Res. Toxicol. 11*, 87-90.

56. Merenyi, G., and Lind, J. (1997) Thermodynamics of peroxynitrite and its CO2 adduct. *Chem. Res. Toxicol. 10*, 1216-1220.

57. Squadrito, G. L., and Pryor, W. A. (1998) Oxidative chemistry of nitric oxide: The roles of superoxide, peroxynitrite, and carbon dioxide. *Free Radical Biol. Med. 25*, 392-403.

58. Squadrito, G. L., and Pryor, W. A. (2002) Mapping the reaction of peroxynitrite with CO2: Energetics, reactive species, and biological implications. *Chem. Res. Toxicol. 15*, 885-895.

59. Beckman, J. S., Beckman, T. W., Chen, J., Marshall, P. A., and Freeman, B. A. (1990) Apparent Hydroxyl Radical Production by Peroxynitrite - Implications for Endothelial Injury from Nitric-Oxide and Superoxide. *Proc. Natl. Acad. Sci. U. S. A. 87*, 1620-1624.

60. Vandervliet, A., Smith, D., Oneill, C. A., Kaur, H., Darleyusmar, V., Cross, C. E., and Halliwell, B. (1994) Interactions of Peroxynitrite with Human Plasma and Its Constituents - Oxidative Damage and Antioxidant Depletion. *Biochem. J. 303*, 295-301.

61. Ischiropoulos, H., Zhu, L., Chen, J., Tsai, M., Martin, J. C., Smith, C. D., and Beckman, J. S. (1992) Peroxynitrite-Mediated Tyrosine Nitration Catalyzed by Superoxide-Dismutase. *Arch. Biochem. Biophys. 298*, 431-437.

62. King, P. A., Anderson, V. E., Edwards, J. O., Gustafson, G., Plumb, R. C., and Suggs, J. W. (1992) A Stable Solid That Generates Hydroxyl Radical Upon Dissolution in Aqueous-Solutions - Reaction with Proteins and Nucleic-Acid. *J. Am. Chem. Soc. 114*, 5430-5432.

63. Radi, R., Beckman, J. S., Bush, K. M., and Freeman, B. A. (1991) Peroxynitrite-Induced Membrane Lipid-Peroxidation - the Cytotoxic Potential of Superoxide and Nitric-Oxide. *Arch. Biochem. Biophys. 288*, 481-487.

64. Hooper, D. C., Spitsin, S., Kean, R. B., Champion, J. M., Dickson, G. M., Chaudhry, I., and Koprowski, H. (1998) Uric acid, a natural scavenger of peroxynitrite, in experimental allergic encephalomyelitis and multiple sclerosis. *Proc. Natl. Acad. Sci. U. S. A. 95*, 675-680.

65. Spitsin, S. V., Scott, G. S., Mikheeva, T., Zborek, A., Kean, R. B., Brimer, C. M., Koprowski, H., and Hooper, D. C. (2002) Comparison of uric acid and ascorbic acid in protection against EAE. *Free Radical Biol. Med. 33*, 1363-1371.

66. Feig, D. I., and Johnson, R. J. (2003) Hyperuricemai in childhood essential hypertension. *Pediatr. Res. 53*, 524A.

67. Feig, D. I., Nakagawa, T., Karumanchi, S. A., Oliver, W. J., Kang, D. H., Finch, J., and Johnson, R. J. (2004) Hypothesis: Uric acid, nephron number, and the pathogenesis of essential hypertension. *Kidney Int. 66*, 281-287.

68. Kang, D. H., Nakagawa, T., Feng, L. L., Watanabe, S., Han, L., Mazzali, M., Truong, L., Harris, R., and Johnson, R. J. (2002) A role for uric acid in the progression of renal disease. *Journal of the American Society of Nephrology. 13*, 2888-2897.

69. Mazzali, M., Kanellis, J., Han, L., Feng, L., Xia, Y. Y., Chen, Q., Kang, D. H., Gordon, K. L., Watanabe, S., Nakagawa, T., Lan, H. Y., and Johnson, R. J. (2002) Hyperuricemia induces a primary renal arteriolapathy in rats by a blood pressure-independent mechanism. *American Journal of Physiology-Renal Physiology. 282*, F991-F997.

70. Nakagawa, T., Tuttle, K. R., Short, R. A., and Johnson, R. J. (2005) Hypothesis: fructose-induced hyperuricemia as a causal mechanism for the epidemic of the metabolic syndrome. *Nature Clinical Practice Nephrology. 1*, 80-86.

71. Nakagawa, T., Hu, H. B., Zharikov, S., Tuttle, K. R., Short, R. A., Glushakova, O., Ouyang, X., Feig, D. I., Block, E. R., Herrera-Acosta, J., Patel, J. M., and Johnson, R. J. (2006) A causal role for uric acid in fructose-induced metabolic syndrome. *American Journal of Physiology-Renal Physiology. 290*, F625-F631.

72. Aruoma, O. I., and Halliwell, B. (1989) Inactivation of Alpha-Antiproteinase by Hydroxyl Radicals - the Effect of Uric-Acid. *FEBS Lett. 244*, 76-80.

73. Bagnati, M., Perugini, C., Cau, C., Bordone, R., Albano, E., and Bellomo, G. (1999) When and why a water-soluble antioxidant becomes pro-oxidant during copper-induced low-density lipoprotein oxidation: a study using uric acid. *Biochem. J. 340*, 143-152.

74. Kittridge, K. J., and Willson, R. L. (1984) Uric-Acid Substantially Enhances the Free Radical-Induced Inactivation of Alcohol-Dehydrogenase. *FEBS Lett. 170*, 162-164.

75. Sanguinetti, S. M., Batthyany, C., Trostchansky, A., Botti, H., Lopez, G. I., Wikinski, R. L. W., Rubbo, H., and Schreier, L. E. (2004) Nitric oxide inhibits prooxidant actions of uric acid during copper-mediated LDL oxidation. *Arch. Biochem. Biophys. 423*, 302-308.

76. Uppu, R. M., and Pryor, W. A. (1996) Synthesis of peroxynitrite in a two-phase system using isoamyl nitrite and hydrogen peroxide. *Anal. Biochem. 236*, 242-249.

77. Janzen, E. G. (1971) Spin Trapping. *Acc. Chem. Res. 4*, 31-&.

78. Bechara, E. J., Massari, J., Fujy, D., Micke, G., Tokikawa, R., and Assuncao, N. (2008) Radical acetylation of amino acids and 2 '-deoxyguanosine coupled to the reaction of diacetyl with peroxynitrite in aerated medium. *Free Radical Biol. Med. 44*, 493.

79. Nonoyama, N., Oshima, H., Shoda, C., and Suzuki, H. (2001) The reaction of peroxynitrite with organic molecules bearing a biologically important functionality. The multiplicity of reaction modes as exemplified by hydroxylation, nitration, nitrosation, dealkylation, oxygenation, and oxidative dimerization and cleavage. *Bull. Chem. Soc. Jpn. 74*, 2385-2395.

80. Safranow, K., and Machoy, Z. (2005) Simultaneous determination of 16 purine derivatives in urinary calculi by gradient reversed-phase high-performance liquid chromatography with UV detection. *J. Chromatogr. , B: Anal. Technol. Biomed. Life Sci. 819*, 229-235.

81. Davies, K. J. A., Sevanian, A., Muakkassahkelly, S. F., and Hochstein, P. (1986) Uric-Acid Iron-Ion Complexes - A New Aspect of the Antioxidant Functions of Uric-Acid. *Biochem. J. 235*, 747-754.

82. Safranow, K., and Machoy, Z. (2005) Methylated purines in urinary stones. *Clinical Chemistry. 51*, 1493-1498.

83. Bhat, V. B., Sridhar, G. R., and Madyastha, K. M. (2001) Efficient scavenging of hydroxyl radicals and inhibition of lipid peroxidation by novel analogues of 1,3,7-trimethyluric acid. *Life Sci. 70*, 381-393.

84. Smith, R. C., Reeves, J., Mckee, M. L., and Daron, H. (1987) Reaction of Methylated Urates with 1,1-Diphenyl-2-Picrylhydrazyl. *Free Radical Biol. Med. 3*, 251-257.

85. Meadows, J., Smith, R. C., and Reeves, J. (1986) Uric-Acid Protects Membranes and Linolenic Acid from Ozone-Induced Oxidation. *Biochem. Biophys. Res. Commun. 137*, 536-541.

86. Nishida, Y. (1991) Inhibition of Lipid-Peroxidation by Methylated Analogs of Uric-Acid. *J. Pharm. Pharmacol. 43*, 885-887.

87. Smith, R. C., and Lawing, L. (1983) Antioxidant Activity of Uric-Acid and 3-N-Ribosyluric Acid with Unsaturated Fatty-Acids and Erythrocyte-Membranes. *Arch. Biochem. Biophys. 223*, 166-172.

88. Telo, J. P. (2003) Radicals derived from uric acid and its methyl derivatives in aqueous solution: an EPR spectroscopy and theoretical study. *Org. Biomol. Chem. 1*, 588-592.

89. Zhou, C. C., and Hill, D. R. (2007) The keto-enol tautomerization of ethyl butylryl acetate studied by LC-NMR. *Magn. Reson. Chem. 45*, 128-132.

90. Arteel, G. E., Briviba, K., and Sies, H. (1999) Protection against peroxynitrite. *FEBS Lett. 445*, 226-230.

91. Douki, T., Cadet, J., and Ames, B. N. (1996) An adduct between peroxynitrite and 2'-deoxyguanosine: 4,5-dihydro-5-hydroxy-4-(nitrosooxy)-2'-deoxyguanosine. *Chem. Res. Toxicol. 9*, 3-7.

92. Merenyi, G., and Lind, J. (1998) Free radical formation in the peroxynitrous acid (ONOOH) peroxynitrite (ONOO-) system. *Chem. Res. Toxicol. 11*, 243-246.

93. Althaus, J. S., Fici, G. J., Plaisted, S. M., Kezdy, F. J., Campbell, C. M., Hoogerheide, J. G., and VonVoigtlander, P. F. (1997) Protein nitration by peroxynitrite: A method for monitoring nitric oxide neurotoxicity. *Microchem. J. 56*, 155-164.

94. Xiong, Y. Q., Rabchevsky, A. G., and Hall, E. D. (2007) Role of peroxynitrite in secondary oxidative damage after spinal cord injury. *J. Neurochem. 100*, 639-649.

95. Kohnen, S. L., Mouithys-Mickalad, A. A., by-Dupont, G. P., Deby, C. M. T., Lamy, M. L., and Noels, A. F. (2001) Oxidation of tetrahydrobiopterin by peroxynitrite or oxoferryl species occurs by a radical pathway. *Free Radical Res. 35*, 709-721.

96. Eberson, L. (1992) Inverted Spin Trapping - Reactions Between the Radical Cation of Alpha-Phenyl-N-Tert-Butylnitrone and Ionic and Neutral Nucleophiles. *J. Chem. Soc., Perkin Trans. 2. 10*, 1807-1813.

97. Eberson, L., Lind, J., and Merenyi, G. (1994) Inverted Spin-Trapping .4. Application to the Formation of Imidyl Spin Adducts from N-Haloimides. *J. Chem. Soc., Perkin Trans. 2. 6*, 1181-1188.

98. Eberson, L. (1994) Inverted Spin-Trapping .3. Further-Studies on the Chemical and Photochemical Oxidation of Spin Traps in the Presence of Nucleophiles. *J. Chem. Soc., Perkin Trans. 2. 2*, 171-176.

99. Kotake, Y., and Janzen, E. G. (1991) Decay and Fate of the Hydroxyl Radical Adduct of Alpha-Phenyl-N-Tert-Butylnitrone in Aqueous-Media. *J. Am. Chem. Soc. 113*, 9503-9506.

100. Mcintire, G. L., Blount, H. N., Stronks, H. J., Shetty, R. V., and Janzen, E. G. (1980) Spin Trapping in Electrochemistry .2. Aqueous and Non-Aqueous Electrochemical Characterizations of Spin Traps. *J. Phys. Chem. 84*, 916-921.

101. Eberson, L., Hartshorn, M. P., and Persson, O. (1996) Inverted spin trapping .5. 1,1,1,3,3,3-hexafluoropropan-2-ol as a solvent for the discrimination between proper and inverted spin trapping. *J. Chem. Soc., Perkin Trans. 2. 2*, 141-149.

102. Gandour, M. A., Kasim, E. A., Amrallah, A. H., and Farghaly, O. A. (1994) Differential-Pulse Polarography of Cadmium-Urate and Lead-Urate and Adsorptive Stripping Voltammetric Determination of Uric-Acid. *Talanta. 41*, 439-444.

BIOGRAPHICAL SKETCH

Witcha Imaram was born in Ratchaburi, a province in the western part of Thailand. Awarded by the Institute for the Promotion of Teaching Science and Technology, he received the Development and Promotion of Science and Technology Talent Project (DPST) scholarship to complete his high school education at Sriboonyanon School, Nonthaburi, Thailand in 1999, and a Bachelor of Science (1^{st} class honours) degree in chemistry from Kasetsart University, Bangkok, Thailand, in 2003. After graduation, he received a Thai scholarship to pursue his Ph.D. degree at the University of Florida in Fall 2003. In his graduate research work, he joined Dr. Alexander Angerhofer's research group to elucidate the mechanisms involved in the biological effects of uric acid, using ESR spin trapping methods to probe the formation of reactive radical species derived from uric acid.